



CENTER FOR INFRASTRUCTURE ENGINEERING STUDIES

BOND BETWEEN CARBON FIBER REINFORCED POLYMER SHEETS AND CONCRETE

by

BRIAN DANIEL MILLER

University of Missouri-Rolla

**CIES
99-03**

Disclaimer

The contents of this report reflect the views of the author(s), who are responsible for the facts and the accuracy of information presented herein. This document is disseminated under the sponsorship of the Center for Infrastructure Engineering Studies (CIES), University of Missouri -Rolla, in the interest of information exchange. CIES assumes no liability for the contents or use thereof.

The mission of CIES is to provide leadership in research and education for solving society's problems affecting the nation's infrastructure systems. CIES is the primary conduit for communication among those on the UMR campus interested in infrastructure studies and provides coordination for collaborative efforts. CIES activities include interdisciplinary research and development with projects tailored to address needs of federal agencies, state agencies, and private industry as well as technology transfer and continuing/distance education to the engineering community and industry.

Center for Infrastructure Engineering Studies (CIES)

University of Missouri-Rolla
223 Engineering Research Lab
1870 Miner Circle
Rolla, MO 65409-0710
Tel: (573) 341-6223; fax -6215
E-mail: cies@umr.edu
www.cies.umr.edu

BOND BETWEEN CARBON
FIBER REINFORCED POLYMER
SHEETS AND CONCRETE

by

BRIAN DANIEL MILLER

A THESIS

Presented to the Faculty of the Graduate School of the

UNIVERSITY OF MISSOURI-ROLLA

In partial Fulfillment of the Requirements for the Degree

MASTER OF SCIENCE IN CIVIL ENGINEERING

1999

Approved by

Antonio Nanni, Advisor

Abdeldjelil Belarbi

K. Chandrashekhara

© 1999
Brian D. Miller
All Rights Reserved

ABSTRACT

The purpose of this investigation is to study the bond between Carbon Fiber Reinforced Polymer (CFRP) sheets and concrete. An experimental investigation was conducted in order to determine the effects of bonded length, concrete strength, and number of plies of CFRP. The specimens used in the study were unreinforced concrete beams that were externally reinforced with CFRP sheets and tested in flexure. Strain gauges were used to monitor the strain at different locations on the CFRP sheet. From this information, strain distribution curves were plotted for different levels of load. After the initial experimental investigation was completed, more specimens were tested to verify results. These specimens were conducted to address the effects of the width of sheet, 0°/90° wrapping technique, and surface preparation.

The failure mode for all of the specimens in the initial investigation resulted from peeling of the CFRP sheet. However, some of the specimens in the verification stage failed by fiber rupture. It was found that the bonded length did not have an effect on the bond strength due to the existence of an effective bonded length. The effective bonded length is defined as the length of sheet that contributes to the bond strength. The concrete strength also did not affect the bond, as the peeling failure occurred in the concrete-epoxy interface. The number of plies (stiffness) of CFRP reinforcement had a considerable influence on the bond. A model was developed based on the stiffness of the CFRP sheet. This model was used to create a design procedure to make sure that the service stress in the CFRP sheet is less than the calculated peeling stress. The width of the sheet was found to have no effect on the bond strength. The 0°/90° wrapping technique and improved surface preparation was found to improve the bond strength to the point where failure occurred by fiber rupture. It was concluded that more experimental evidence is needed to provide a complete answer to the problem. Suggestions were made for future research in order to build on the current study.

ACKNOWLEDGEMENTS

I would like to express my gratitude to NSF for funding this research project. I would also like to thank Master Builders Technologies for the donation of materials.

I would also like to express my appreciation to Dr. Antonio Nanni for his guidance and the opportunity to complete this experimental study. I would also like to thank Dr. Abdeldjelil Belarbi and Dr. K. Chandrashekhara for their support and advice.

I would like to recognize the following people who helped in one way or another with the experimental portion of this research project: Ahmed Khalifa, Arnold Yan, Bob Eskens, Gustavo Tumialan, Matt Mettemeyer, Tarek Alkhrdaji, and William Gold. To all of them I would like to express my gratitude.

Finally, to my wife Amy and my family, I express my deepest appreciation for their love, help, understanding, and support.

TABLE OF CONTENTS

	Page
ABSTRACT.....	iii
ACKNOWLEDGMENTS	iv
LIST OF FIGURES	viii
LIST OF TABLES	xi
SECTION	
1. INTRODUCTION.....	1
1.1. BACKGROUND AND PROBLEM STATEMENT.....	1
1.2. PREVIOUS RESEARCH ON BOND.....	1
1.3. OBJECTIVES	8
2. CONSTITUENT MATERIALS.....	9
2.1. CARBON FIBER TOW SHEET.....	9
2.2. EPOXY RESINS	10
2.3. COMPOSITE SYSTEM	11
2.4. CONCRETE BEAM.....	12
3. METHODOLOGY.....	14
3.1. INTRODUCTION	14
3.2. DESIGN OF SPECIMEN	14
3.3. SPECIMEN PREPARATION	24
3.3.1. Surface Preparation.....	24
3.3.2. Application of CFRP Sheets.....	25
3.4. TEST PROCEDURE	28
3.5. VERIFICATION OF RESULTS	29

3.6. MISCELLANEOUS SPECIMENS	31
3.7. SUMMARY OF TEST SPECIMENS	34
4. EXPERIMENTAL RESULTS	36
4.1. INTRODUCTION	36
4.2. SERIES I	36
4.3. SERIES II	43
4.4. SERIES III	47
4.5. VERIFICATION SPECIMENS	51
4.6. MISCELLANEOUS SPECIMENS	56
5. COMPARISON OF EXPERIMENTAL RESULTS	64
5.1. BONDED LENGTH	64
5.2. CONCRETE STRENGTH	69
5.3. PLIES OF CFRP SHEET	73
5.4. WIDTH OF SHEET	76
5.5. TRANSVERSE SHEET	77
5.6. SURFACE PREPARATION	80
5.7. SUMMARY	81
6. MODELING OF RESULTS	83
6.1. ANALYTICAL MODEL	83
6.2. DESIGN RECOMMENDATIONS	92
7. RECOMMENDATIONS, CONCLUSIONS, AND SUMMARY	95
7.1. RECOMMENDATIONS FOR FUTURE RESEARCH	95
7.2. CONCLUSIONS	98

7.3. SUMMARY.....	99
APPENDICES	
A. STRAIN vs. LOCATION DIAGRAMS	100
B. LOAD vs. DEFLECTION DIAGRAMS.....	114
C. DESIGN EXAMPLE.....	128
LIST OF REFERENCES.....	136
VITA.....	138

LIST OF FIGURES

Figure	Page
1.1 Stress Distribution in Steel Plates	2
1.2 Shear Test Specimen.....	3
1.3 Direct Tensile Test Specimen	4
1.4 Stress Distribution in CFRP Sheet at Ultimate Load.....	6
1.5 Strain vs. Location Schematic.....	7
2.1 Application of FRP Sheets.....	11
2.2 Thickness of each Layer of Composite System.....	12
3.1 Effect of Cracking on Stress Distribution.....	15
3.2 Location of Hinge and Detail of Hinge.....	17
3.3 Free Body Diagram of Beam at Midspan	21
3.4 Layout of Specimen	23
3.5 Sandblasted Concrete Surface.....	25
3.6 Position of Strain Gauges for the 4-inch (102-mm) Bonded Length.....	27
3.7 Position of Strain Gauges for the 8-inch (203-mm) Bonded Length.....	27
3.8 Position of Strain Gauges for the 12-inch (305-mm) Bonded Length.....	28
3.9 Picture of Test Setup.....	29
3.10 Location of Strain Gauges for Verification Testing	30
3.11 Procedure for Applying Sheets at 0° and 90°	32
3.12 Specimen with 2-inch (51-mm) Wide Sheet and Transverse Sheet	33
3.13 Specimen with 4-inch (102-mm) Wide Sheet and Transverse Sheet	33
3.14 Surface of Specimen 6-1-12-S	34
4.1 Load vs, Deflection for Specimen with 4-inch (102-mm) Bonded Length	38
4.2 Load vs. Deflection for Specimen with 8 or 12-inch (203 or 305 mm) Bonded Length	39
4.3 Typical Strain vs. Location for 4-inch (102 mm) Bonded Length	41
4.4 Strain vs. Location for 8-inch (203-mm) Bonded Length	41
4.5 Strain vs. Location for 12-inch (305-mm) Bonded Lengths.....	42
4.6 Comparison of Quadratic and Linear Curves	42
4.7 Load vs. Deflection for 4-inch (102-mm) Bonded Length.....	45

4.8	Typical Load vs. Deflection for 8 or 12-inch (203 or 305-mm) Bonded Length .	45
4.9	Strain vs. Location for 4-inch (102-mm) Bonded Length	46
4.10	Strain vs. Location for 8-inch (203-mm) Bonded Length	46
4.11	Strain vs. Location for 12-inch (305-mm) Bonded Length	47
4.12	Load vs. Deflection for 4-inch (102 mm) Bonded Length	49
4.13	Typical Load vs. Deflection for 8 or 12-inch (203 or 305-mm) Bonded Length .	49
4.14	Strain vs. Location for 4-inch (102-mm) Bonded Length	50
4.15	Typical Strain vs. Location for 8-inch (203-mm) Bonded Length	50
4.16	Typical Strain vs. Location for 12-inch (305-mm) Bonded Length	51
4.17	Load vs. Deflection for Verification Specimen	53
4.18	Strain vs. Location for Verification Specimen	54
4.19	Comparison of the Strain Gauges in the Unbonded Region with the Theoretical Value	54
4.20	Location of Strain Gauges in the Unbonded Region	55
4.21	Adjusted Strain in Unbonded Region vs. Load	55
4.22	Strain vs. Location for Specimen with 4-inch (102-mm) Wide Sheet.....	58
4.23	Load vs. Deflection for Specimen 2-0-90.....	59
4.24	Strain vs. Location for Specimen 2-0-90	60
4.25	Load vs. Deflection for Specimen 4-0-90.....	61
4.26	Strain vs. Location for Specimen 4-0-90	61
4.27	Failure Mode of 4-0-90.....	62
4.28	End View of 6-1-12-S after Failure	63
5.1	Average Bond Strength vs. Bond Length for Series I	65
5.2	Average Bond Strength vs. Bond Length for Series II.....	65
5.3	Average Bond Strength vs. Bond Length for Series III.....	66
5.4	Comparison of Strain Distributions for Series I	67
5.5	Comparison of Strain Distributions for Series II	68
5.6	Comparison of Strain Distributions for Series III.....	68
5.7	Surface of Bonded Area After Peeling (6-1-8-2).....	69
5.8	Surface of Bonded Area After Peeling (3-1-8-2).....	70
5.9	Comparison of Average Bond Strength for Different Concrete Strengths.....	72

5.10	Comparison of Strain Distribution for Series I and Series III	72
5.11	Comparison of Average Bond Strength for Series I and II.....	75
5.12	Comparison of Strain Distributions Series I and Series II.....	75
5.13	Comparison of Strain Distributions for Different Widths of CFRP	77
5.14	Contribution of Transverse Sheet (2-inch (51-mm) Width)	79
5.15	Contribution of Transverse Sheet (4-inch (102-mm) Width)	80
5.16	Sandblasted Surface	80
5.17	Roughened Surface	81
6.1	Curves Used to Calculate $d\varepsilon/dx$ for Series I.....	84
6.2	Curves Used to Calculate $d\varepsilon/dx$ for Series II.....	85
6.3	Effective Bond Length vs. Stiffness	88
6.4	Effective Bond Length vs. Stiffness (Maeda et al.).....	89
6.5	$d\varepsilon/dx$ vs. Stiffness	89
6.6	Free-Body Diagram of Sheet with Length dx	91
6.7	Ultimate Load vs. Stiffness of CFRP Sheet.....	92
7.1	Anchor System for FRP Sheets.....	96
7.2	Surface Before Application.....	97
7.3	Location of Indentations	97

LIST OF TABLES

Table	Page
2.1 Properties of Fiber Tow Sheet	9
2.2 Physical Properties of Epoxy Resins	10
2.3 Tension: Neat Resin Properties ASTM D-638	10
2.4 Compressive Strength of Concrete Beams	13
3.1 Description of Specimens	24
3.2 Description of Verification Specimen	31
3.3 Details of Miscellaneous Specimens	34
3.4 Summary of all Test Specimens	35
4.1 Details of Specimens for Series I.....	38
4.2 Details of Specimens for Series II	44
4.3 Details of Specimens for Series III.....	48
4.4 Details of Verification Specimens	53
4.5 Details of Miscellaneous Specimens	58
4.6 Comparison of the Ultimate Load with Change in the Width of Sheet.....	59
5.1 Cracking and Ultimate Load for Series I and III	71
5.2 Comparison of Cracking and Ultimate Load for Series I and III	71
5.3 Ultimate Load of Series I and II	73
5.4 Comparison of Ultimate Load for Series I and II.....	74
5.5 Comparison of Ultimate Load for Different Width of CFRP Sheet.....	76
5.6 Influence of Transverse Sheet on Ultimate Load	78
5.7 Comparison of Specimens with Different Surface Preparation.....	80
6.1 Values Used to Find L_e (Series I)	85
6.2 Values Used to Find L_e (Series II).....	86
6.3 Values for the Ultimate Design.....	94
6.4 Values for Service Loads	94
7.1 Recommended Sheet Stiffness to Test.....	95

1. INTRODUCTION

1.1. BACKGROUND AND PROBLEM STATEMENT

The use of Fiber Reinforced Polymer (FRP) for reinforcement of concrete members has emerged as one of the most exciting and promising technologies in materials and structural engineering (Nanni, 1995). The type of application includes both new construction and repair/rehabilitation. The subject of this research is externally bonded Carbon FRP (CFRP) sheets, which are used in the area of repair/rehabilitation. In particular, the bond between CFRP sheets and concrete will be addressed.

The bond between CFRP sheets and concrete is an issue that is in need of attention. The importance of bond is that it is the means for the transfer of stress between the concrete and CFRP in order to develop composite action. To properly reinforce a concrete structure with CFRP sheets, it is mandatory that development lengths be determined. Development length is defined as the shortest length necessary to attain failure of the reinforcement. The development length can only be determined after the failure mode and stress distribution of the CFRP sheets are understood.

1.2. PREVIOUS RESEARCH ON BOND

There has been much research conducted in the area of epoxy bonded steel plates and concrete. The following is one example of the research that has been conducted. Van Gemert (1996) conducted a series of test on the bonding of steel plates to concrete. The specimen used in these tests consisted of two concrete prisms connected by steel plates bonded on two opposite sides of the prisms. The goal of this research was to develop design guides for the anchorage of steel plates. The stress distributions, given in

Figure 1.1 were presented. The first is at service loads and the other is at ultimate load. (Van Gemert, 1996).

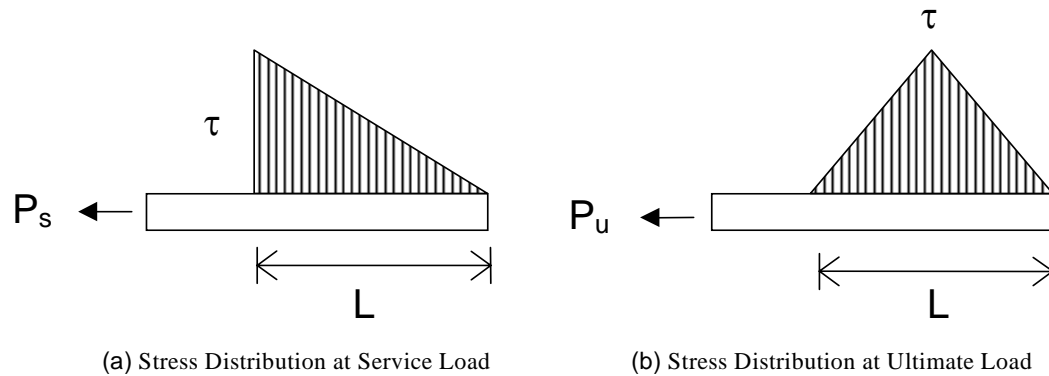


Figure 1.1: Stress Distribution in Steel Plates

While there is a lot of experimental data for steel plates, it cannot be directly applied to CFRP sheets (Brosens and Van Gemert, 1997). The problem is that steel has different physical properties and behavior from FRP. At present, data on the bond between CFRP sheets and concrete is reported in the following literature (Frigo, 1996; Yoshizawa et al, 1996; Brosens and Van Gemert, 1997; Horiguchi and Saeki, 1997; Maeda et al, 1997; Nanni et al, 1997; Takahashi et al, 1997; Taljsten, 1997; Dolan et al, 1998; Green et al, 1998; Lee et al, 1998; Malek et al, 1998; Bizindavyi and Neale, 1999; Tripi et al, 1999). The following paragraphs will outline some of the research efforts that have been reported.

A group of researchers conducted a study on the effect of the type of concrete surface preparation on the bond of CFRP sheets (Yoshizawa et al, 1996). The specimen used in these tests was a concrete prism with CFRP sheets applied to two opposite sides (see Figure 1.2). The specimen was tested in tension, causing direct shear to be placed on the sheets. The concrete surface of the specimens was prepared either by water jet or sand blasting. They found that the water jet doubled the capacity of the specimen as compared to the sand blasted specimens. The bonded length of the CFRP sheet, which is the length of sheet that is physically glued to the concrete, was determined to have little effect on the ultimate load of the specimen.

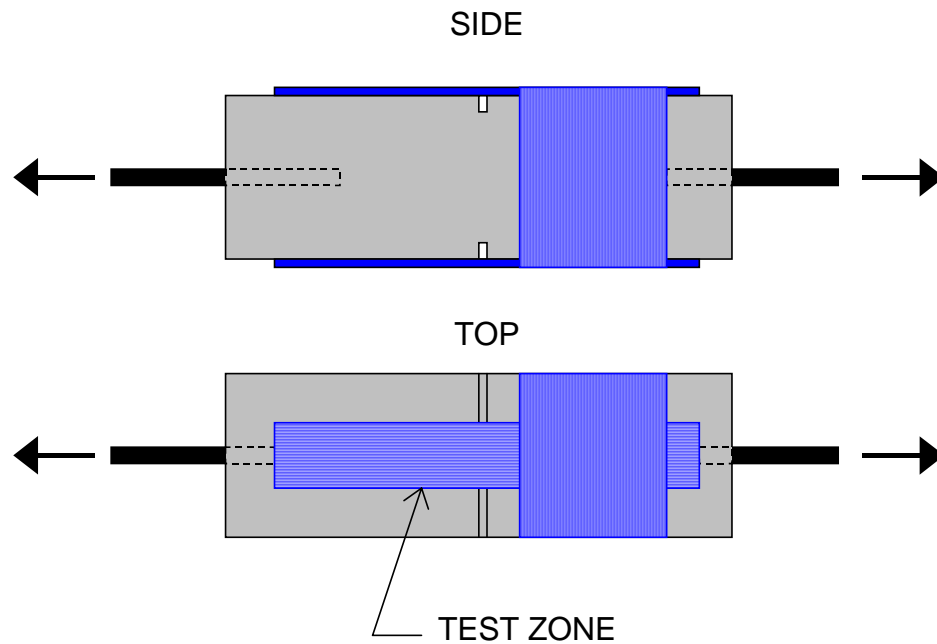


Figure 1.2: Shear Test Specimen

Another group of researchers studied the effect of the type of test method and quality of concrete on the bond of CFRP sheets (Horiguchi and Saeki, 1997). There were three different test methods investigated: the shear test, flexure test, and direct tensile test. The shear test is the same as shown in Figure 1.2. The flexure test is similar to the test conducted for this thesis and will be discussed in later chapters. The direct tensile can be seen in Figure 1.3. It consists of bonding a dolley to the CFRP sheet and cutting a groove through the sheet and concrete. Direct tension is then applied to the dolley until failure occurs. It was found that depending on the type of test method different values of average bond strength were determined. The tensile test produced the largest average bond strength, the bending test gave the second highest, and the shear test gave the lowest average bond strength.

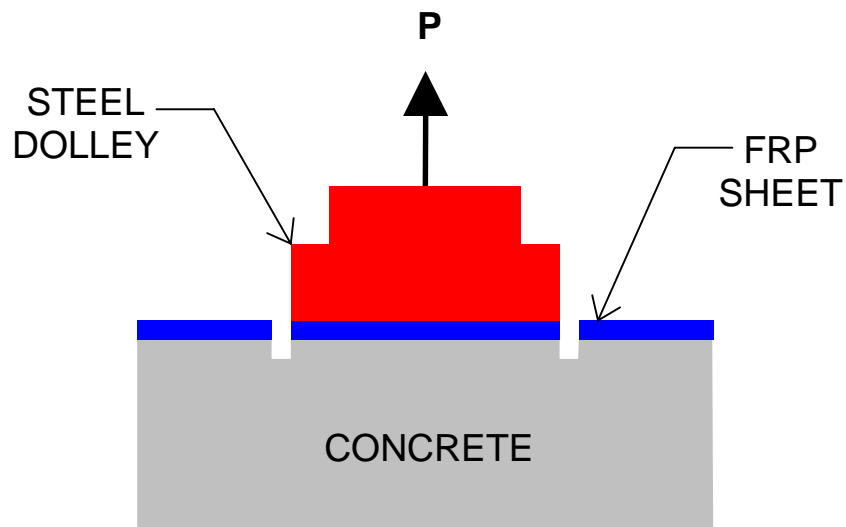


Figure 1.3: Direct Tensile Test Specimen

Another objective of this study was to determine the effect of concrete quality on the bond strength of the CFRP sheets. It was found that if the compressive strength of the concrete is low, less than 3600 psi (25 MPa), then the failure occurs in the concrete. For normal strength concrete, failure occurred by peeling of the CFRP sheet. When high strength concrete was used, the fiber ruptured for the bending test specimen. As a conclusion, bond strength should increase as concrete compressive strength increases.

The bonded length of the CFRP sheet had minimal effect on the ultimate load. The average bond strength decreased as the bonded length increased implying that an effective bond length exists. The effective bond length is a function of the reinforcing system properties.

Brosens and Van Gemert (1997) tested specimens similar to the one in Figure 1.2. Their findings showed that an increase in bonded length increases the fracture load. This is contrary to findings of other researchers. However, they did find that the influence of bonded length decreases at longer lengths. They concluded that for computational purposes the stress distributions in the FRP sheet may be taken as the same shape as seen in steel plates (see Figure 1.1).

They also developed the following design equation for the ultimate load, which is based on the stress distribution seen in Figure 1.4.

$$P_{\max} = \frac{w_f l_b f_{ct}}{2} \quad (1-1)$$

P_{\max} = the load at which failure occurs

w_f = width of the FRP sheet

l_b = bonded length of the sheet

f_{ct} = pull-off strength of concrete surface

The value of f_{ct} is found from pull-off tests of the existing concrete. It should be noted that a large safety factor should be used with this equation.

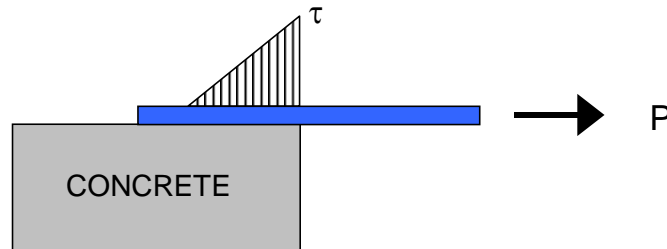


Figure 1.4: Stress Distribution in CFRP Sheet at Ultimate Load

Another study on the bond mechanism of CFRP sheets was performed using the same specimen as seen in Figure 1.2 (Maeda et al, 1997). The variables in this testing were the bonded length, number of layers of FRP, and type of FRP sheet. Results of the test showed that the stiffness of the fiber sheet increases the ultimate load. Also, for bonded lengths above approximately 4 inches (100 mm), the ultimate load does not change. This implies that an effective bond length exists. This paper also described the failure mechanism known as peeling as follows. The effective length of the CFRP sheet takes the entire load to a certain point at which localized peeling occurs causing the effective bond length to shift. This shifting of the effective bond length continues until the CFRP sheet has completely peeled from the concrete. This mechanism is described by Figure 1.5. The figure is an idealized plot of the strain vs. the location of that strain.

As can be seen, the curve is quadratic at low levels of loading. Then, the strain reaches a maximum level and the distribution becomes linear and the CFRP sheet peels over the effective length. This phenomenon continues until the sheet completely peels from the concrete surface.

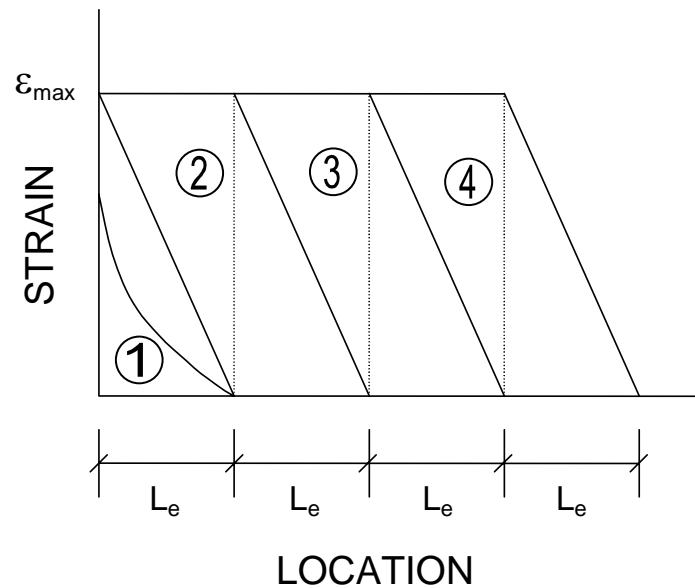


Figure 1.5: Strain vs. Location Schematic

Based on the present level of knowledge, it can be concluded that more work is needed to determine the strain distribution in the FRP sheet. Therefore, the work of this thesis will address the factors that affect the strain distribution. Based on the work by Horiguchi and Saeki (1997), the flexure specimen was chosen. It was chosen to avoid concrete cracking over the bonded length.

1.3. **OBJECTIVES**

The main objective of this thesis was to address the factors affecting the bond between CFRP sheets and concrete. The factors that were addressed were:

- bonded length
- compressive strength of concrete
- number of plies (stiffness) of FRP.

A series of test specimens were fabricated to address each of the factors. The results of these tests were analyzed in order to determine their effect on bond. Of particular interest was the strain distribution in the CFRP sheet.

The failure mode known as peeling was investigated and design recommendations were made to address this failure mode. Furthermore, attempts were made to address the issue of why CFRP rupture could not be achieved by these specimens.

The ultimate goal is to develop design guidelines for determining the required development length of the CFRP sheet. The foundation for achieving this goal was set in place, and recommendations were made for future work that will eventually lead to the achievement of this goal.

2. CONSTITUENT MATERIALS

Two primary materials were used in the construction of the test specimen. The beam was made from plain concrete, and CFRP sheets were used to reinforce the beam. There are many commercially available systems, and they all have great similarities. Each of these systems consists of carbon fiber tow sheets impregnated with epoxy resins. Also, primer and putty are used to prepare the concrete surface. The MBrace system (MBrace, 1998) was chosen for this project. Each of these materials along with the concrete beam will be discussed in this chapter.

2.1 CARBON FIBER TOW SHEET

FRP manufacturers make available systems with different properties. For example, MBrace has three different tow sheets that can be used with their system. They are the CF-130, CF-530, and EG-900. The properties of each of these sheets can be seen in Table 2.1. The properties of the sheet are the values obtained from the manufacturer. The type of sheet used in the testing was the MBrace CF-130. This tow sheet is a unidirectional fiber tow sheet. (MBrace, 1998).

Table 2.1: Properties of Fiber Tow Sheet

Fiber Tow Sheet	Ultimate Strength (ksi)	Design Strength (ksi)	Tensile Modulus (ksi)	Thickness (in)
High Tensile Carbon	620	550	33,000	0.0065
High Modulus Carbon	584	510	54,000	0.0065
E-Glass	251	220	10,500	0.014

Note: 1 ksi = 6.89 MPa; 1 in = 25.4 mm

2.2 EPOXY RESINS

There are three different resins used in the application of CFRP sheets to concrete, primer, putty, and saturant. The physical properties of these resins can be seen in Table 2.2 (MBrace, 1998). For this project, the method of mixing the resins was by mass. The properties of the resins in tension are shown in Table 2.3. The values shown are the theoretical values obtained from the manufacturer.

Table 2.2: Physical Properties of Epoxy Resins

Properties	Primer	Putty	Saturant
Color			
-Part A	Amber	Tan	Blue
-Part B	Clear	Charcoal	Clear
-Mixed	Amber	Tan	Blue
Mix Ratio by Volume PartA/Part B	3/1	3/1	3/1
Mix Ratio by Mass PartA/Part B	100/30	100/30	100/34
Working Time at 77°F (25°C)	20 minutes	40 minutes	45 minutes

Table 2.3: Tension: Neat Resin Properties ASTM D-638

	Primer	Putty	Saturant
Maximum Stress psi (MPa)	2500 (17.2)	2200 (15.2)	8000 (55.2)
Stress at Yield psi (MPa)	2100 (14.5)	1900 (13.1)	7800 (53.8)
Stress at Rupture psi (MPa)	2500 (17.2)	2100 (14.5)	7900 (54.5)
Strain at Max. Stress	0.400	0.060	0.030
Strain at Yield	0.040	0.020	0.025
Strain at Rupture	0.400	0.070	0.035
Elastic Modulus psi (MPa)	104,000 (715)	260,000 (1790)	440,000 (3035)
Poisson's Ratio	0.48	0.48	0.40

2.3 COMPOSITE SYSTEM

In this section, the properties of the system itself will be discussed. Figure 2.1 shows the order of application in which the materials are applied. As can be seen, the first layer applied is the primer. It can be applied either by a brush or roller. The next layer is the putty, which is applied using a trowel. A layer of saturant is then placed on top of the putty. Next, the tow sheet is placed on the saturant followed by another layer of saturant. Normally, a protective coating is then placed on top, however; this is not necessary in the lab.

The thickness of each layer of resin and fiber sheet was determined in previous work conducted at the University of Missouri-Rolla (Tumialan, 1998). The method for determining the thickness of each layer was by a Scanning Electron Microscope (SEM). The SEM is a microscope that uses electrons rather than light to form an image. By employing a SEM, more control in the amount of magnification can be obtained. Figure 2.2 shows the resulting thicknesses obtained from the SEM.

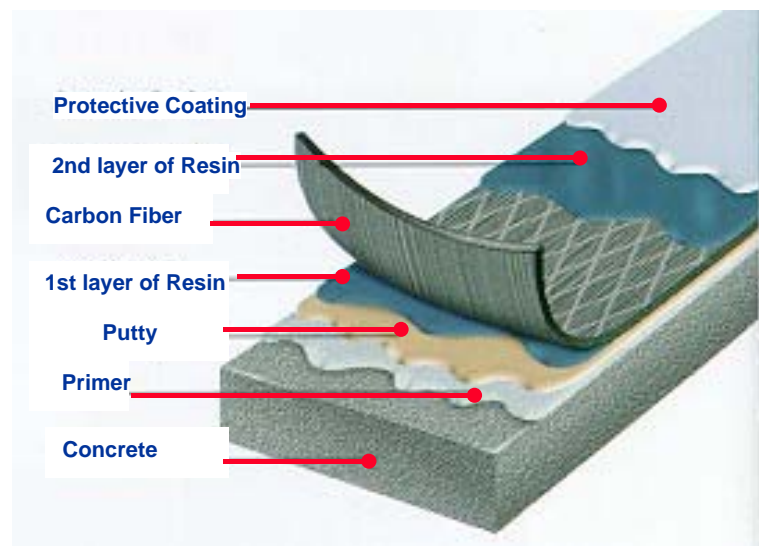


Figure 2.1: Application of FRP Sheets

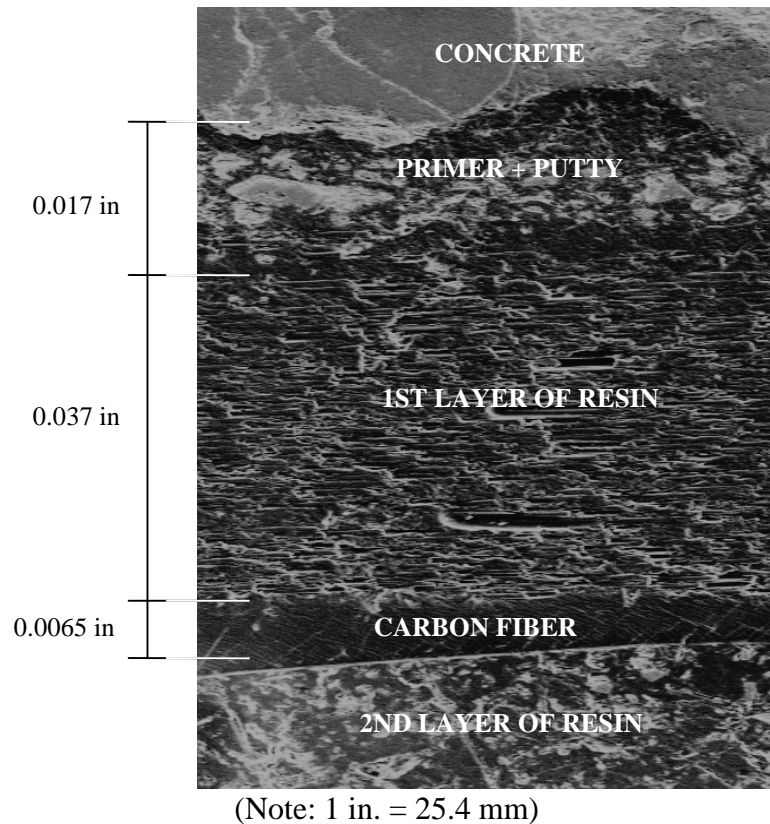


Figure 2.2: Thickness of each Layer of Composite System

2.4 CONCRETE BEAM

A local contractor prepared the concrete beams used in this study. A ready-mix concrete company supplied the concrete. The specified strengths of the concrete to be used were 3000 and 6000 psi (20.68 and 41.37 Mpa). Concrete compression cylinders were made according to ASTM C 31 each time a set of beams was poured in order to determine the compressive strength of the concrete. The cylinders were tested 28 days after the pour date according to ASTM C 39. The testing of the specimen was completed

no more than two days before or after the cylinders were tested. The actual strength of each beam is shown in Table 2.4.

After the beams had cured for 10-14 days, the surface on which the CFRP was to be applied was sandblasted. The beams were sandblasted to remove the top layer of mortar, just until the aggregate was visible. The approximate depth of sandblasting was 0.06 in. (1.5 mm). Next, the beams were saw cut at midspan in order to force the beam to crack at midspan.

Table 2.4: Compressive Strength of Concrete Beams

Series Number	Specimen	Compressive Strength (psi)		Series Number	Specimen	Compressive Strength (psi)	
		Target	Actual			Target	Actual
I	6-1-4-1	6000	6860	III	3-1-4-1	3000	3550
	6-1-4-2				3-1-4-2		
	6-1-8-1				3-1-8-1		
	6-1-8-2				3-1-8-2		
	6-1-12-1				3-1-12-1		
	6-1-12-2				3-1-12-2		
II	6-2-4-1	6000	5900	IV	6-1-8-R-1	6000	6240
	6-2-4-2				6-1-8-R-2		
	6-2-8-1				6-1-8-NR-1		
	6-2-8-2				6-1-8-NR-2		
	6-2-12-1			V	4-8		
	6-2-12-2			4-12			
VI	2-0-90	6000	5870	VI	4-0-90	6000	5870
VII	6-1-12-S						

Note: 1 psi = 6.89 kPa

3. METHODOLOGY

3.1. INTRODUCTION

This section will discuss the procedure of the experimental phase of the research. It will begin with a discussion on the design of the specimen. The preparation of the specimen for testing will then be discussed. This will be followed by a discussion of the actual testing of the specimens.

3.2. DESIGN OF SPECIMEN

As discussed in Section 1, there have been three types of specimens used for bond testing of FRP sheets: shear specimen, flexure specimen, and tensile specimen. The work by Horiguchi and Saeki (1997) was used to select the best specimen. It was concluded that the flexure specimen would be used because it is possible to prevent cracking in the bonded length with the flexure specimen. The reason that it is important to prevent cracking is because the stress distribution changes if a crack occurs in the bonded length. Figure 3.1 shows the effect cracking in the bonded length would have on the stress distribution. At the location of the crack, a reversal of stress occurs.

Before designing the specimen, an experimental plan had to be developed. This involved determining the variables to be studied. The variables of interest are bonded length, concrete strength, and number of plies of CFRP. The concrete strength was selected to be 3000 and 6000 psi (20.7 and 41.4 MPa). The number of plies was set at one and two. For the bonded length of CFRP it was decided that three different lengths would be used. The actual lengths were to be determined during the design process. It was also determined that there would be two repetitions for each case.

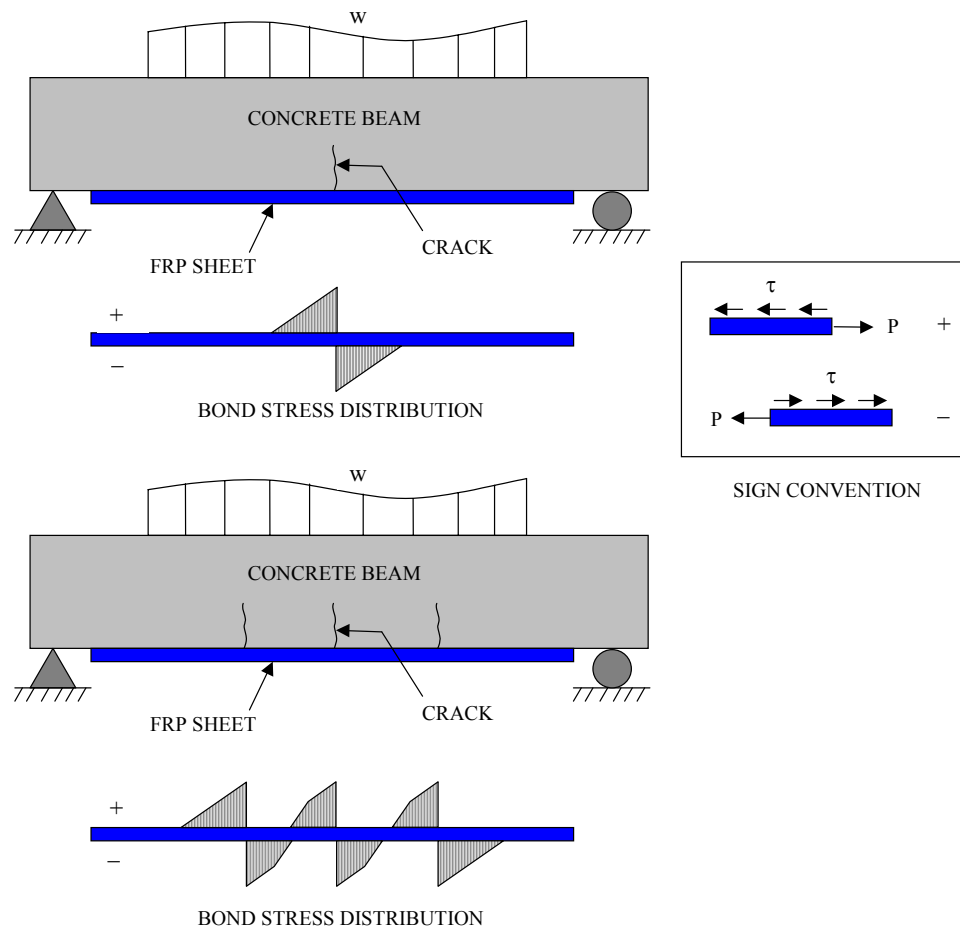


Figure 3.1: Effect of Cracking on Stress Distribution

The length of the beam was selected to be 48 inches (1219 mm) with the distance between supports of 42 in (1067 mm). Also, a hinge was to be placed at the top of the beam at midspan along with a saw cut (see Figure 3.2). It should also be noted that the FRP sheet would be unbonded two inches on both sides of the center. The purpose of the hinge and saw cut was to aid in the analysis of the specimen. During the loading of the specimen, the beam would crack up to the hinge. This would cause the compressive force in the beam to be positioned at the center of the hinge and therefore the internal

moment arm would remain constant throughout the test. The purpose of the unbonded area was that if any cracking occurred, it would be in the area close to the center of the beam. Also, since this area was unbonded, a strain gauge could be used to measure the strain in this area. From this strain, the load applied to the FRP sheet could then be calculated by the following equation.

$$T = \varepsilon_f t_f w_f E_f \quad (3-1)$$

T = tensile load applied to the sheet

ε_f = strain in the CFRP sheet

t_f = thickness of the fibers

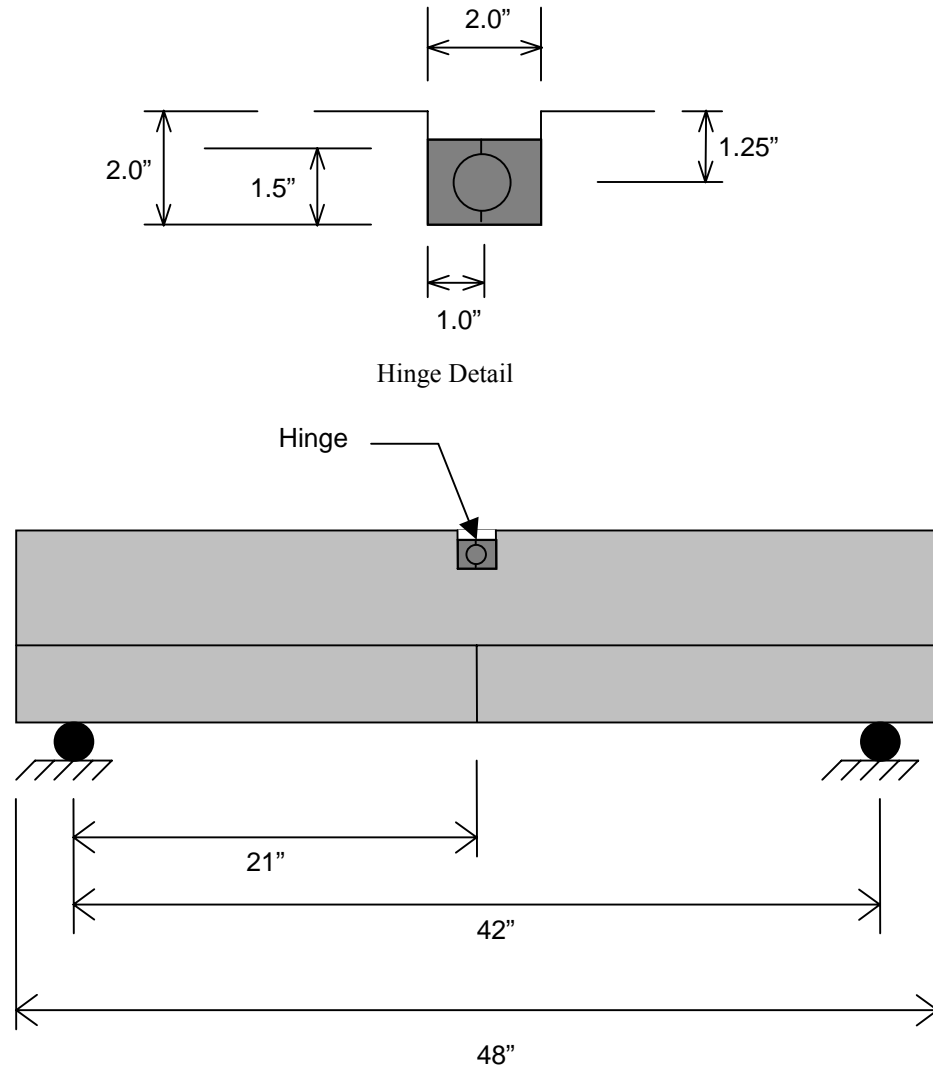
w_f = width of the CFRP sheet

E_f = tensile modulus of elasticity of the fibers

In order to achieve the desired results, the following constraints were placed on the design of the beam.

1. The specimen would not crack due to flexural loads except at mid span.
2. The specimen would not crack due to shear loads.
3. The specimen would weigh approximately 300 lbs. (1.33 kN) or less.
4. Width of sheet and bonded length would be such that CFRP breakage should be the cause of failure in at least one specimen.

In order to meet these requirements, equations were developed for the applied load that would cause each of the conditions to occur.



(Note: 1 inch = 25.4 mm)

Figure 3.2: Location of Hinge and Detail of Hinge

Flexural cracking is assumed to occur when the bending stress is equal to the modulus of rupture for concrete. ACI 318 defines the modulus of rupture as seen in Equation (3-2).

$$f_r = 7.5\sqrt{f'_c} \quad (3-2)$$

f_r = modulus of rupture (psi)

f'_c = compressive strength of concrete (psi)

$$f_r = 0.623\sqrt{f'_c} \quad (3-2M)$$

f_r = modulus of rupture (MPa)

f'_c = compressive strength of concrete (MPa)

The bending stress is defined by Equation (3-3).

$$\sigma_b = \frac{My}{I} \quad (3-3)$$

σ_b = bending stress

M = applied moment

I = moment of inertia of the cross-section

y = distance from tension face of beam to centroid

The equation for the maximum moment can be seen in Equation (3-4).

$$M_{\max} = \frac{P}{4}(L - x) \quad (3-4)$$

M_{\max} = maximum moment

P = applied load

L = clear span of the specimen

x = distance between applied loads

Setting (3-2) equal to (3-3), then substituting (3-4) into (3-3) and solving for P gives

Equation (3-5).

$$P_{cr} = \left(\frac{7.5\sqrt{f'_c}I}{y} \right) \left(\frac{4}{L - x} \right) \quad (3-5)$$

$$P_{cr} = \left(\frac{0.623\sqrt{f'_c I}}{y} \right) \left(\frac{4}{L-x} \right) \quad (3-5M)$$

P_{cr} = applied load to cause flexural cracking

ACI states that shear failure will occur when the shear force at any section is equal to Equation (3-6).

$$V = 2\sqrt{f'_c} b_w h \quad (3-6)$$

$$V = 0.166\sqrt{f'_c} b_w h \quad (3-6M)$$

V = shear force to cause shear failure

b_w = width of the beam web

h = height of the beam

The maximum shear force for this beam will be equal to half the applied load. Therefore, setting half the applied load equal to V and solving for P gives Equation (3-7).

$$P_v = 4\sqrt{f'_c} b_w h \quad (3-7)$$

$$P_v = 0.332\sqrt{f'_c} b_w h \quad (3-7M)$$

P_v = applied load that will cause shear failure

To determine the length at which the CFRP would break an equation for both peeling failure and CFRP rupture had to be developed. The load that will cause CFRP rupture can be determined using a Mechanics of Materials approach. Since the CFRP sheet will be loaded in direct tension, Equation (3-8) can be used.

$$\sigma_t = \frac{T}{A} \quad (3-8)$$

σ_t = tensile stress

T = tensile force

A = cross-sectional area

Cutting a free-body diagram at the center of the beam and summing moments at the hinge will allow the applied load to be related to the tensile load on the CFRP sheet (see Figure 3.3).

$$\Sigma M = 0 = \frac{P}{2} \left(\frac{x}{2} \right) - \frac{P}{2} \left(\frac{L}{2} \right) + T(h - 1.25) \quad (3-9)$$

$$T = \frac{P}{(h - 1.25)} \left(\frac{L - x}{4} \right) \quad (3-10)$$

Substituting T into Equation (3-8) and solving for P gives,

$$P = \frac{4 \sigma_t A (h - 1.25)}{L - x} \quad (3-11)$$

The ultimate stress of the CFRP sheet can be denoted as f_{fu} and the cross-sectional area, A, is equal to the thickness multiplied by the width. This gives Equation (3-12), which is the load that will cause CFRP rupture.

$$P_f = \frac{4 w_f t_f f_{fu} (h - 1.25)}{(L - x)} \quad (3-12)$$

P_f = applied force that will cause fiber rupture

w_f = width of the FRP sheet

t_f = thickness of the FRP sheet

f_{fu} = ultimate stress of the FRP sheet

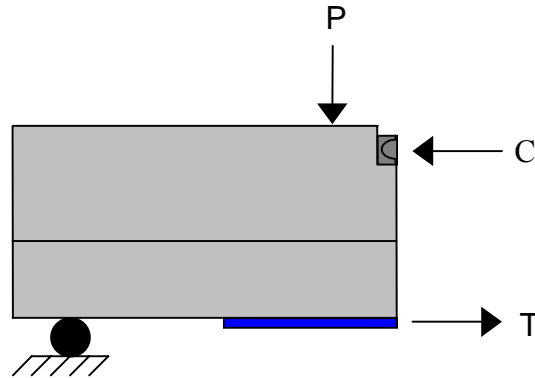


Figure 3.3: Free Body Diagram of Beam at Midspan

The equation for CFRP peeling can be derived similarly except the stress will be the peeling stress. According to Van Gemert (1996), the peeling stress is equivalent to a triangular block. The peak stress of the triangular block is assumed to be the modulus of rupture as defined by ACI-318. This leads to Equation (3-13).

$$T = \frac{7.5 \sqrt{f'_c} w_f l_b}{2} \quad (3-13)$$

$$T = \frac{0.623 \sqrt{f'_c} w_f l_b}{2} \quad (3-13M)$$

l_b = bonded length of the FRP sheet

Substituting this value into (3-10) and solving for P gives Equation (3-14).

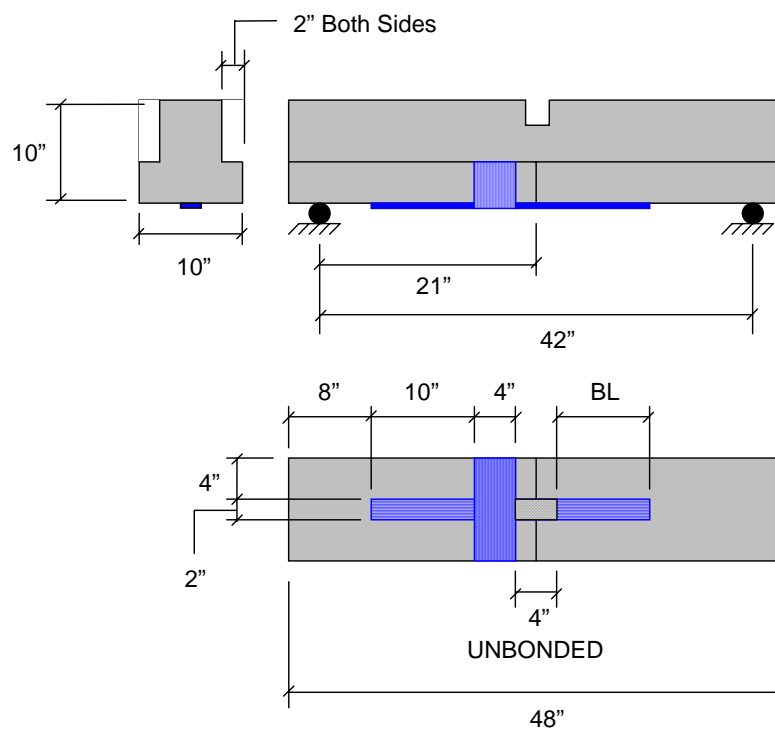
$$P_p = 7.5 \sqrt{f'_c} w_f l_b (h-1.25) \left(\frac{2}{L-x} \right) \quad (3-14)$$

$$P_p = 0.623 \sqrt{f'_c} w_f l_b (h-1.25) \left(\frac{2}{L-x} \right) \quad (3-14M)$$

P_p = applied force to cause the FRP sheet to peel

Equations (3-5), (3-7), (3-12), and (3-14) were used to determine the specimen size and the lengths at which the CFRP would be bonded. To begin, the width of the CFRP sheet was set at 2 inches (51 mm). A trial size for the beam cross-section was then selected, and it was checked to see if it met the previously stated requirements. This process was iterated until the requirements were met. The initial problem in selecting the specimen size was that a rectangular section would not meet the cracking and weight requirements. Therefore, a cross-section in the shape of an inverted T-beam was chosen. This increased the area of concrete that was in tension. Also, the longest bonded length of CFRP was chosen to be 12 inches (305 mm). The other two lengths chosen were 4 and 8 inches (102 and 203 mm). The specimen was expected to fulfill all of the design requirements. The actual weight of the beam is 296 lbs (1.32 kN). No flexural cracking would occur and it would not fail in shear. Also, a beam of 6000 psi (41.37 MPa) concrete with a 12-inch (305 mm) bonded length was expected to fail by CFRP rupture. Figure 3.4 shows the dimensions of the beam that was selected. A transverse strip of CFRP was placed across the sheet on the side opposite of the test region. This was used to ensure that failure would occur in the test region. At this point, it was decided that two beams would be made and tested to verify that the specimen would perform as expected. After the two preliminary beams were tested, the remaining specimens were tested.

Table 3.1 shows all specimens that were tested and the code that will be used to identify them. The definition of the code is as follows: f_c' (ksi) – number of plies – bonded length – specimen number. The specimen number is used to distinguish between two specimens that are identical. For example, 6-1-4-1 would be a specimen with a compressive strength of 6 ksi (41.37 MPa), one ply of CFRP, a 4-inch (102-mm) bonded length, and it would be the first of two identical specimens. 6-1-4-2 would be identical to 6-1-4-1. It should be noted that from a statistics standpoint, more than one repetition would normally be tested. The intention for this study was to test two of each type of specimen, and if the results were not in agreement another specimen would be tested. However, since the results were very similar for each specimen, there was no need to have more repetitions.



(Note: 1 inch = 25.4 mm)

Figure 3.4: Layout of Specimen

Table 3.1: Description of Specimens

Specimen Code	Compressive Strength (psi)	Number of Plies	Bond Length (inches)
3-1-4-1 3-1-4-2	3000	1	4
3-1-8-1 3-1-8-2			8
3-1-12-1 3-1-12-2			12
6-1-4-1 6-1-4-2			4
6-1-8-1 6-1-8-2			8
6-1-12-1 6-1-12-2			12
6-2-4-1 6-2-4-2	6000	2	4
6-2-8-1 6-2-8-2			8
6-2-12-1 6-2-12-2			12

(Note: 1 inch = 25.4 mm; 1 psi = 6.89 kPa)

3.3. SPECIMEN PREPARATION

The preparation of the specimens for testing included surface preparation, application of CFRP sheets, and application of strain gauges. Surface preparation and application of CFRP sheets was performed in accordance with recommendations made by the manufacturer.

3.3.1. Surface Preparation. After the beams had cured properly, the surface where the CFRP sheets were to be applied was sandblasted. This was done in order to remove the laitance that forms at the finished surface of concrete. The machine used for sandblasting was had a 90 cfm (2548 liter/min) air requirement. It was operated at 100-psi (689 kPa) air pressure with 250-lb (1112 N) sand pot. This is a smaller machine than

is normally used in field application. The typical size has a 250 cfm (7079 liters/min) air requirement with a 300-lb (1334 N) sand pot. However, the air pressure at which they operate is also 100 psi (689 kPa). The only difference in the two machines is that the machines used in the field are capable of covering more area of concrete in a smaller amount of time. The beam was sandblasted approximately 0.06 in (1.5 mm), which was just until the aggregate began to be exposed. Figure 3.5 shows a typical concrete surface after sandblasting.

The beam was also saw cut at midspan to create a weakened plane at which the beam would crack. The nominal depth of this cut was 2 inches (51 mm).



Figure 3.5: Sandblasted Concrete Surface

3.3.2. Application of CFRP Sheets. There are three steps to applying CFRP sheets. First, primer is applied to the concrete surface. Next, putty is used to level the surface. Then, a saturant layer, followed by the carbon sheet and another layer of saturant is applied.

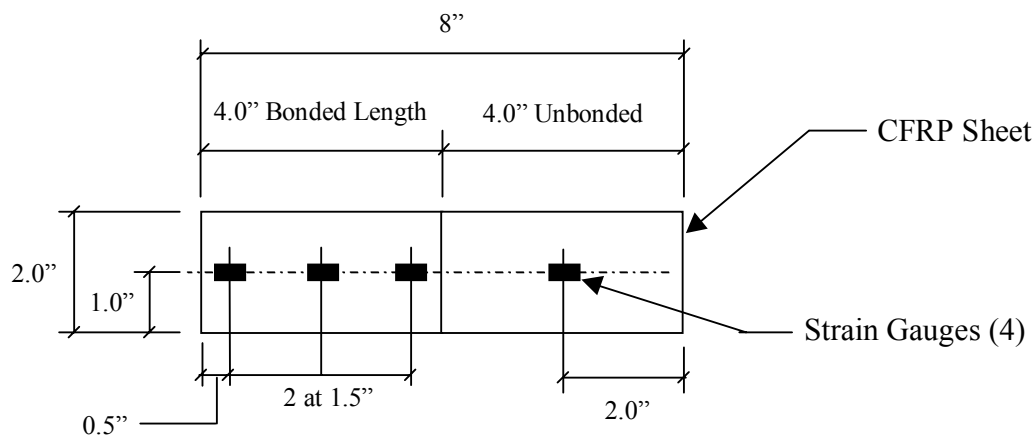
The primer is applied to the surface of the concrete beam in the area where the CFRP sheet is to be applied. The reason the primer is used is to fill the microscopic holes in the concrete. This can be applied either by a roller or brush.

Next, the putty is applied on top of the primer using a trowel. It is not necessary to allow the primer to dry before applying the putty. The putty is used to fill larger holes and level the surface of the concrete. For the beams used in this research, the surface was very smooth and level. Therefore, only a very thin layer of putty was used. The putty was then allowed to dry until it was tack free.

After the putty had dried for a sufficient time, a layer of saturant was rolled on top of the putty. At the same time, saturant was rolled on the carbon sheets to allow it to soak into the sheets. This is an optional step in the application, but it helps ensure that the sheets are properly saturated. After about 20 minutes, the carbon sheets were placed on the saturant layer. Plastic rollers were then used to remove any air that was trapped under the sheet, and further impregnate the sheets with saturant. After 30 minutes, a top layer of saturant was applied to the sheet and plastic rollers were again used to impregnate the sheets. If multiple plies were to be applied, the steps beginning with the application of the first layer saturant were repeated. A period of 30 minutes was allowed to pass between the completion of one layer and the beginning of the next layer.

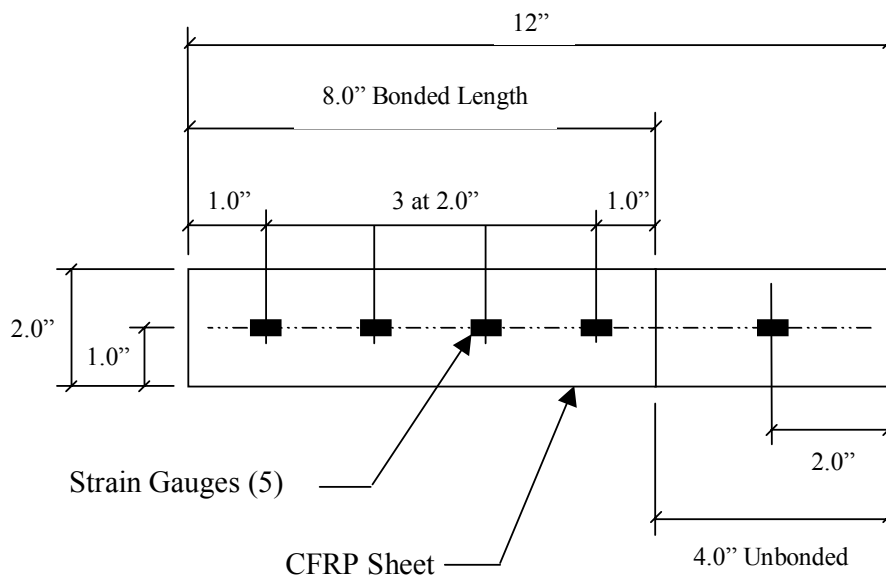
After the CFRP sheets were allowed to cure for three days, strain gauges were applied. Figure 3.6, Figure 3.7, and Figure 3.8 show the location of strain gauges for each length of CFRP sheet. As can be seen, one strain gauge was placed at the center of the unbonded region for each bonded length. For the 4-inch (102-mm) bonded length, there were three strain gauges placed along the centerline of the CFRP sheet in the

bonded region. For the 8-inch (203-mm) bonded length, there were four strain gauges in the bonded region, and for the 12-inch (305-mm) bonded length, there were six strain gauges in the bonded region.



(Note: 1 inch = 25.4 mm)

Figure 3.6: Position of Strain Gauges for the 4-inch (102-mm) Bonded Length



(Note: 1 inch = 25.4 mm)

Figure 3.7: Position of Strain Gauges for the 8-inch (203-mm) Bonded Length

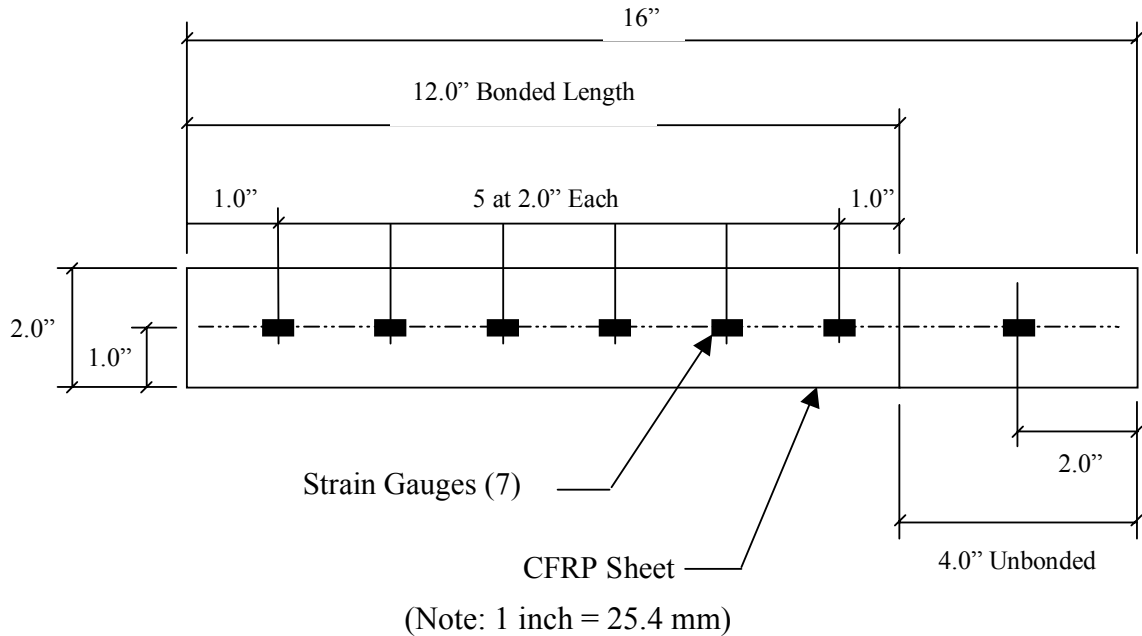


Figure 3.8: Position of Strain Gauges for the 12-inch (305-mm) Bonded Length

3.4. TEST PROCEDURE

The CFRP sheets were allowed to cure for at least 7 days prior to the testing of the beams. The testing of the beams was performed on a Tinius-Olsen testing machine. A LVDT was used to measure the deflection at the center of the beam. The load, deflection and strain were all recorded at one-second intervals by a Labtech data acquisition system. A picture of the test setup can be seen in Figure 3.9.

The testing was performed by first loading the beam with 1500 lbs (6.67 kN) and then unloading to 500 lbs (2.22 kN). This was to make sure that all data was being recorded properly. Next, the beam was loaded until a crack formed at midspan of the beam, and then unloaded to 500 lbs (2.22 kN). Load was then applied until failure resulted.



Figure 3.9: Picture of Test Setup

3.5. VERIFICATION OF RESULTS

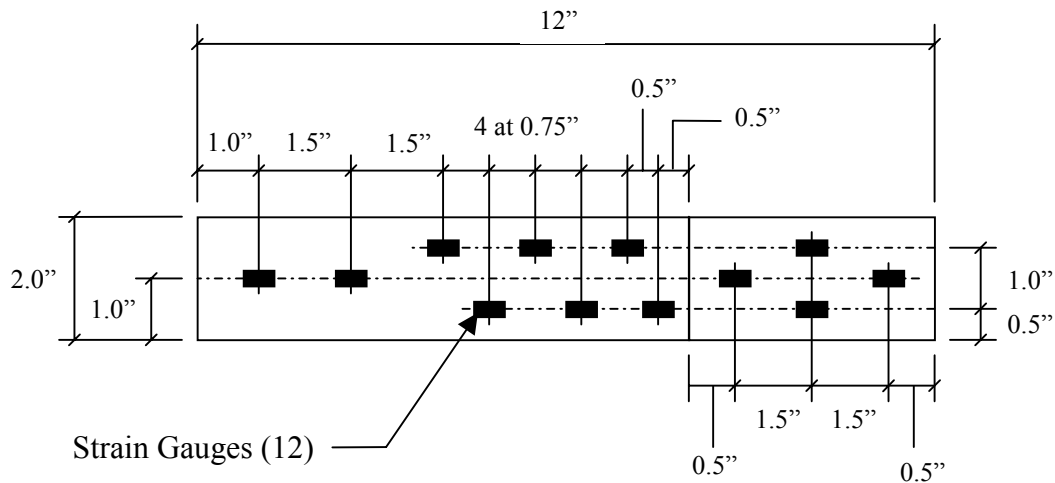
After the testing of the three series of specimens was completed, it was decided that more testing must be performed to verify some of the results. A problem was observed in some of the beams. The strain measured in the unbonded region at midspan did not agree with the theoretical strain that was expected. From equilibrium and mechanics of materials, the strain can easily be related to the load applied to the beam. Strain is related to the tensile force in the sheet as seen in equation (3-15).

$$\varepsilon_f = \frac{T}{t_f w_f E_f} \quad (3-15)$$

Using equation (3-10) in (3-15), strain is related to the applied load P.

$$\varepsilon_f = \frac{P}{t_f w_f E_f} \left(\frac{L-x}{4(h-1.25)} \right) \quad (3-16)$$

It was not certain as to the cause of the discrepancy between the theoretical and measured strain. It was proposed that the strain gauge in the unbonded area was bent due to the deflection of the specimen, therefore causing the gauge to read a higher strain than what actually existed. In order to determine the actual strain, specimens were tested with more strain gauges. To attempt to correct the problem of the bending of the gauge, the corners of the saw cut was rounded on some of the beams. Figure 3.10 shows the location of the strain gauges for these specimens.



(Note: 1 inch = 25.4 mm)

Figure 3.10: Location of Strain Gauges for Verification Testing

Another question to be addressed was whether the CFRP sheet was being damaged or not when the beam was undergoing first cracking. To correct this problem, the cracking load was decreased by increasing the size of the saw cut at the center of the

beam. It was assumed that if the load at which the cracking occurred was lower than the ultimate load, then the cracking was not causing any damage to the CFRP sheet. Table 3.2 shows the name and description of the verification specimens.

Table 3.2: Description of Verification Specimen

Series	Specimen	Compressive Strength (psi)	Bonded Length (in)	Saw Cut Rounded
IV	6-1-8-R-1	6240	8	Yes
	6-1-8-R-2			
	6-1-8-NR-1			No
	6-1-8-NR-2			

(Note: 1 inch = 25.4 mm; 1 psi = 6.89 kPa)

3.6. MISCELLANEOUS SPECIMENS

After the testing of the verification specimens was complete, a few more specimens were tested. Two specimens were made with 4-inch (102-mm) wide CFRP sheets instead of 2-inch (51-mm) sheets. The purpose of these two specimens was to determine whether the width of the sheet had an effect on the strain distribution in the sheet. The bonded lengths of the specimens were 8 and 12 inches (203 and 305 mm), while the strength of the concrete was 6000 psi (41.37 MPa). The specimens were instrumented similar to the specimens from the first three series.

Two other specimens were tested to determine the contribution of applying CFRP sheets at 0° and 90°. This type of application is often used for shear reinforcement. The concrete beam is the same as the previous one. One of the specimens had a 2-inch (51-mm) wide sheet, while the other specimen had a 4-inch (102-mm) wide sheet. The bonded length of both specimens was 8 inches (203 mm). The only difference in this test

is the arrangement of the CFRP sheets. First, a longitudinal strip with a width of either 2 or 4 inches (51 or 102 mm) was applied at the center of the beam (see Figure 3.11 Label #1). This is the same as the previous specimens. Next, a longitudinal strip was placed on each side of the first strip (see Figure 3.11 Label #2). Then, a transverse strip was placed over all three strips (see Figure 3.11 Label #3). Finally, another transverse strip is placed on the opposite end to prevent the sheet from peeling. The complete specimen with the 2-inch (51-mm) wide sheet is shown in Figure 3.12 while the specimen with the 4-inch (102-mm) wide sheet is shown in Figure 3.13. The specimens were instrumented the same as the specimens of the base series with the 8-inch (203-mm) bonded length. The test procedure was the same as described for the first three series.

After testing of all the specimens, a specimen was tested in which the surface preparation was changed. The surface was roughened by adding notches in the surface using a hammer and chisel (see Figure 3.14). The purpose of this test was to determine if surface preparation affected the average bond strength. No strain gauges were used in this testing because the main interest was to see if the ultimate load was increased by the different surface preparation. The details of the specimens can be seen in Table 3.3.

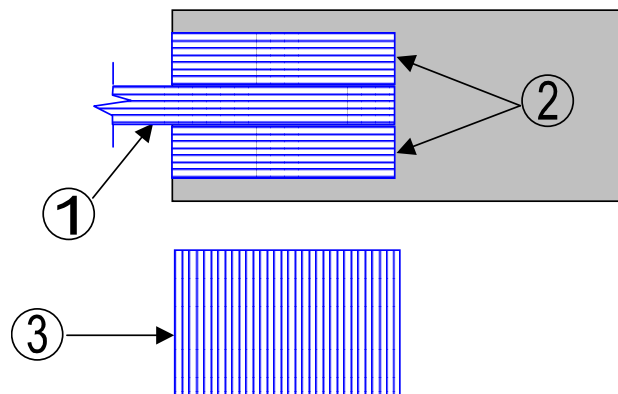


Figure 3.11: Procedure for Applying Sheets at 0° and 90°

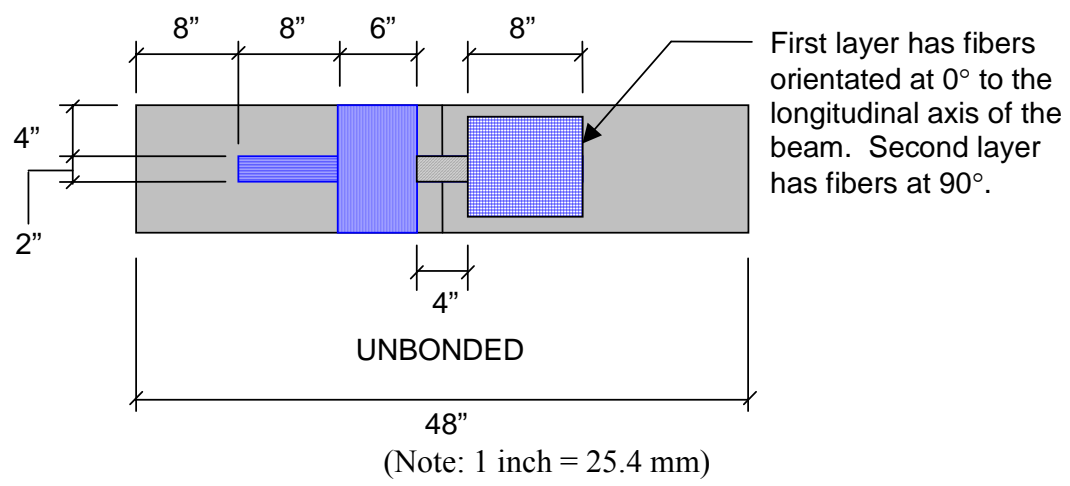


Figure 3.12: Specimen with 2-inch (51-mm) Wide Sheet and Transverse Sheet

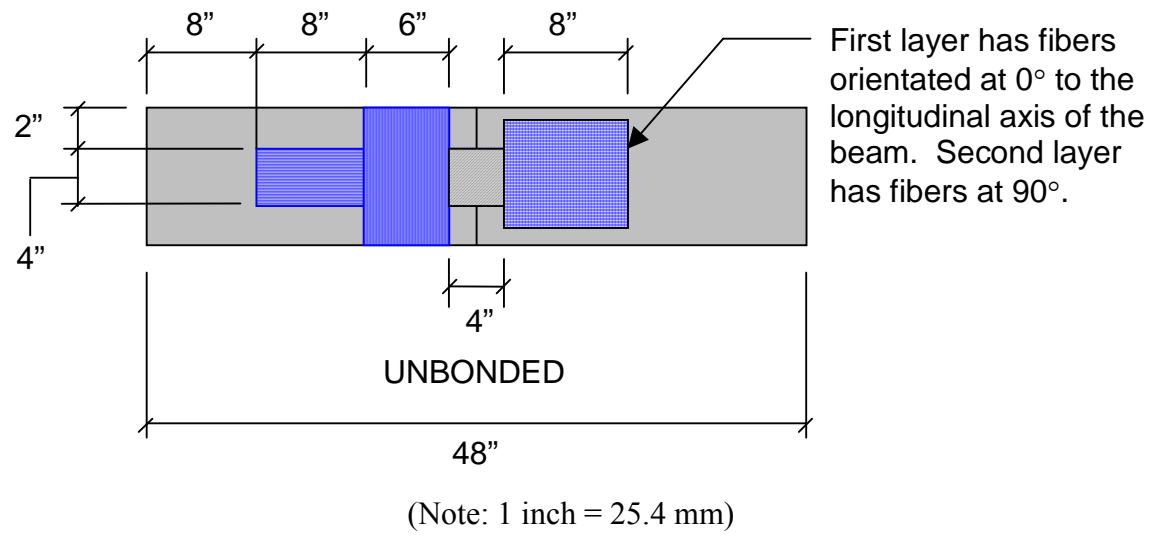


Figure 3.13: Specimen with 4-inch (102-mm) Wide Sheet and Transverse Sheet



Figure 3.14: Surface of Specimen 6-1-12-S

Table 3.3: Details of Miscellaneous Specimens

Series	Specimen	Compressive Strength of Concrete (psi)	Width of CFRP Sheet (in)	Bonded Length (in)	0° and 90°	Surface Anchor
V	4-8	6240	4	8	NO	NO
	4-12			12		
VI	2-0-90	5870	2	8	YES	
	4-0-90		4			
VII	6-1-12-S	5870	2	12	NO	YES

(Note: 1 inch = 25.4 mm; 1 psi = 6.89 kPa)

3.7. SUMMARY OF TEST SPECIMENS

A complete listing of all the specimens that were tested can be seen in Table 3.4. The code used to identify the specimen is seen in the first column. The target compressive strength is the next column followed by the number of plies. The bonded

length and width of sheet make up the next two columns. The next column is for the specimens that were tested to determine the contribution of adding a sheet with fibers that are perpendicular to the original sheet. The last two columns are special features that were tested for verification purposes.

Table 3.4: Summary of all Test Specimens

Specimen Code	f'_c (psi)	Plies	Bond Length (in)	Width of Sheet (in)	0°-90°	Rounded Corners	Increased Saw Cut				
3-1-4-1	3550	1	4	2	NO	NO	NO				
3-1-4-2			8								
3-1-8-1			12								
3-1-8-2			4								
3-1-12-1			8								
3-1-12-2			12								
6-1-4-1	6860	1	4								
6-1-4-2			8								
6-1-8-1			12								
6-1-8-2			4								
6-1-12-1			8								
6-1-12-2			12								
6-2-4-1	5900	2	4	2	NO	NO	NO				
6-2-4-2			8								
6-2-8-1			12								
6-2-8-2			4								
6-2-12-1			8								
6-2-12-2			12								
6-1-8-R-1	6240	1	8					2	NO	NO	YES
6-1-8-R-2											
6-1-8-NR-1											
6-1-8-NR-2			4								
4-8											
4-12											
2-0-90	5870	2	8	2	YES	NO					
4-0-90			4								
6-1-12-S		1	12	2	NO						

(Note: 1 inch = 25.4 mm; 1 psi = 6.89 kPa)

4. EXPERIMENTAL RESULTS

4.1. INTRODUCTION

The following sections will discuss the results obtained from the experimental testing. Before beginning the full testing phase, two preliminary tests were performed to ensure that the specimen would perform properly. It was found that the specimen would perform as required, and therefore it was determined that the specimen would be used for the full experimental phase. The testing was performed in three separate series followed by a series of tests aimed at verifying results. Each series consisted of six specimens with each specimen of a series having the same concrete strength and number of plies of CFRP. The variable in each series is the bonded length of the sheet.

4.2. SERIES I

The first series of testing was for the specimens with 6000-psi (41.37 kN) concrete and one-ply of CFRP sheet. Six specimens were prepared and designated as 6-1-4-1, 6-1-4-2, 6-1-8-1, 6-1-8-2, 6-1-12-1, and 6-1-12-2. This series of specimens was designated as Series I and was the reference point for the other two series of specimens. The details of these specimens can be seen in Table 4.1. This table shows the bonded length and actual compressive strength of each specimen. The load at which the beam first cracked at the notched section is shown in the next column. The next column shows the ultimate load, which is the highest load achieved after first cracking. The last column, average bond strength, is calculated from the following equation.

$$\tau_b = \frac{P_{\max}}{l_b w_f} \quad (4-1)$$

τ_b = average bond strength

P_{\max} = maximum load

l_b = bonded length

w_f = width of CFRP sheet

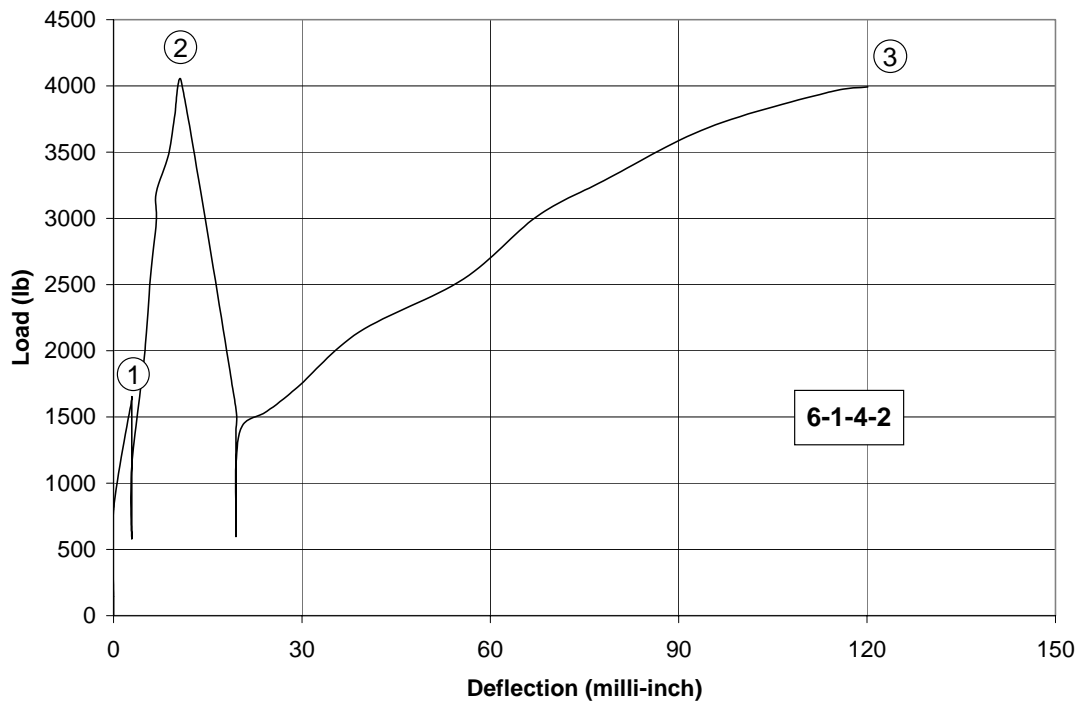
After the testing of the specimens, the data was compiled and displayed graphically in different manners. First, load vs. deflection graphs were plotted. These can be used to see the behavior of the beam during the test. From Figure 4.1, it can be seen that the beam was loaded in three steps. It was first loaded to 1500 lbs. (6.67 kN) to check to make sure the instrumentation was working. It was then unloaded to 500 lbs. (2.22 kN) and then reloaded until the beam cracked. The load was then decreased to 500 lbs. (2.22 kN) and then loaded until failure occurred.

There were two different behaviors noticed at failure for Series I. When the bond length was 4 in. (102 mm), the failure was sudden as seen in Figure 4.1. However, for the specimens with a bond length of 8 or 12 inches (203 or 305 mm), the failure was prolonged as the sheet progressively peeled toward the end of the sheet. As the load increased, the sheet began peeling from the center of the beam. This caused the strain in the sheet to shift to the portion of the sheet that remained bonded. This caused the deflection to increase even though the load decreased as seen in Figure 4.2. The load was never able to increase above the point at which peeling first occurred.

Table 4.1. Details of Specimens for Series I

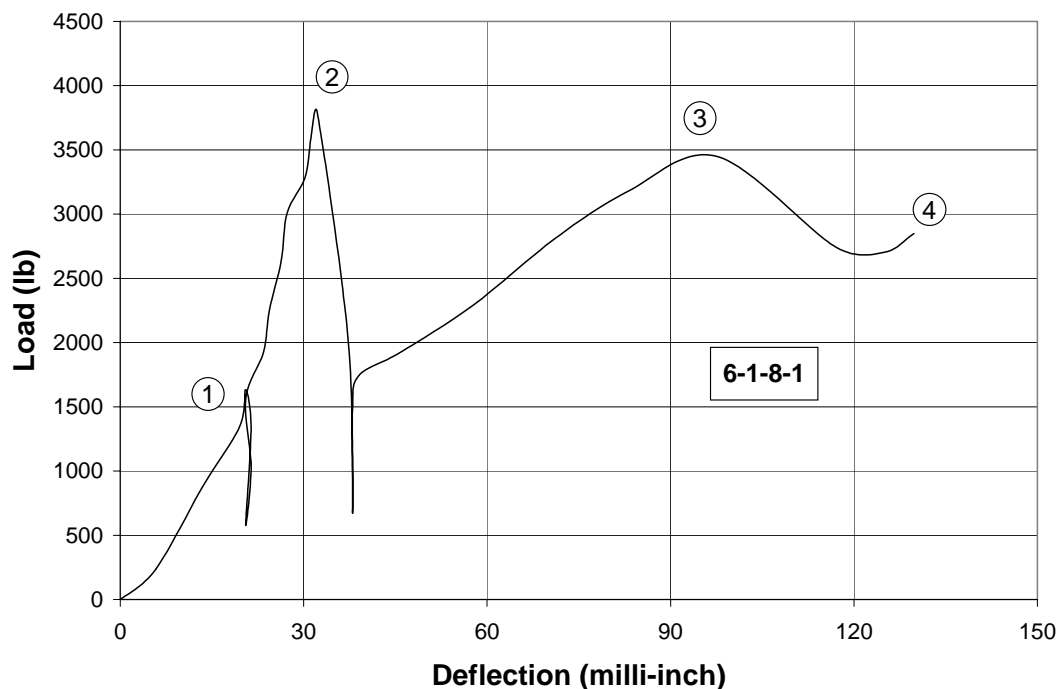
Specimen	Bond Length (in)	Compressive Strength of Concrete (psi)	Cracking Load (lb)	Ultimate Load (lb)	Average Bond Strength (psi)
6-1-4-1	4	6860	3140	3720	465
6-1-4-2			4100	3990	499
6-1-8-1	8		3920	3560	223
6-1-8-2			3230	3190	200
6-1-12-1	12		4250	3830	160
6-1-12-2			3720	3390	142

Note: 1 in = 25.4 mm; 1 psi = 6.89 kPa; 1 lb = 4.45 N



Note: 1 lb = 4.45 N; 1 in = 25.4 mm

Figure 4.1: Load vs. Deflection for Specimen with 4-inch (102-mm) Bonded Length

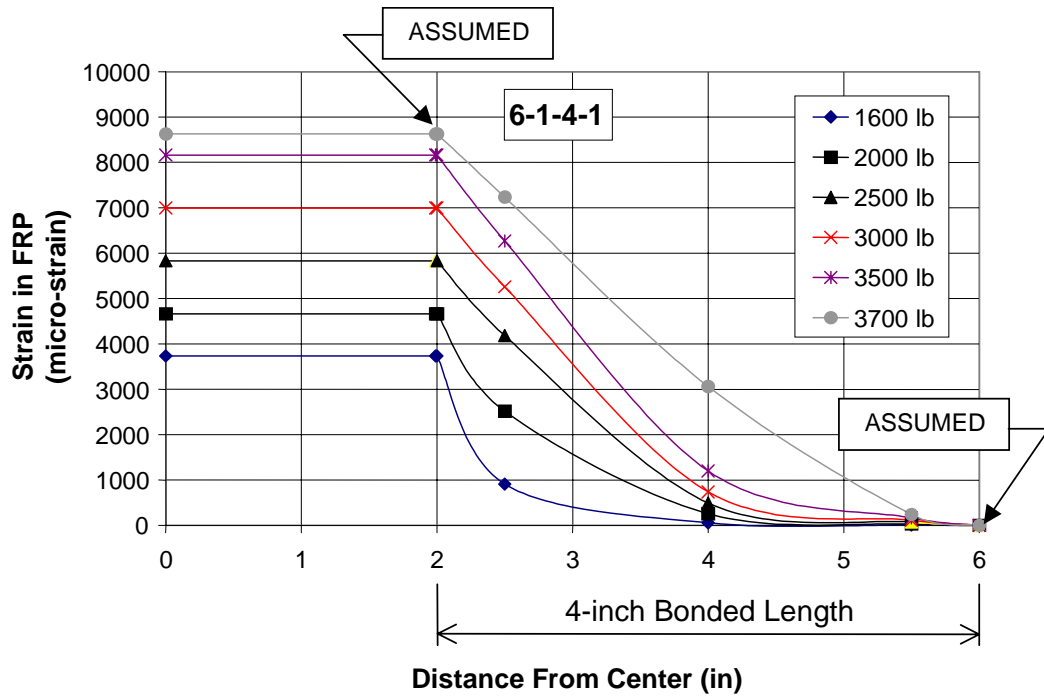


Note: 1 lb = 4.45 N; 1 in = 25.4 mm

Figure 4.2. Load vs. Deflection for Specimen with 8 or 12-inch (203 or 305 mm) Bonded Length

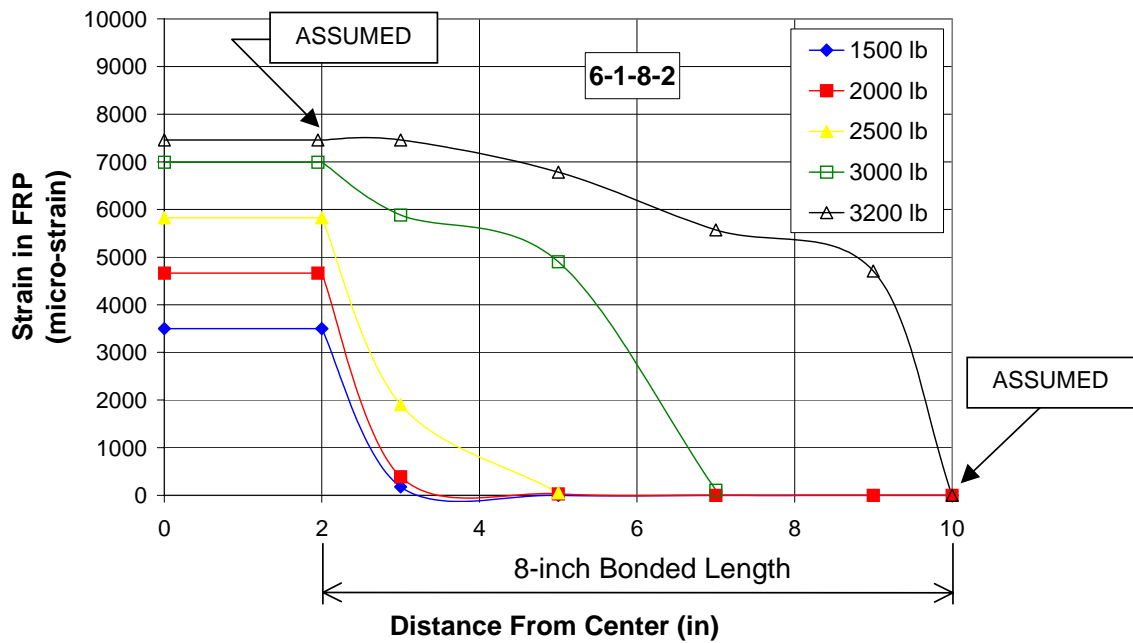
The data from the strain gauges was used to create strain vs. location graphs. This is a graph of the value of the strain vs. the distance the strain gauge is from the center of the beam. A typical graph for the 4-inch (102-mm) bonded length can be seen in Figure 4.3. This graph consists of several curves. Each curve is a plot of the strain in the FRP sheet at a particular level of load. The portion of the curve that is a horizontal line is the strain in the unbonded region. This distribution is actually assumed since there is only one strain gauge in the unbonded area. Also, the point where the strain is shown as zero at the end of the sheet is assumed. This graph can be compared with Figure 4.4 and

Figure 4.5. It can be seen that at early stages of loading, the curves are almost identical. They both have a quadratic shape, and the strain gauges located 5 inches (127 mm) or more from the center do not read strain. Also, as the load increases, the curves change from quadratic to linear (see Figure 4.6). It is assumed that peeling began to occur immediately after the point when the curve becomes linear. Once peeling begins, the behavior of the two cases is different. The specimens with the 4-inch (102-mm) bonded length seem to fail suddenly as soon as the peeling process begins. For the 8 and 12-inch (203 and 305-mm) bonded lengths, the longer bonded length causes the peeling failure to occur in stages. For example, refer to Figure 4.5. The curves labeled 1500 lb, 2000 lb and 2500 lb (6.67 kN, 8.90 kN, and 11.12 kN) have a quadratic shape. The curve labeled 3000 lb (13.34 kN) shows a more linear shape. The curve labeled 3300 lb (14.68 kN) shows that the sheet is beginning to peel off of the concrete. This can be seen due to the large increase in strain in the gauges located at 3 and 5 inches (76 and 127 mm). The curve labeled 3700 lb (16.46 kN) is the strain distribution just before failure. A considerable amount of strain is seen at 11 inches (279 mm), which is only 3 inches (76 mm) from the end of the sheet.



Note: 1 lb = 4.45 N; 1 in = 25.4 mm

Figure 4.3. Typical Strain vs. Location for 4-inch (102 mm) Bonded Length



Note: 1 lb = 4.45 N; 1 in = 25.4 mm

Figure 4.4: Strain vs. Location for 8-inch (203-mm) Bonded Length

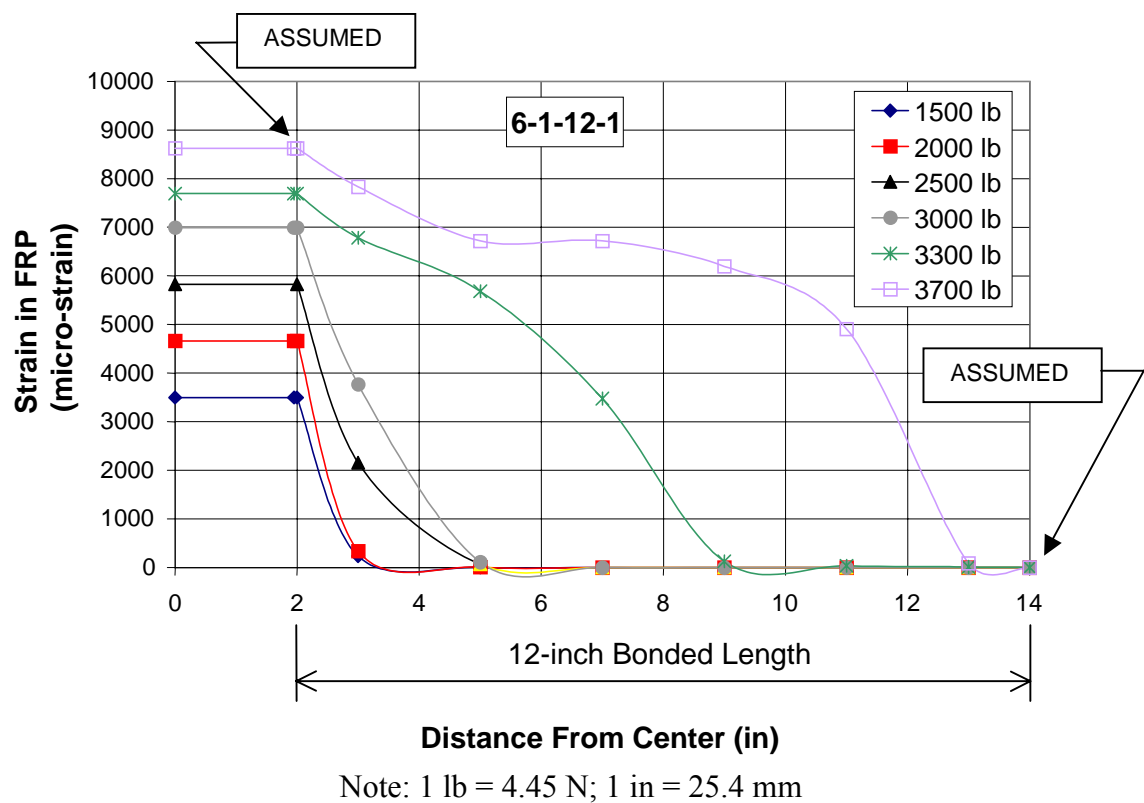


Figure 4.5: Strain vs. Location for 12-inch (305-mm) Bonded Lengths

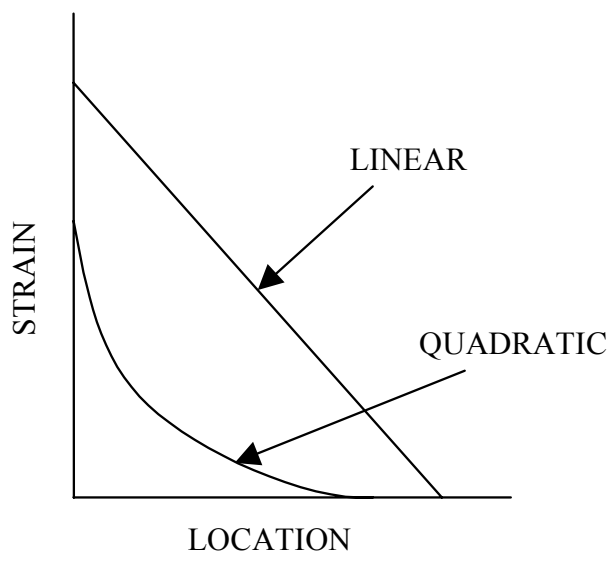


Figure 4.6: Comparison of Quadratic and Linear Curves

4.3. SERIES II

This series of specimens was the same as Series I except two plies of CFRP sheets were used as reinforcement as opposed to one. There were six specimens in Series II, and they will be referred to as 6-2-4-1, 6-2-4-2, 6-2-8-1, 6-2-8-2, 6-2-12-1, and 6-2-12-2.

Table 4.2 shows the details of the specimens from Series II. The first two columns show the specimen code and bond length. The next column is the actual compressive strength of the concrete. The next column is the load at which the specimen experienced first cracking. The ultimate load reached before failure of the specimen follows this. The last column shows the average bond strength, which is calculated by equation (4-1).

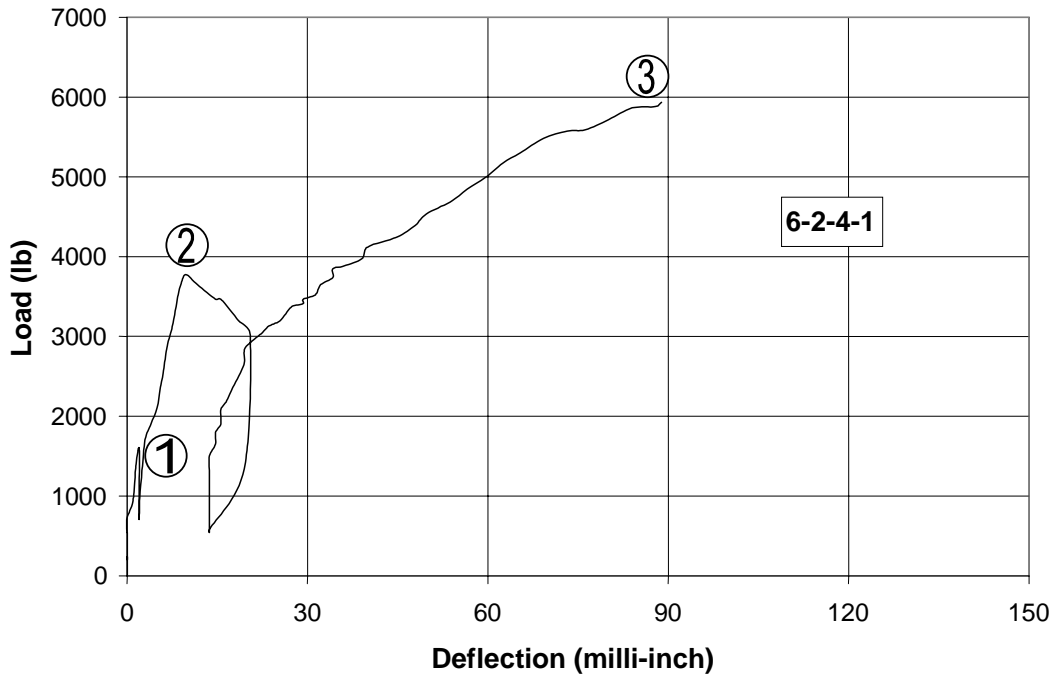
The data from this series of tests was processed the same as Series I. Load vs. deflection graphs were plotted. It can be seen from Figure 4.3 that the specimens with 4-inch (102-mm) bonded lengths demonstrated similar behavior to Series I specimens with 4-inch (102-mm) bonded lengths (compare Figure 4.3 and Figure 4.7). There is no sign of the progressive delamination phenomenon occurring in the specimens. This is due to the shorter bonded length peeling the entire length at once. Figure 4.8 shows the load-deflection of a 12-inch (305-mm) bonded length specimen. The 8 and 12-inch (203 and 305-mm) bonded lengths displayed almost identical behavior, therefore; only one graph will be displayed for both of the lengths. The CFRP sheet progressively delaminated during failure for the specimen in Figure 4.8. This is evident because after the maximum load was reached at point #3, the load decreased significantly and the deflection continued to increase.

Also, strain vs. location diagrams were plotted for the series with two ply of CFRP sheets. Figure 4.9 shows the diagram for the 4-inch (102-mm) bonded length. The shapes of these curves are similar to the diagram of the 4-inch (102-mm) bonded length of Series I, but the values of load and strain are significantly different. The maximum load for the specimen with one ply is 3700 lb. (16.46 kN) while the maximum load for the specimen with two plies is 5900 lb. (26.24 kN). However, since Series II has two plies, the strain is half that of the specimens in Series I at the same load. This is the reason the strains in Figure 4.9 are less than seen in Figure 4.3. The curves for the 8-inch (203-mm) bonded length can be seen in Figure 4.10, and the curves for the 12-inch (305-mm) bonded length can be seen in Figure 4.11. It can be seen that both of these specimens experienced progressive delamination at failure.

Table 4.2. Details of Specimens for Series II

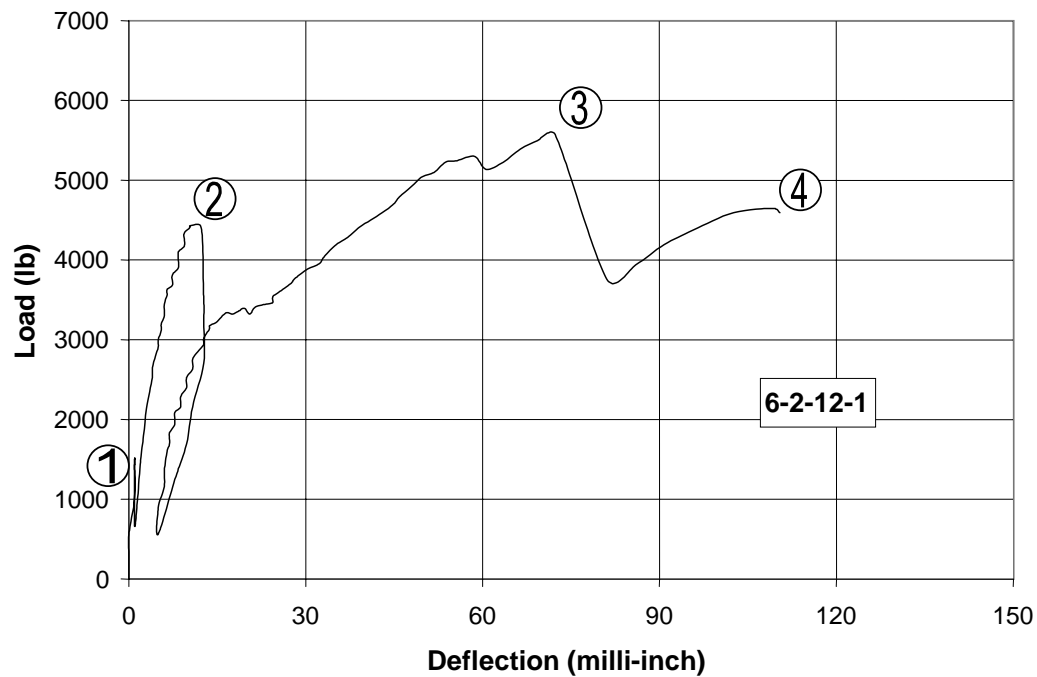
Specimen	Bond Length (in)	Compressive Strength of Concrete (psi)	Cracking Load (lb)	Ultimate Load (lb)	Average Bond Strength (psi)
6-2-4-1	4	5900	3850	5930	741
6-2-4-2			4390	5140	643
6-2-8-1	8		3560	4630	289
6-2-8-2			3880	6260	391
6-2-12-1	12		4500	5590	233
6-2-12-2			3900	5080	212

Note: 1 in = 25.4 mm; 1 psi = 6.89 kPa; 1 lb = 4.45 N



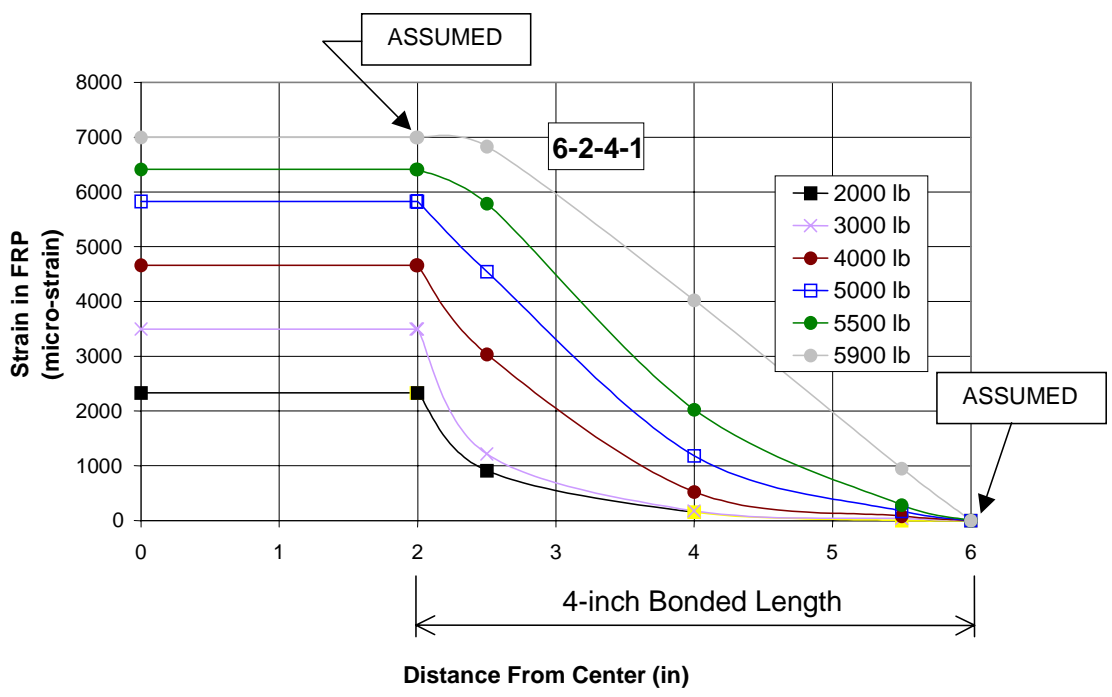
Note: 1 lb = 4.45 N; 1 in = 25.4 mm

Figure 4.7: Load vs. Deflection for 4-inch (102-mm) Bonded Length



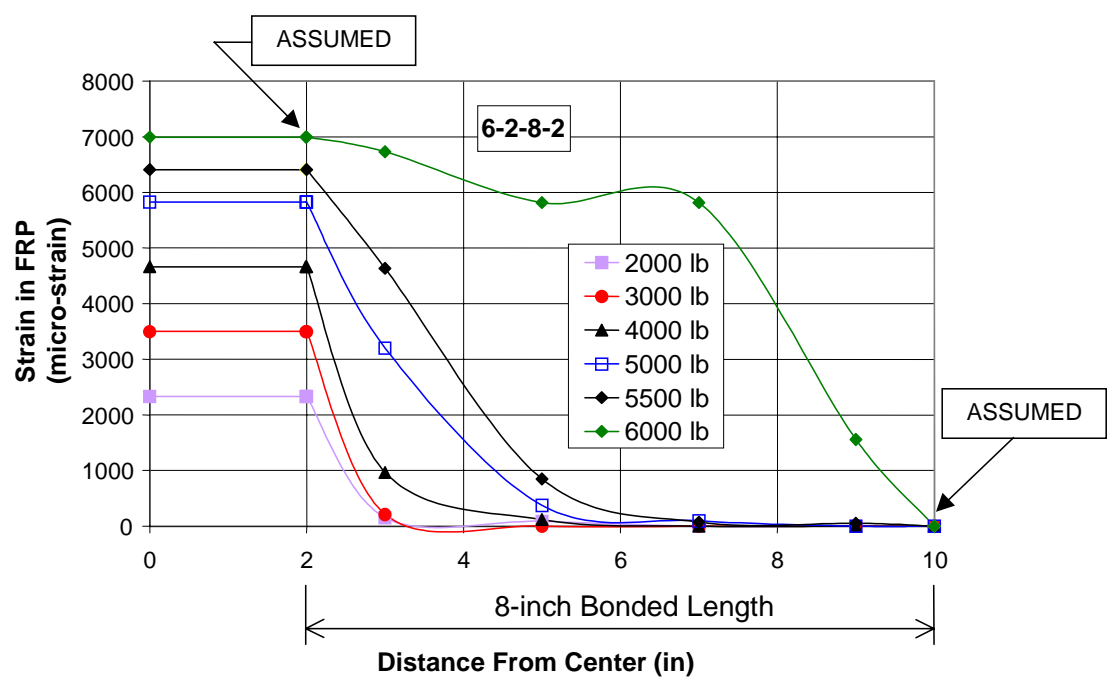
Note: 1 lb = 4.45 N; 1 in = 25.4 mm

Figure 4.8: Typical Load vs. Deflection for 8 or 12-inch (203 or 305-mm) Bonded Length



Note: 1 lb = 4.45 N; 1 in = 25.4 mm

Figure 4.9: Strain vs. Location for 4-inch (102-mm) Bonded Length



Note: 1 lb = 4.45 N; 1 in = 25.4 mm

Figure 4.10: Strain vs. Location for 8-inch (203-mm) Bonded Length

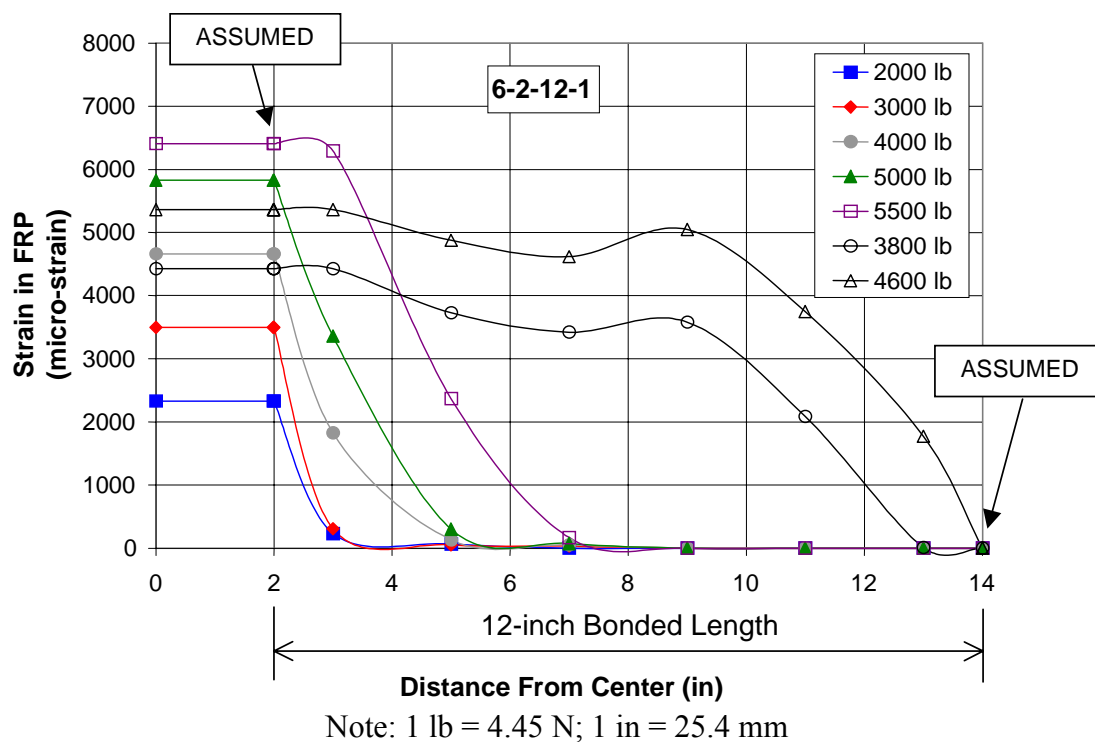


Figure 4.11: Strain vs. Location for 12-inch (305-mm) Bonded Length

4.4. SERIES III

This series of specimens was the same as the Series I except 3000 psi (20.68 MPa) concrete was used instead of 6000 psi (41.37 MPa) concrete. There were six specimens in this series, and they will be referred to as 3-1-4-1, 3-1-4-2, 3-1-8-1, 3-1-8-2, 3-1-12-1, and 3-1-12-2.

Table 4.3 shows the details of the specimens from Series III. The first two columns show the specimen code and bond length. The next column is the actual compressive strength of the concrete. The next column is the load at which the specimen experienced first cracking. The ultimate load reached before failure of the specimen follows this. The last column shows the average bond strength, which is calculated by equation (4-1).

Load vs. Deflection diagrams were plotted for the data of this series. These can be seen in Figure 4.12 and Figure 4.13. The load vs. deflection for the 4-inch (102-mm) bonded length varies slightly from Series I. It shows that a small amount of peeling occurred prior to failure instead of the entire sheet peeling instantly as in Series I. However, the load vs. deflection diagrams for the 8 and 12-inch (203 and 305 mm) bonded lengths are identical to the Series I.

Strain vs. Location diagrams were also plotted for this series. Figure 4.14 verifies that there was partial peeling in the specimen with the 4-inch (102-mm) bonded length. Figure 4.15 and Figure 4.16 show that the specimens with 8 and 12-inch (203 and 305 mm) bonded lengths are similar to Series I.

Table 4.3. Details of Specimens for Series III

Specimen	Bond Length (in)	Compressive Strength of Concrete (psi)	Cracking Load (lb)	Ultimate Load (lb)	Average Bond Strength (psi)
3-1-4-1	4	3550	2740	3300	413
3-1-4-2			2720	3120	390
3-1-8-1	8		2760	4450	278
3-1-8-2			2380	2920	183
3-1-12-1	12		2920	4770	199
3-1-12-2			2790	3450	144

Note: 1 in = 25.4 mm; 1 psi = 6.89 kPa; 1 lb = 4.45 N

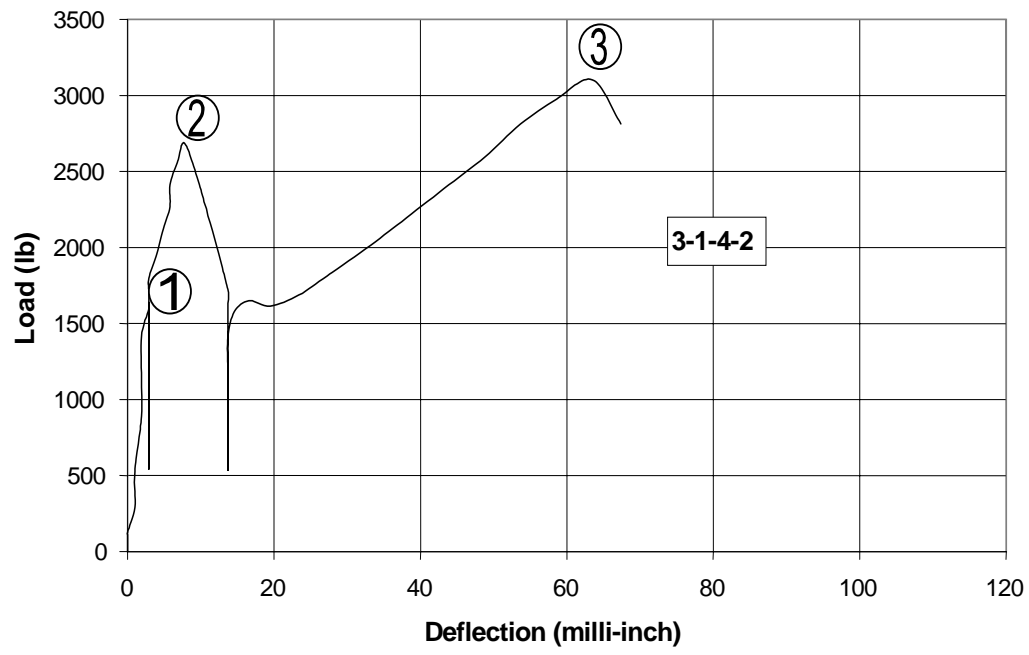


Figure 4.12: Load vs. Deflection for 4-inch (102 mm) Bonded Length

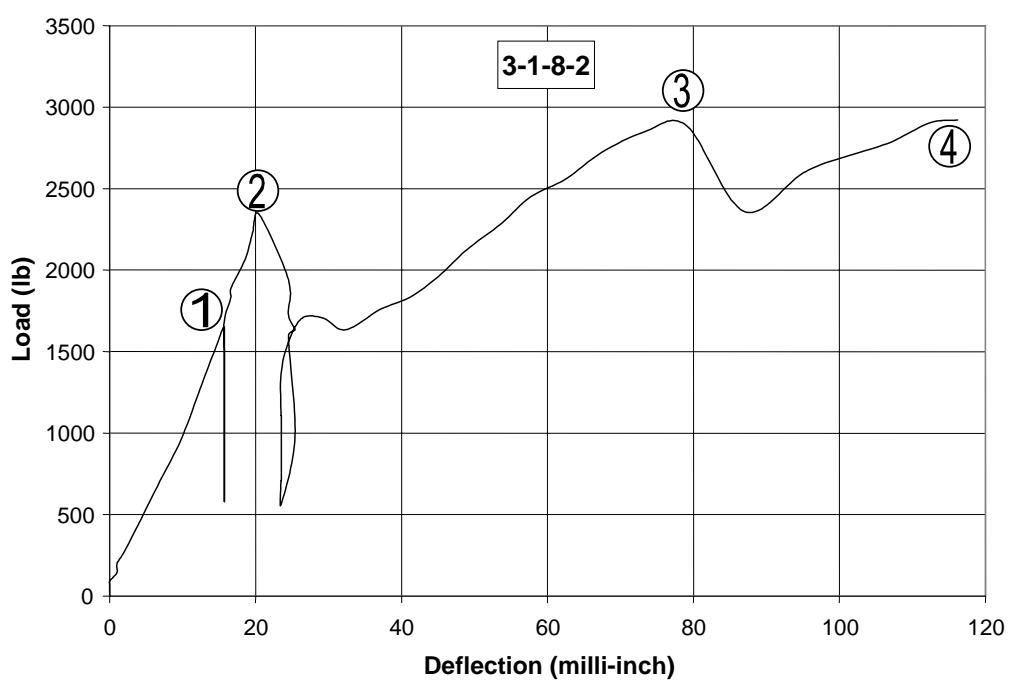
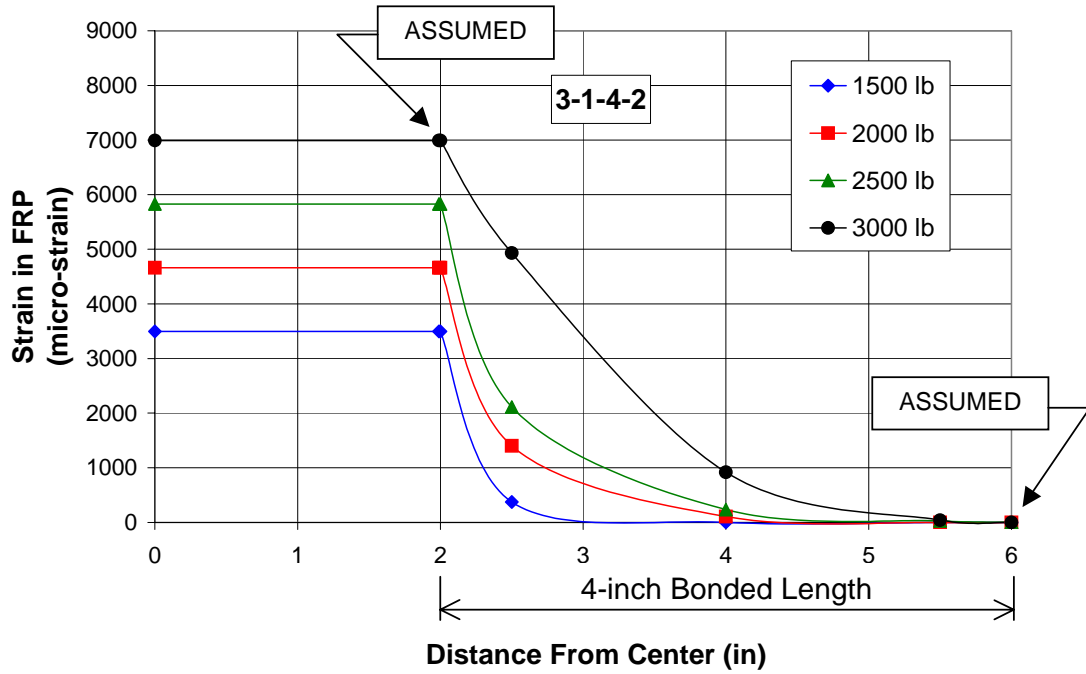
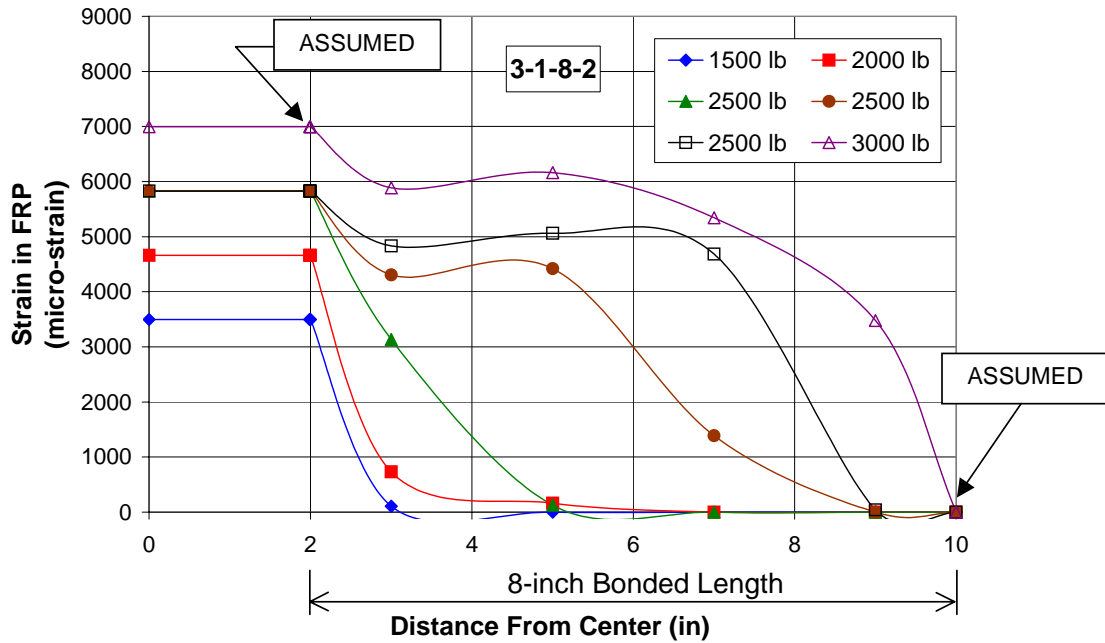


Figure 4.13: Typical Load vs. Deflection for 8 or 12-inch (203 and 305-mm) Bonded Length



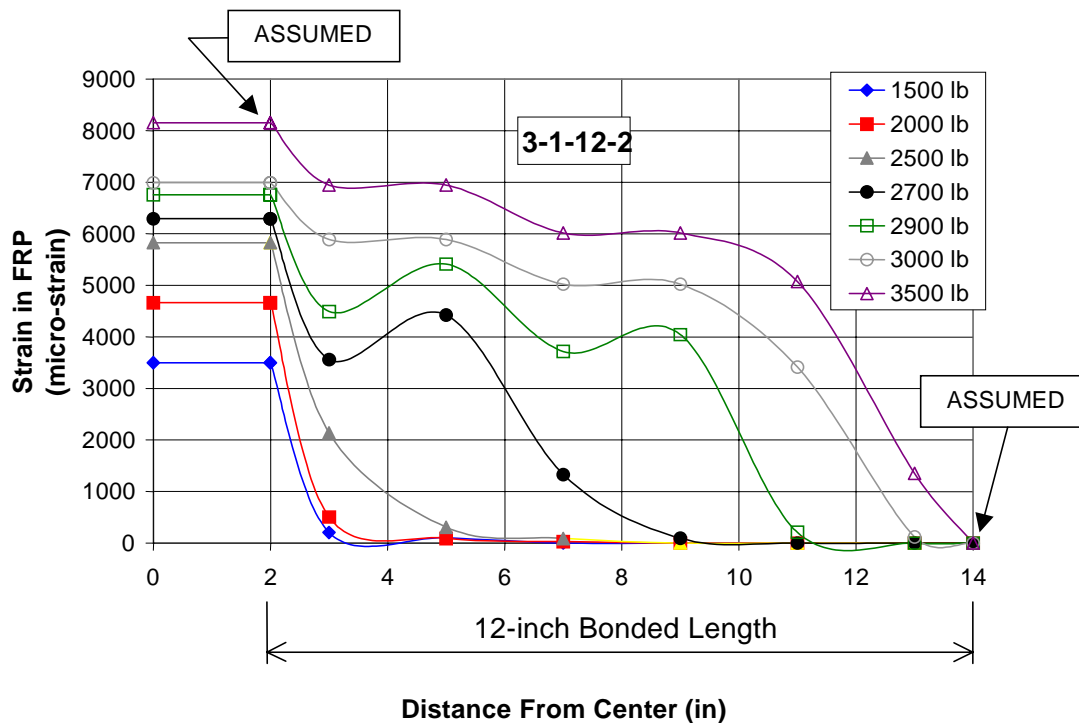
Note: 1 lb = 4.45 N; 1 in = 25.4 mm

Figure 4.14: Strain vs. Location for 4-inch (102-mm) Bonded Length



Note: 1 lb = 4.45 N; 1 in = 25.4 mm

Figure 4.15: Typical Strain vs. Location for 8-inch (203-mm) Bonded Length



Note: 1 lb = 4.45 N; 1 in = 25.4 mm

Figure 4.16: Typical Strain vs. Location for 12-inch (305-mm) Bonded Length

4.5. VERIFICATION SPECIMENS

This group of specimens was tested with the purpose of verifying results from the first three series of specimens.

Table 4.4 shows the details of the specimens from Series IV. The first two columns show the specimen code and bond length. The next column is the actual compressive strength of the concrete. The next column is the load at which the specimen experienced first cracking. The ultimate load reached before failure of the specimen follows this. The last column shows the average bond strength, which is calculated by equation (4-1).

The data from these specimens was plotted in the same manner as the previous three series. The load-deflection graph can be seen in Figure 4.17. It can be seen that the cracking load is much lower than the ultimate load in this graph.

As discussed earlier, many of the specimens failed at the same load at which they cracked. The load vs. deflection graph seen in Figure 4.17 can be used to prove that the specimen is not damaged when the specimen cracks. It can be seen that the cracking load is much lower than the ultimate load.

A typical strain vs. location graph for the verification specimens is shown in Figure 4.18. This graph is similar to the graph of specimens from Series I. The only difference is the location and number of strain gauges for these specimens. It should be noted that even though the cracking load of the specimen was reduced, the strain-location curve has the same shape and behavior as the specimens from Series I. It can be concluded from this information that the results were not changed due to the decrease in cracking load.

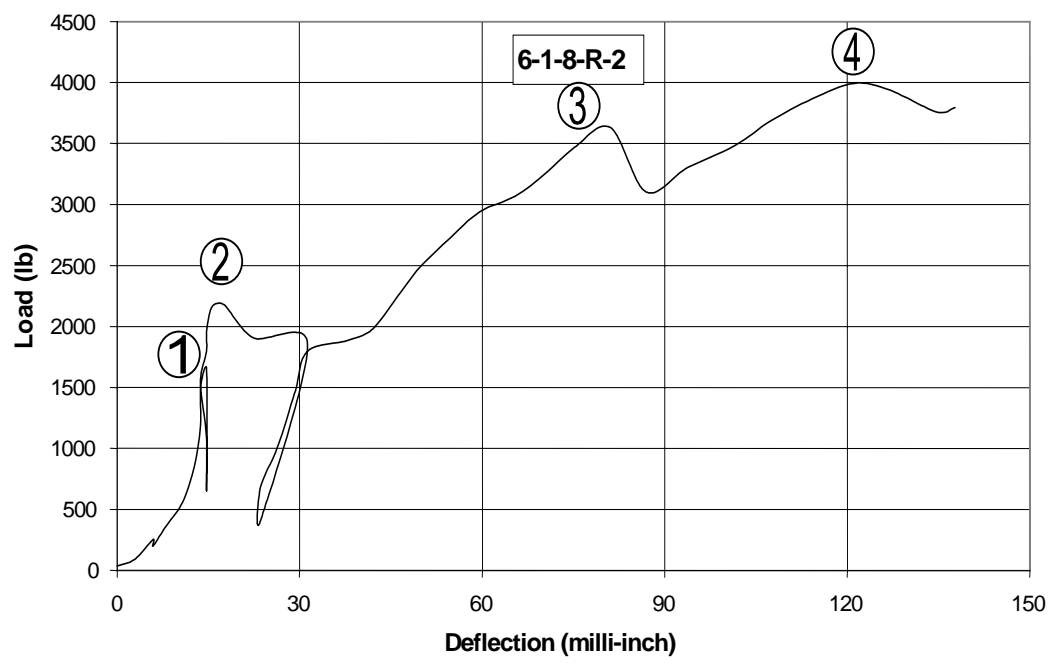
An additional plot of load vs. strain for the strain gauges in the unbonded area was plotted. This plot, shown in Figure 4.19, is used to compare the readings of the strain in the unbonded area to the theoretical strain. The plot is of the strain measured after the specimen had cracked. The location of each of the strain gauges is shown in Figure 4.20. It can be seen from the figure that the gauges labeled Strain1 and Strain2 measured values close to the theoretical strain, while Strain3 and Strain4 are quite different from the theoretical value. However, the slope of all four curves is basically the same, which means the change in strain was read properly. This leads to the conclusion that the zero point of the strain reading was not correct. Therefore, the zero value of the strain was

adjusted to the theoretical value at the point after cracking and plotted in Figure 4.21. The values of strain are very close to the theoretical values for all four strain gauges. From this it was concluded that there is a good correlation between the analytical and experimental data after the zero adjustment.

Table 4.4: Details of Verification Specimens

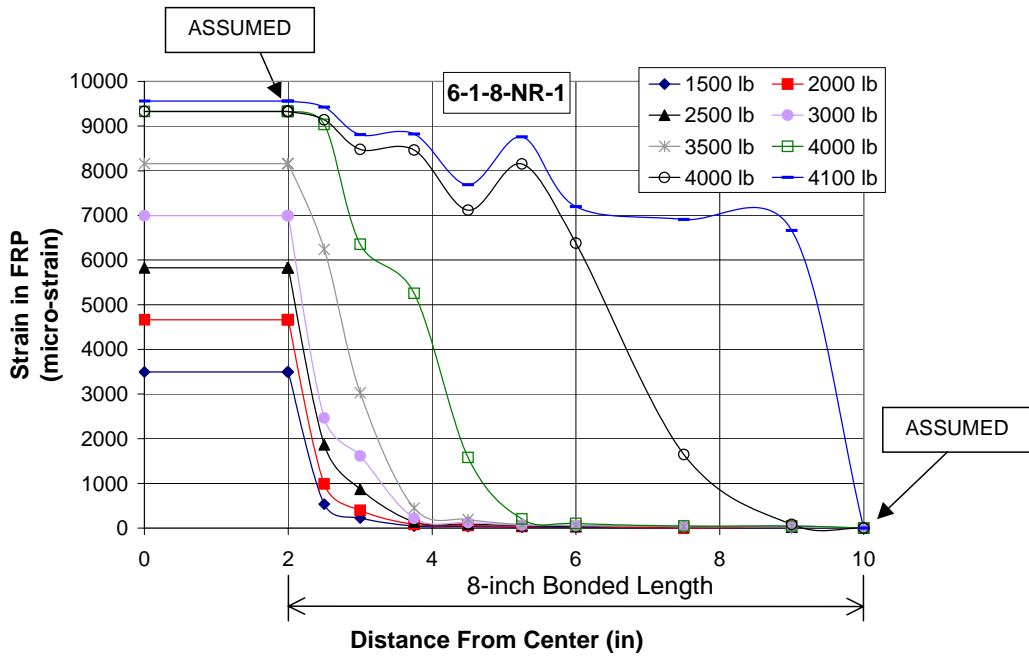
Specimen	Bond Length (in)	Compressive Strength of Concrete (psi)	Cracking Load (lb)	Ultimate Load (lb)	Average Bond Strength (psi)
6-1-8-R-1	8	6240	2010	3450	216
6-1-8-R-2			2180	4100	256
6-1-8-NR-1			2230	4170	261
6-1-8-NR-2			2470	3880	242

Note: 1 in = 25.4 mm; 1 psi = 6.89 kPa; 1 lb = 4.45 N



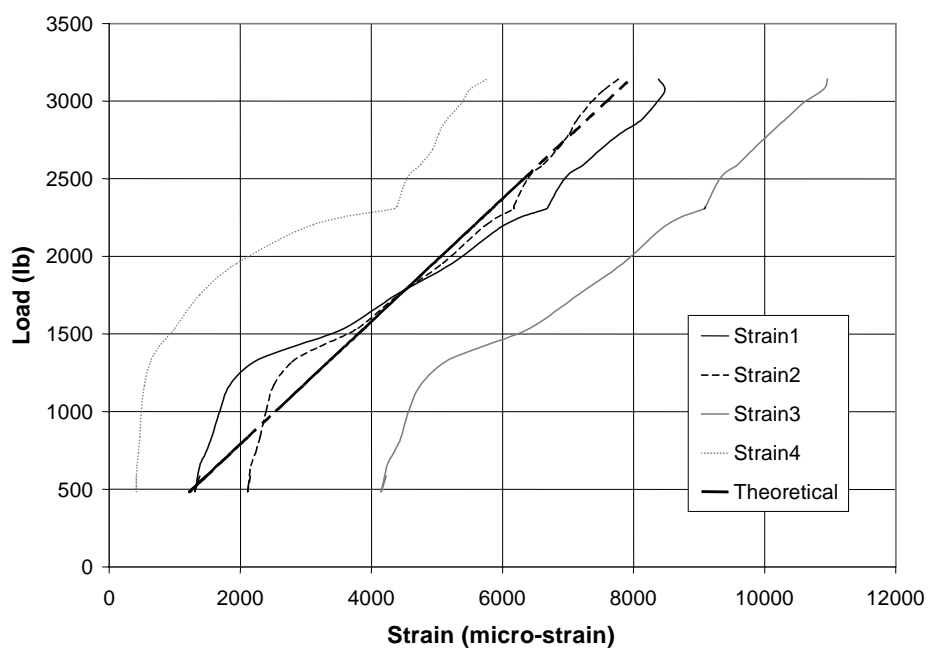
Note: 1 lb = 4.45 N; 1 in = 25.4 mm

Figure 4.17: Load vs. Deflection for Verification Specimen



Note: 1 lb = 4.45 N; 1 in = 25.4 mm

Figure 4.18: Strain vs. Location for Verification Specimen



Note: 1 lb = 4.45 N

Figure 4.19: Comparison of the Strain Gauges in the Unbonded Region with the Theoretical Value

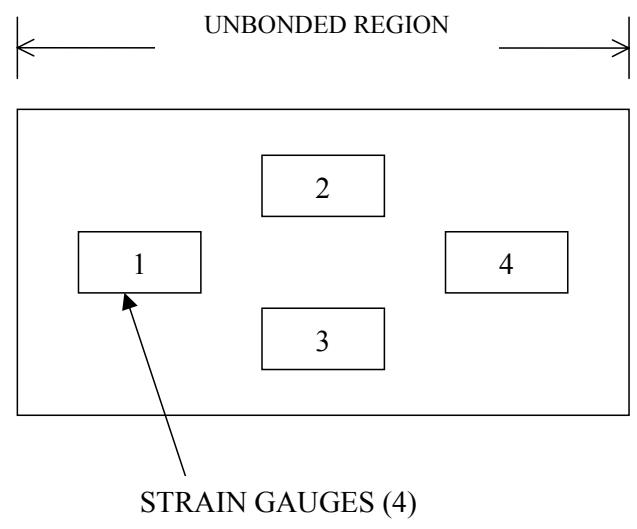
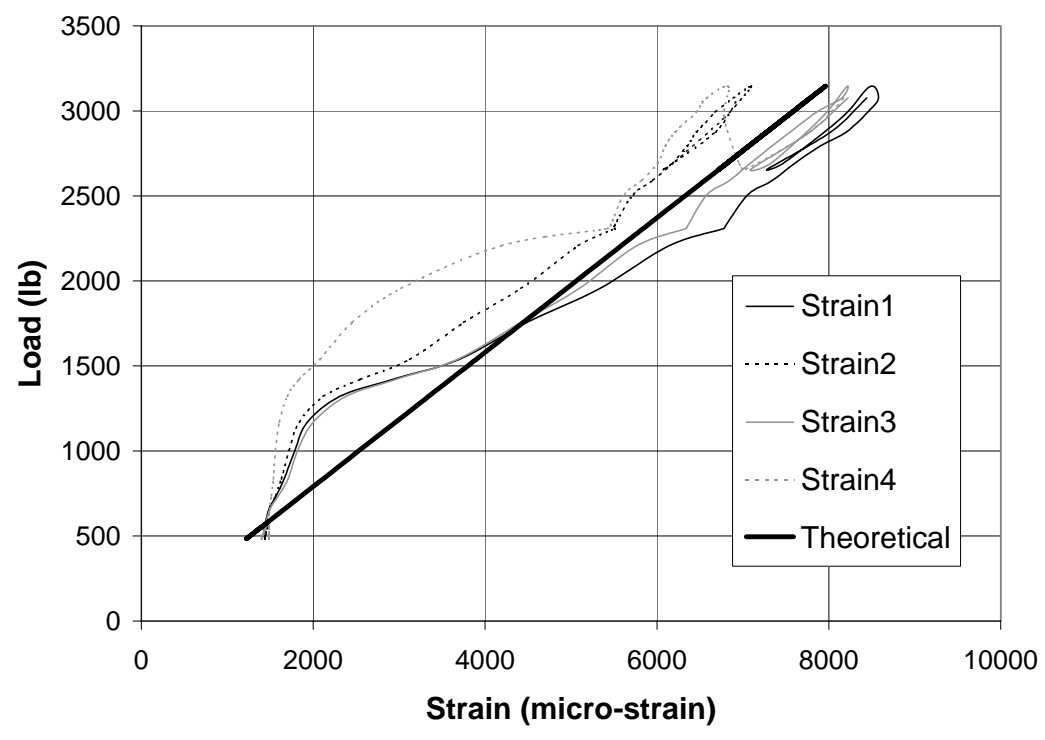


Figure 4.20: Location of Strain Gauges in the Unbonded Region



Note: 1 lb = 4.45 N

Figure 4.21: Adjusted Strain in Unbonded Region vs. Load

4.6. MISCELLANEOUS SPECIMENS

The miscellaneous specimens consist of three types of specimens. One type had a 4-inch (102-mm) wide sheet. Another type had CFRP sheets bonded at 0° and 90° . The other type had a roughened concrete surface. The specimens with the 4-inch (102-mm) wide sheet are designated as 4-8 and 4-12. The specimens with the 0° and 90° CFRP sheets are designated as 2-0-90 and 4-0-90. The specimen with the roughened surface is designated as 6-1-12-S. (Refer to Section 3 for more details.) The details of the specimens can be seen in Table 4.5. The first two columns show the specimen code and bond length. The next column is the actual compressive strength of the concrete. The next column is the load at which the specimen experienced first cracking. The ultimate load reached before failure of the specimen follows this. The last column shows the average bond strength, which is calculated by equation (4-1).

The results of interest for specimens 4-8 and 4-12 are the strain vs. location graphs and the ultimate load. These two pieces of information can be used to determine whether the width of the sheet has any effect on the bond between the concrete and CFRP sheet. The strain vs. location graph can be seen in Figure 4.22. Note that the sheet shows that peeling has begun when the load exceeds 6000 lb. (26.69 kN). This compares to a 3000-lb (13.34 kN) load on a 2-inch (51 mm) wide sheet. Also, there are two curves labeled 7000 lb. (31.14 kN). The second one is after extensive peeling has occurred and the load has decreased.

It can be seen that the strain distribution for this specimen is the same as the specimens with 2-inch (51-mm) wide sheets. The load is two times that of the other specimens, but that is to be expected since the sheet is twice as wide. However, the value

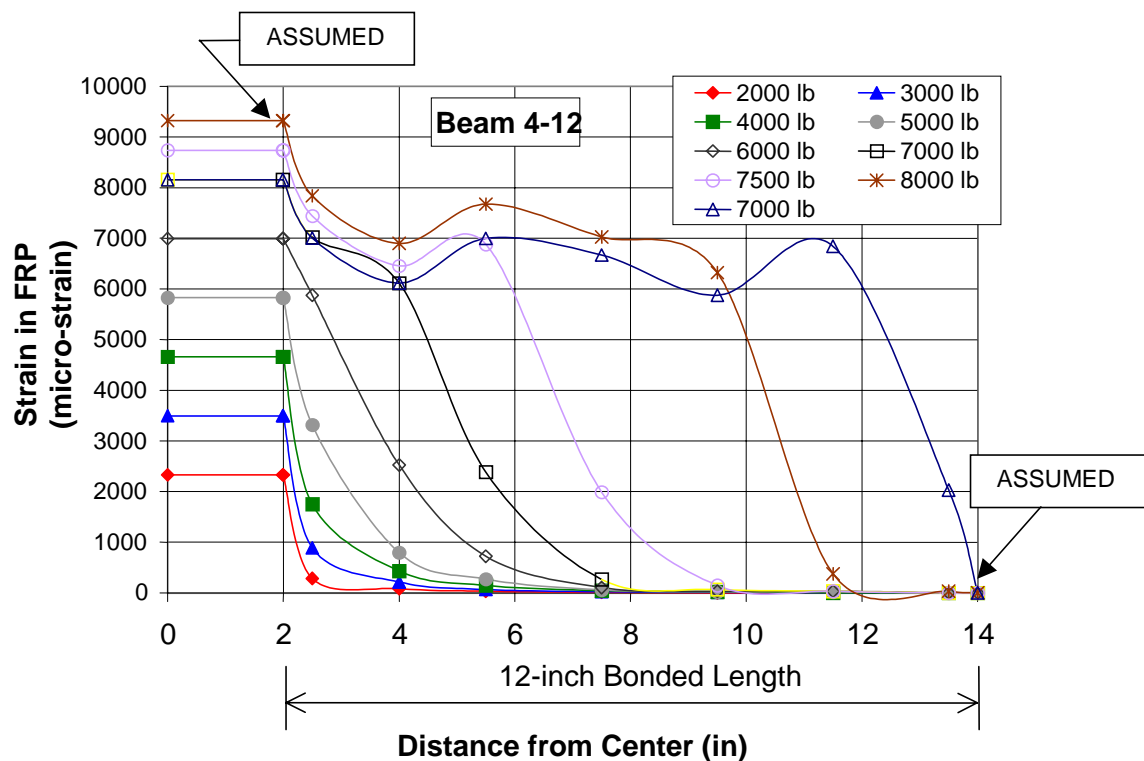
of the strain is almost identical to that of the 2-inch (51-mm) wide sheet. Also, the failure mode of these specimens was the same as the specimens with a 2-inch (51-mm) wide sheet. Table 4.6 compares the ultimate loads of specimens that are the same except for the width of the sheet. As previously stated, the capacity approximately doubled and therefore it is concluded that the change in width does not affect the bond between CFRP sheets and concrete.

The data for the specimens with the 0° and 90° sheets, 2-0-90 and 4-0-90, was plotted the same as for the other specimens. Load vs. deflection and strain vs. location graphs were plotted for each specimen. Figure 4.23 shows the load vs. deflection graph for specimen 2-0-90. From this graph it can be seen that the ultimate load and deflection of the specimen dramatically increased as compared to the specimens from Series I. The failure mode of the specimen was also different from all of the other specimens. The failure occurred by fiber rupture instead of peeling. The load-deflection curve shows a decrease in load and increase in deflection just before the failure point. This occurred because local failures in the CFRP sheet occurred before the CFRP sheet completely failed. The strain vs. location graph for 2-0-90 in Figure 4.24 shows that only a small amount of peeling occurred just before failure. As seen from the curves labeled 5000 lb. (22.24 kN) and Failure, the peeling occurred only in the first half-inch (13 mm). It should be noted that for the curve labeled Failure, the actual load is less than the ultimate load. However, the strain is higher because the cross-section of the CFRP sheet was reduced due to the local failure that occurred.

Table 4.5: Details of Miscellaneous Specimens

Specimen	Bond Length (in)	Compressive Strength of Concrete (psi)	Cracking Load (lb)	Ultimate Load (lb)	Average Bond Strength (psi)
4-8	8	6240	2400	7890	247
4-12	12		2700	7990	166
2-0-90	8	5870	1830	5030	314
4-0-90			2540	10530	329
6-1-12-S	12	5870	2685	5590	233

Note: 1 in = 25.4 mm; 1 psi = 6.89 kPa; 1 lb = 4.45 N



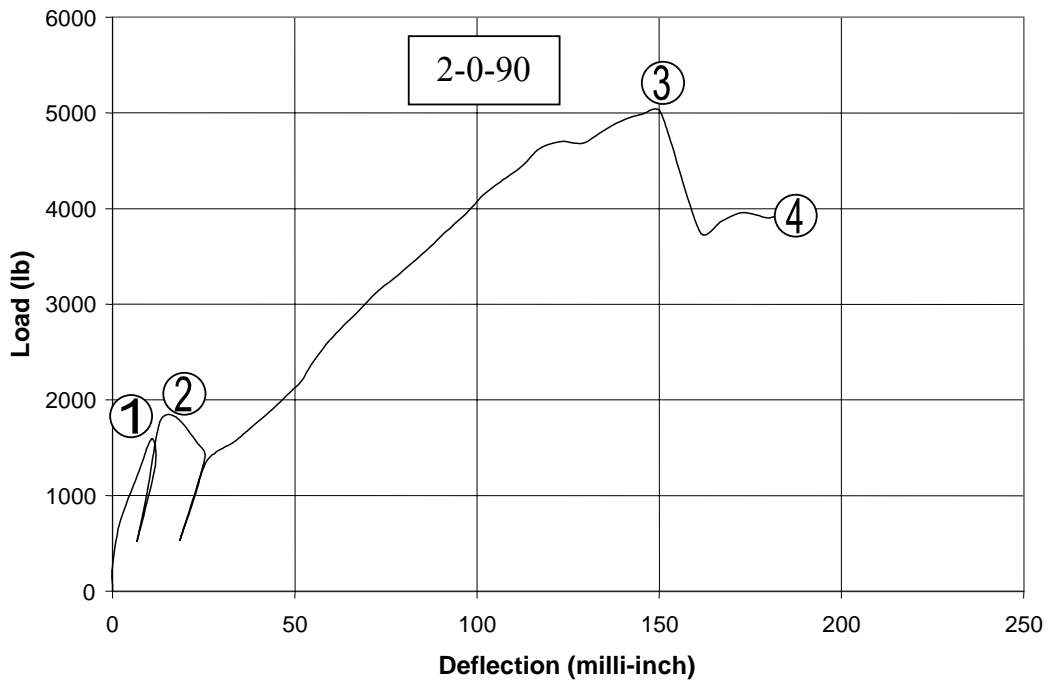
Note: 1 lb = 4.45 N; 1 in = 25.4 mm

Figure 4.22: Strain vs. Location for Specimen with 4-inch (102-mm) Wide Sheet

Table 4.6: Comparison of the Ultimate Load with Change in the Width of Sheet

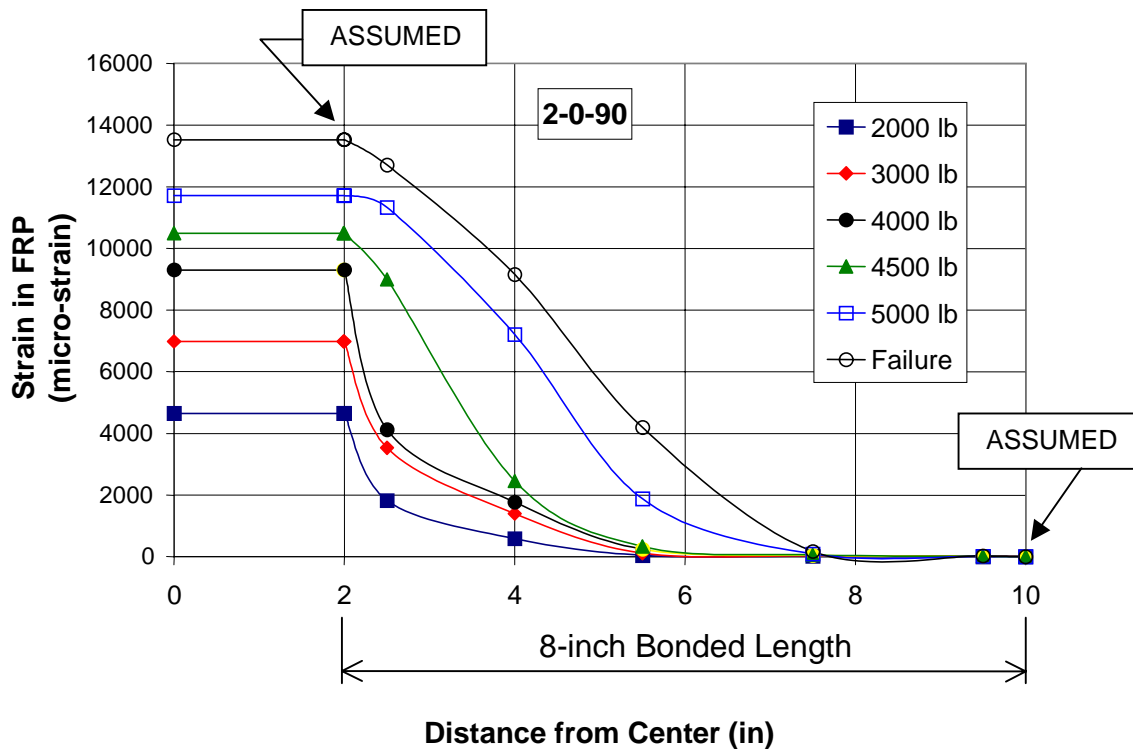
Bond Length (in)	Ultimate Load (lb.)		Ratio 4-inch : 2-inch
	2-inch Wide Sheet (avg.)	4-inch Wide Sheet	
8	3380	7890	2.33:1
12	3610	7990	2.21:1

Note: 1 in = 25.4 mm; 1 lb = 4.45 kN



Note: 1 lb = 4.45 N; 1 in = 25.4 mm

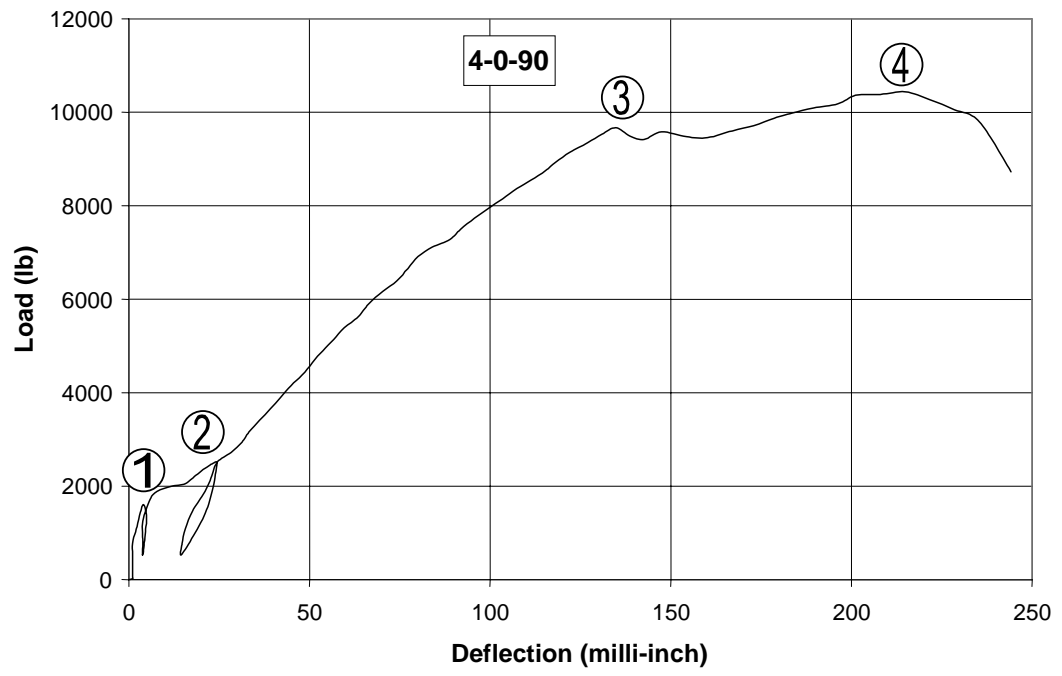
Figure 4.23: Load vs. Deflection for Specimen 2-0-90



Note: 1 lb = 4.45 N; 1 in = 25.4 mm

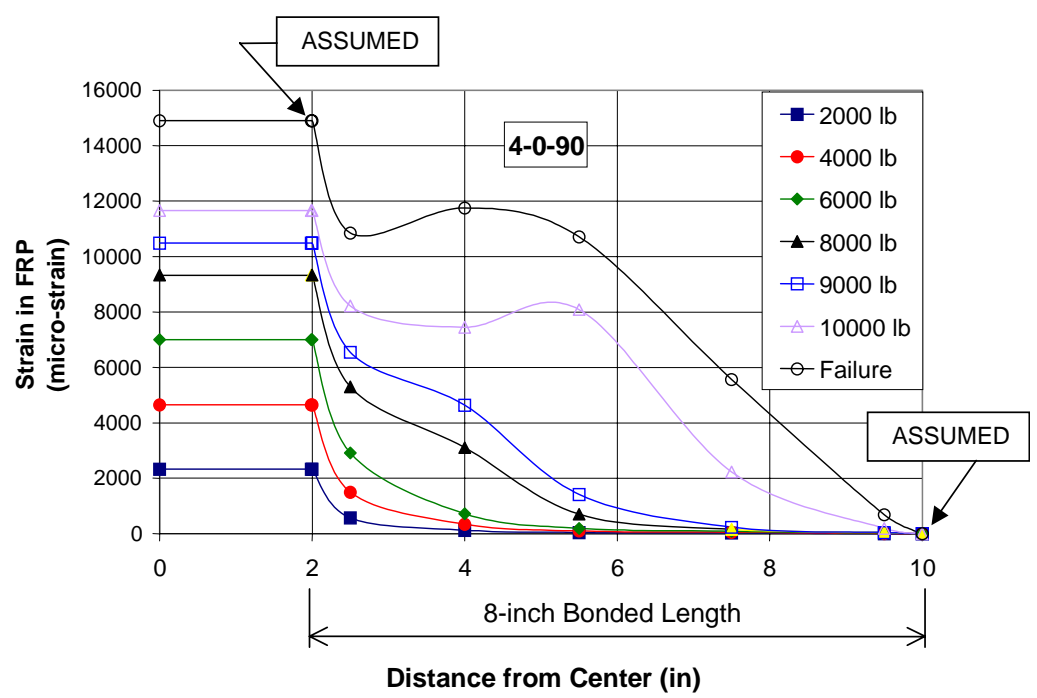
Figure 4.24: Strain vs. Location for Specimen 2-0-90

Specimen 4-0-90 behaved similar to 2-0-90 as can be seen in the load-deflection curve in Figure 4.25. Comparing this specimen to specimen 4-8, the ultimate load and deflection both increased. The strain distribution is also different as can be seen in Figure 4.26. It appears that more peeling occurred prior to failure in this specimen as opposed to 2-0-90. However, the failure mode was again by CFRP rupture and not peeling. The failure occurred in the same manner as 2-0-90 with local failures occurring followed by complete rupture of the sheet. Figure 4.27 shows the failure mode of specimen 4-0-90.



Note: 1 lb = 4.45 N; 1 in = 25.4 mm

Figure 4.25: Load vs. Deflection for Specimen 4-0-90



Note: 1 lb = 4.45 N; 1 in = 25.4 mm

Figure 4.26: Strain vs. Location for Specimen 4-0-90



Figure 4.27: Failure Mode of 4-0-90

The results obtained from specimen 6-1-12-S are very important to the issue of bond. It was found that the surface preparation of the concrete significantly affects the average bond strength. By roughening the surface of the concrete before application of the CFRP sheet, CFRP rupture was attained. Figure 4.28 shows the specimen after failure. It can be seen that the sheet began peeling until it reached the location of the first set of notches. The notches seemed to anchor the sheet to the concrete. If this is the case, then concrete strength will play a significant role in the bond because the concrete could become the weak link.

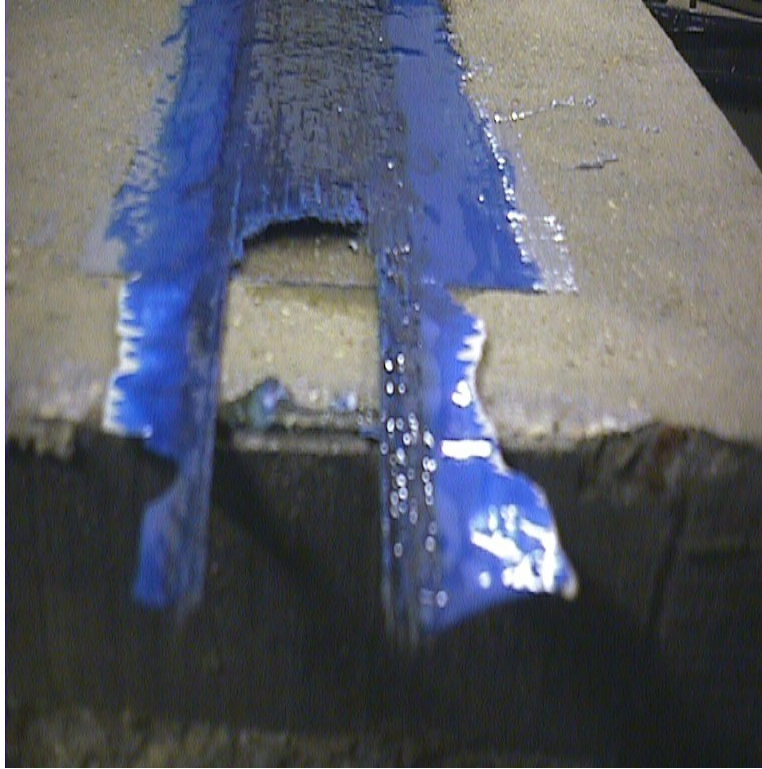


Figure 4.28: End View of 6-1-12-S after Failure

5. COMPARISON OF EXPERIMENTAL RESULTS

In this section, the results presented in Section 4 will be compared in order to determine how each variable influenced bond. In particular, the bonded length, concrete strength, and number of layers will be addressed. Also, the contribution of the transverse wrapping and surface preparation will be discussed.

5.1 BONDED LENGTH

The different bonded lengths of the CFRP sheet that were studied in this experiment showed to have no effect on the ultimate strength of the specimen. There was no change in the ultimate load of the specimens due to the change in bonded length. Figure 5.1 shows the average bond strength vs. the bond length for Series I. It can be seen that the average bond strength decreased as the bonded length increased. The average bond strength is calculated by equation (5-1). The curve was created by plotting a point for each specimen of the series, and then a curve was fitted to the set of points. Similar graphs for Series II and III can be seen in Figure 5.2 and Figure 5.3 respectively. The cause of this decrease in average bond strength with an increase in bond length is due to the effective bond length. Since only a portion of the bonded length is actually taking load, the average bond strength becomes diluted as the bond length becomes larger.

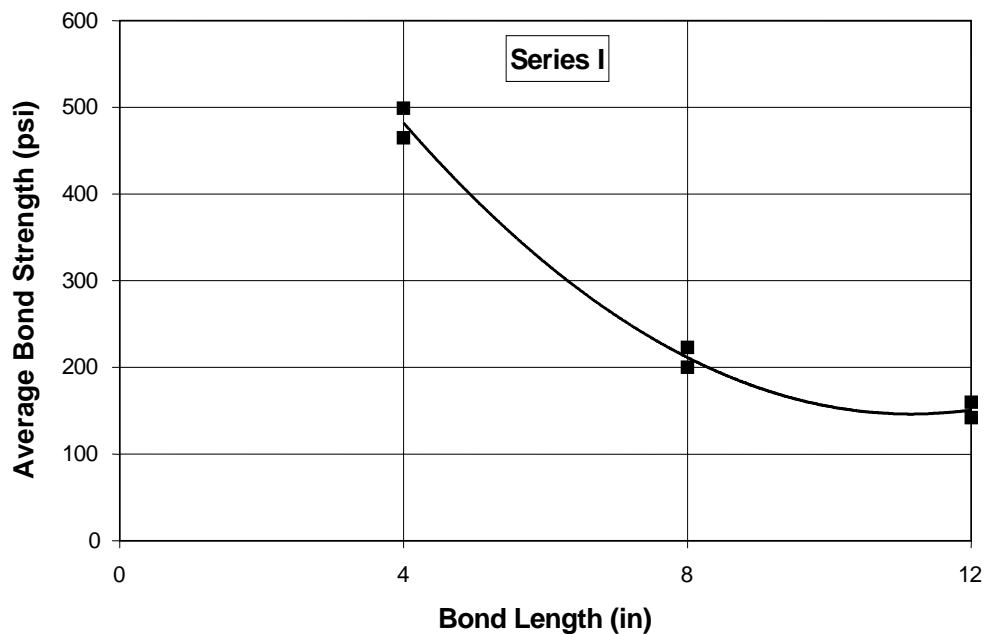
$$\tau_b = \frac{P_{\max}}{l_b w_f} \quad (5-1)$$

τ_b = average bond strength

P_{\max} = ultimate load

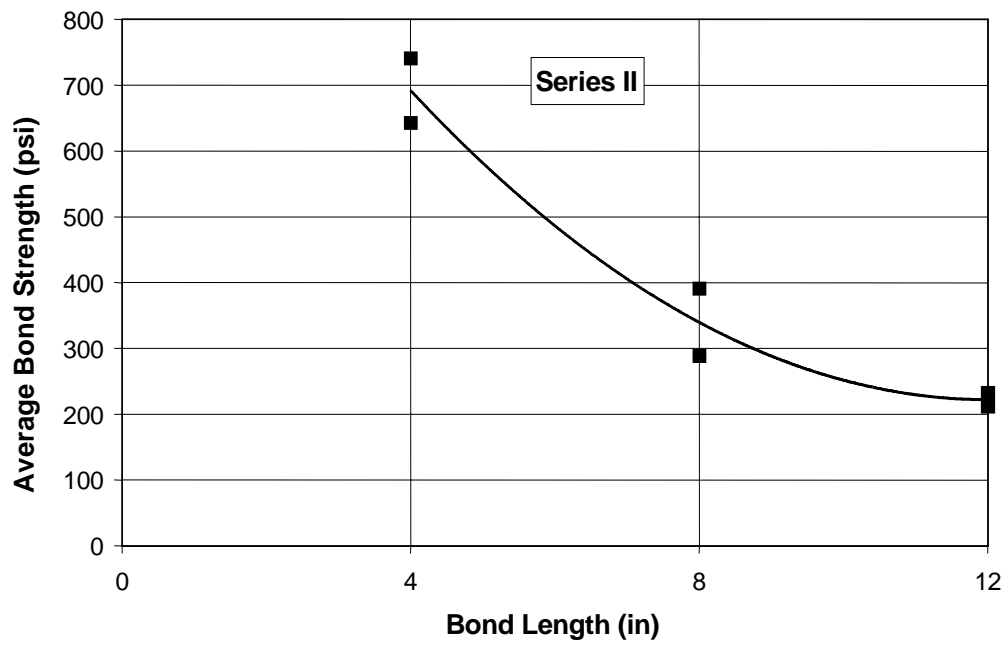
l_b = bonded length

w_f = width of sheet



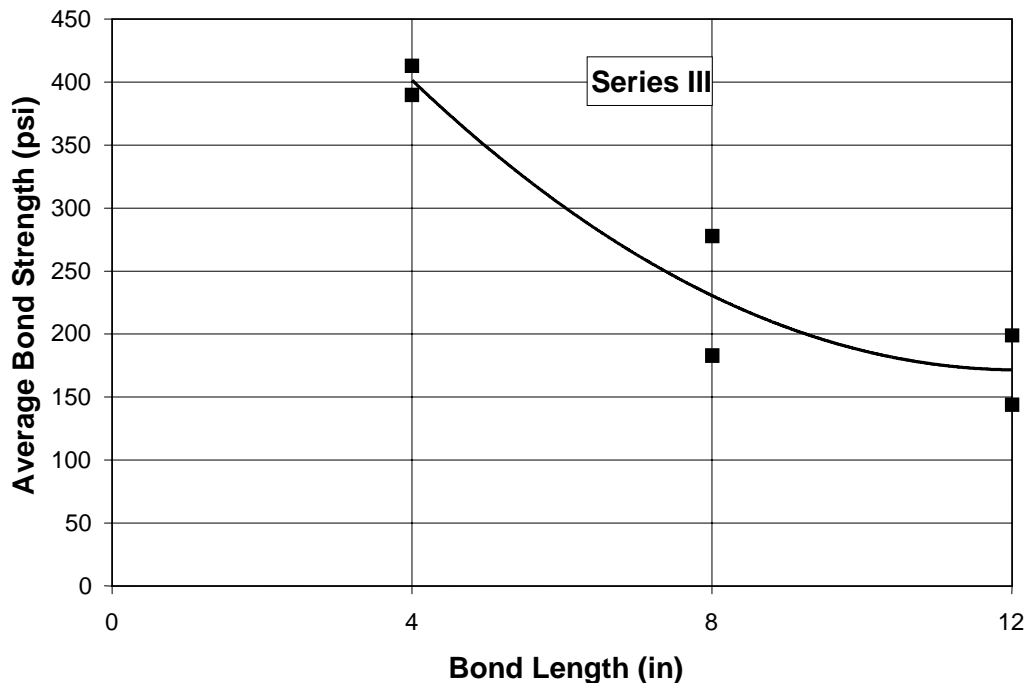
Note: 1 psi = 6.89 kPa 1 in = 25.4 mm

Figure 5.1: Average Bond Strength vs. Bond Length for Series I



Note: 1 psi = 6.89 kPa 1 in = 25.4 mm

Figure 5.2: Average Bond Strength vs. Bond Length for Series II

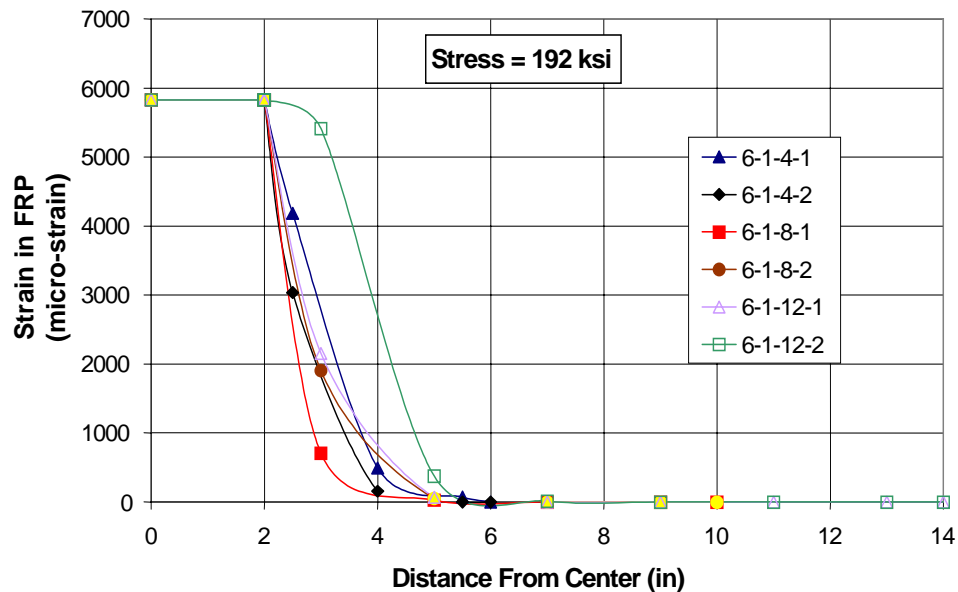


Note: 1 psi = 6.89 kPa 1 in = 25.4 mm

Figure 5.3: Average Bond Strength vs. Bond Length for Series III

Also, the strain distribution in the sheet was virtually the same for each bonded length. Figure 5.4 shows the strain distribution for each specimen of Series I for a tensile stress of 192 ksi (1324 MPa). The tensile stress is used to label the curves instead of load so that the comparison between each series is relevant. The applied load cannot be used to compare because the cross-sectional area of the sheet in Series I is different than Series II. The curve for 6-1-12-2 is slightly different from the other curves, but this is only because peeling occurred in the sheet just before the 192 ksi (1324 MPa) stress was reached. The curve would be the same as the others if it were shifted back over the length that had peeled. Figure 5.5 shows the strain distribution of each specimen of Series II for a tensile stress of 192 ksi (1324 MPa). Specimen 6-2-8-1 is not shown here

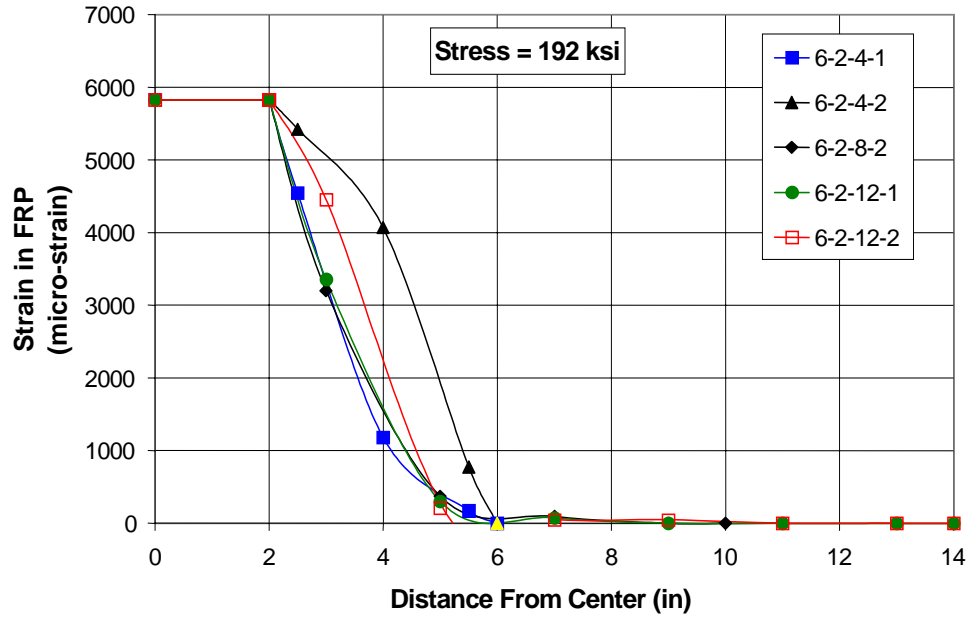
because it failed before the 192 ksi (1324 MPa) stress level was reached. The curve for specimen 6-2-4-2 shows that peeling had begun at this stress level. Figure 5.6 shows the strain distribution for the specimens of Series III for a tensile stress of 192 ksi (1324 MPa). The curves show that the distribution is basically the same for all bonded lengths.



Note: 1 ksi = 6.89 MPa 1 in = 25.4 mm

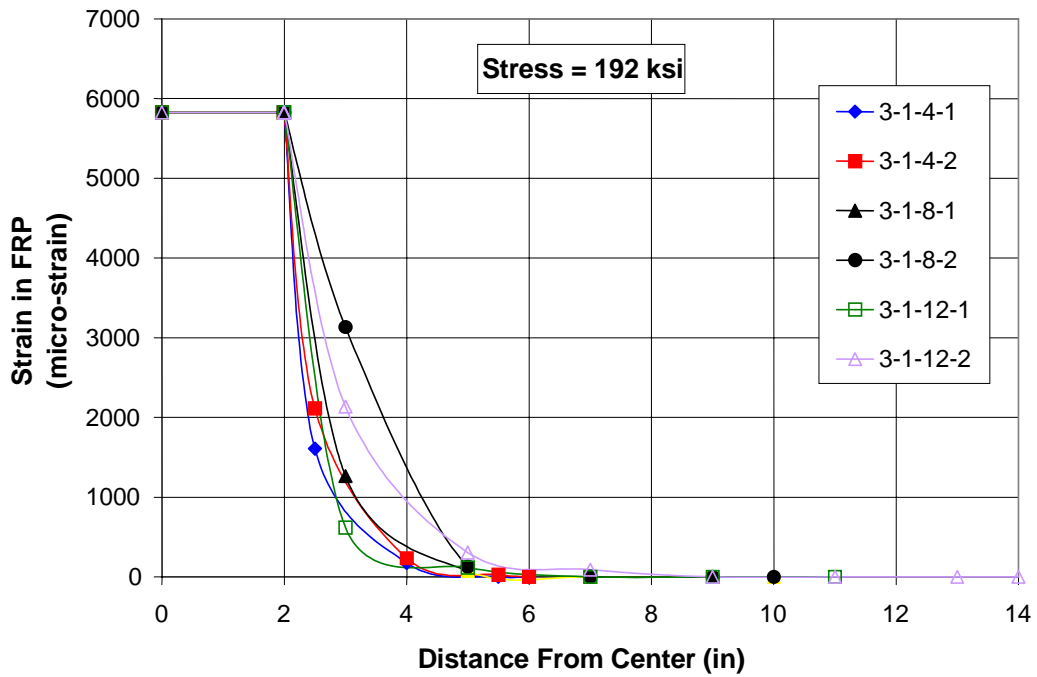
Figure 5.4: Comparison of Strain Distributions for Series I

It was concluded that an effective length exists in which no stress is transferred beyond until peeling occurs. Other researchers have reported the existence of an effective development length (Maeda et al, 1997; Takahashi et al, 1997; Brosens and Van Gemert, 1997; Bakis et al, 1998); however, the actual length reported is not consistent. From the present investigation, it was found that the effective length is approximately 3 inches (76 mm).



Note: 1 ksi = 6.89 MPa 1 in = 25.4 mm

Figure 5.5: Comparison of Strain Distributions for Series II



Note: 1 ksi = 6.89 MPa 1 in = 25.4 mm

Figure 5.6: Comparison of Strain Distributions for Series III

5.2 CONCRETE STRENGTH

It was initially expected that the concrete strength would have an influence on the bond strength of CFRP sheets to concrete. However, in this investigation, no significant differences were seen when the concrete had different strengths. It was concluded that the concrete did not control the peeling failure experienced by the specimens, but the failure occurred in the concrete-epoxy interface. Figure 5.7 and Figure 5.8 are pictures of the concrete surface where the CFRP sheet was bonded. They show that the concrete surface did not fail, except at the end of the sheet. This failure occurred after most of the sheet had peeled and only a short length of the sheet remained attached. With only a short length of the sheet still bonded to the concrete, most of the load would be transferred into the concrete causing it to fail.

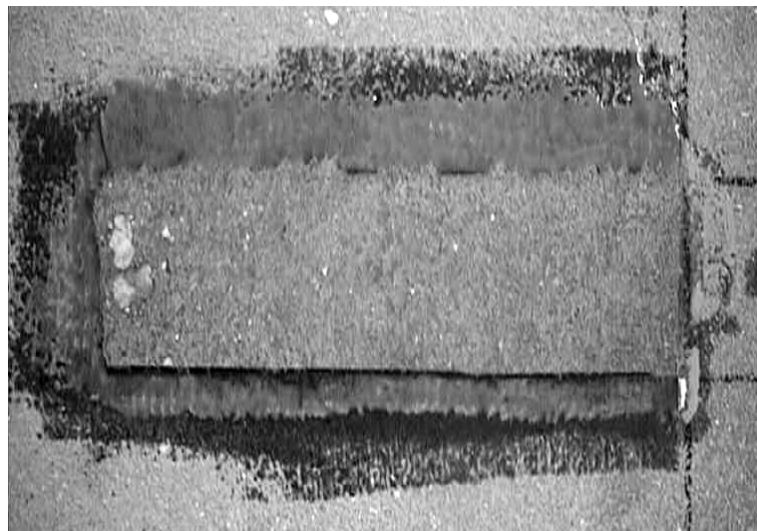


Figure 5.7: Surface of Bonded Area After Peeling (6-1-8-2)

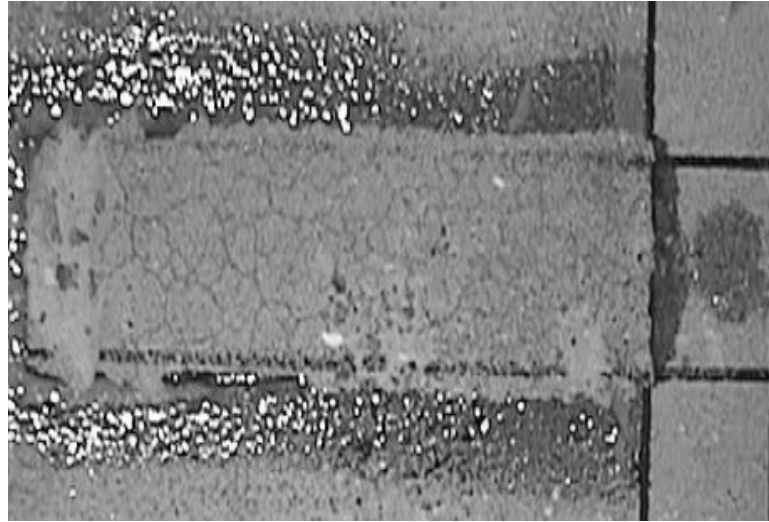


Figure 5.8: Surface of Bonded Area After Peeling (3-1-8-2)

Table 5.1 shows the load at which first cracking occurred along with the ultimate load for specimens of Series I and Series III. The average of these loads is also shown at the bottom of each column. These averages along with the compressive strengths are then compared in Table 5.2. The consistency of the results is very good. This can be seen by the values shown for the standard deviation and coefficient of variation. The significance of this table is to show that the concrete strength did have an effect on the cracking load, but it did not effect the ultimate load. The concrete strength should vary as a function of $\sqrt{f'_c}$. The table shows that the ratio $\sqrt{f'_c}$ and the cracking load are the same. However, the ultimate load is virtually the same for Series I and III.

Table 5.1: Cracking and Ultimate Load for Series I and III

Specimen	Cracking Load (lb)	Ultimate Load (lb)	Specimen	Cracking Load (lb)	Ultimate Load (lb)
6-1-4-1	3140	3720	3-1-4-1	2740	3300
6-1-4-2	4100	3990	3-1-4-2	2720	3120
6-1-8-1	3920	3560	3-1-8-1	2760	4450
6-1-8-2	3230	3190	3-1-8-2	2380	2920
6-1-12-1	4250	3830	3-1-12-1	2920	4770
6-1-12-2	3720	3390	3-1-12-2	2790	3450
Average	3727	3613	Average	2718	3668
Standard Deviation	456	294	Standard Deviation	180	757
Coefficient of Variation	12.2%	8.1%	Coefficient of Variation	6.6%	20.6%

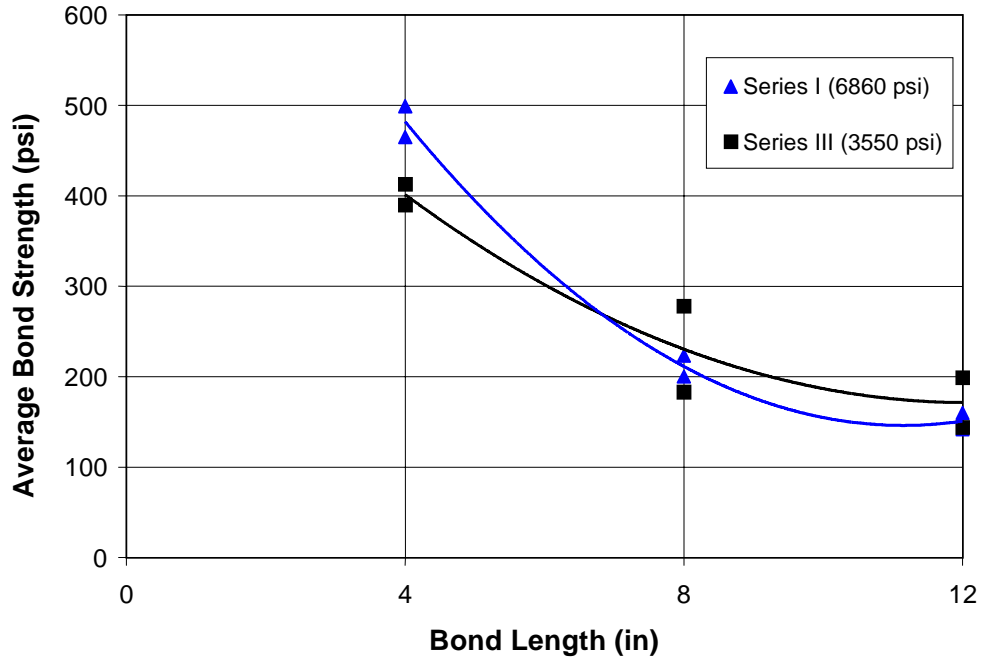
Note: 1 lb = 4.45 N

Table 5.2: Comparison of Cracking and Ultimate Load for Series I and III

	Series I	Series III	% of Series I
f_c' (psi)	6860	3550	52%
$(f_c')^{0.5}$ ((psi)^{0.5})	82.8	59.6	72%
Cracking Load (lb)	3727	2718	73%
Ultimate Load (lb)	3613	3668	102%

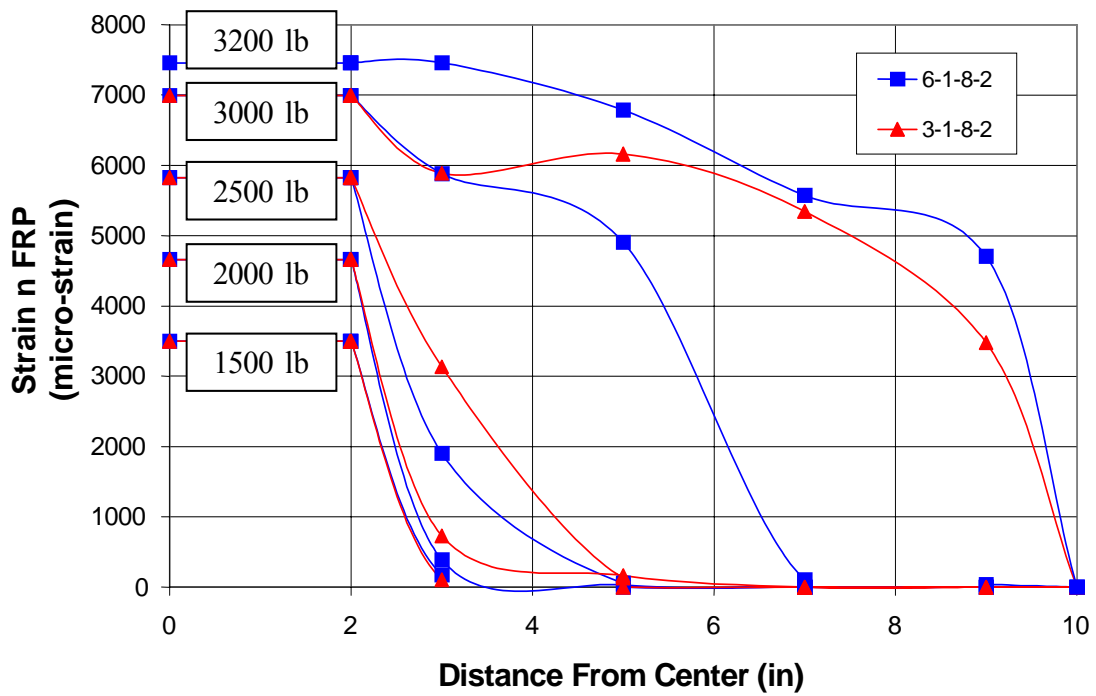
Note: 1 lb = 4.45 N 1 psi = 6.89 kPa

Figure 5.9 compares the average bond strength vs. bond length curve for Series I and III. The average bond strength at the 4-inch (102-mm) bonded length is higher for Series I, but at the 8 and 12-inch (203 and 305 mm) bonded lengths the average bond strengths are basically the same. Figure 5.10 shows the strain distributions for a specimen of Series I and a specimen of Series III. The two specimens are 6-1-8-2 and 3-1-8-2. The strain distributions show that peeling occurred earlier in specimen 3-1-8-2 than in specimen 6-1-8-2. However, when 6-1-8-2 is at a load of 3200 lbs (14.2 kN) and 3-1-8-2 is at a load of 3000 lbs (13.3 kN), the peeling is almost the same.



Note: 1 psi = 6.89 kPa 1 in = 25.4 mm

Figure 5.9: Comparison of Average Bond Strength for Different Concrete Strengths



Note: 1 lb = 4.45 kN 1 in = 25.4 mm

Figure 5.10: Comparison of Strain Distribution for Series I and Series III

5.3 PLIES OF CFRP SHEETS

The number of plies used to make the CFRP laminate will affect the average bond strength of the laminate. In order for two plies of CFRP sheet to be as efficient as one ply, the average bond strength would have to double. However, it is not expected that this will occur, and the results of this research indicate that the increase in average bond strength is not proportional to number of plies. The ultimate load for the specimens of Series I and II is shown in Table 5.3. The consistency of the results is also very good. This can be seen by the values shown for the standard deviation and coefficient of variation. The averages of the ultimate loads are compared in Table 5.4, and it shows that the increase is only 1.5 times Series I.

Table 5.3: Ultimate Load of Series I and II

Specimen	Ultimate Load (lb)	Specimen	Ultimate Load (lb)
6-1-4-1	3720	6-2-4-1	5930
6-1-4-2	3990	6-2-4-2	5140
6-1-8-1	3560	6-2-8-1	4630
6-1-8-2	3190	6-2-8-2	6260
6-1-12-1	3830	6-2-12-1	5590
6-1-12-2	3390	6-2-12-2	5080
Average	3613	Average	5438
Standard Deviation	294	Standard Deviation	602
Coefficient of Variation	8.1%	Coefficient of Variation	11.1%

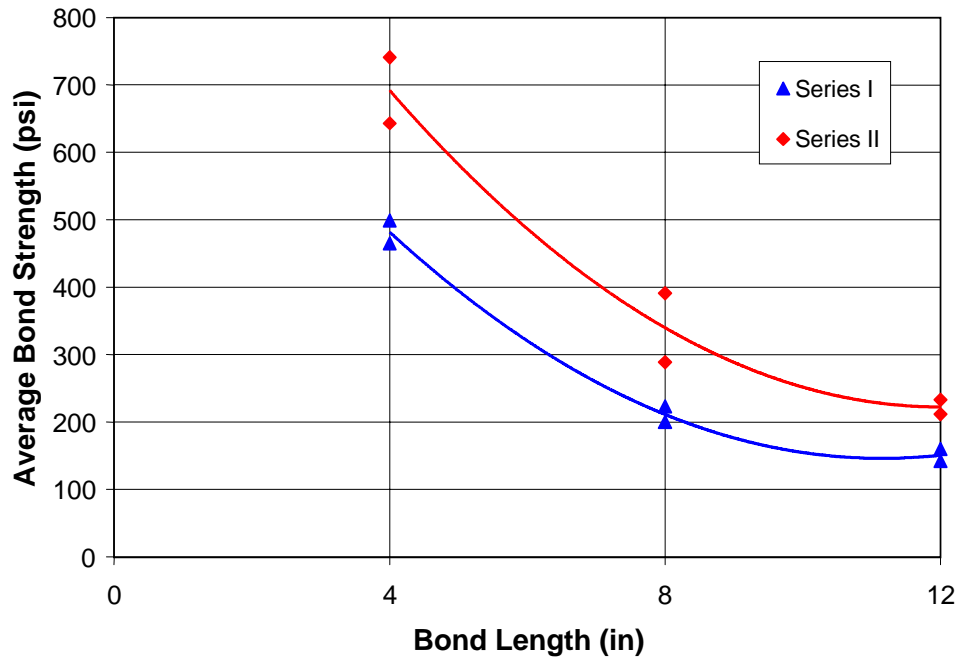
Note: 1 lb = 4.45 kN

Table 5.4: Comparison of Ultimate Load for Series I and II

Ultimate Condition	Series I	Series II	% of Series I
Load (lb)	3613	5438	151%
Normal FRP Stress (ksi)	278	209	75%

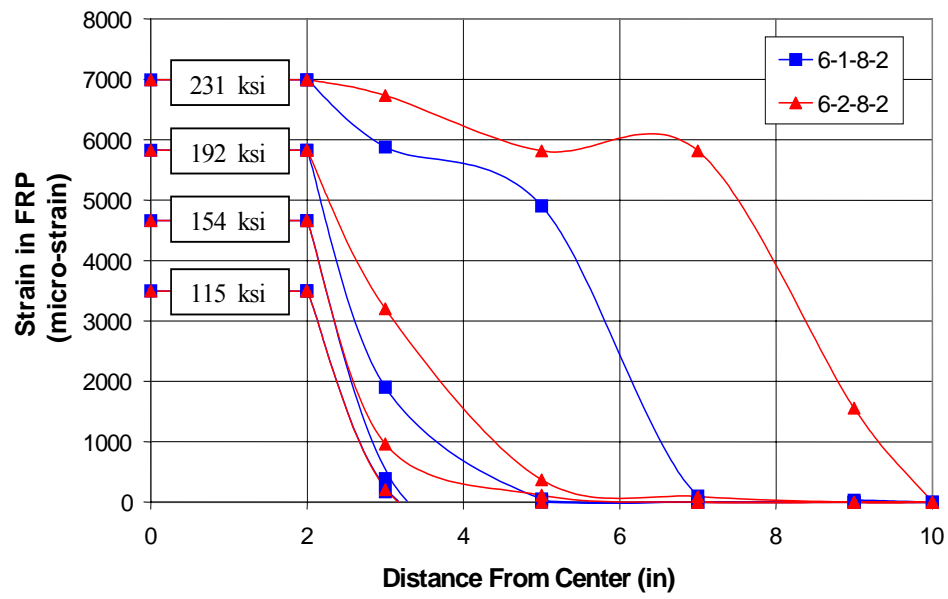
Note: 1 lb = 4.45 kN

The average bond strength is proportional to the ultimate load, and since the ultimate load increased by a factor of 1.5 the average bond strength also increased by a factor of 1.5. Figure 5.11 shows the average bond strength vs. bond length for Series I and II. The curve for Series II is the same as Series I, except it is shifted upwards. The strain distributions for specimens 6-1-8-2 and 6-2-8-2 are compared in Figure 5.12. It should be noted that in this graph, the tensile stress in the sheet is used to label the curves instead of tensile load. This is necessary because the cross-sectional area of the CFRP sheet of Series II is larger than Series I. It can be seen that peeling occurred at lower levels of stress for Series II than Series I.



Note: 1 psi = 6.89 kPa 1 in = 25.4 mm

Figure 5.11: Comparison of Average Bond Strength for Series I and II



Note: 1 ksi = 6.89 MPa 1 in = 25.4 mm

Figure 5.12: Comparison of Strain Distributions Series I and Series II

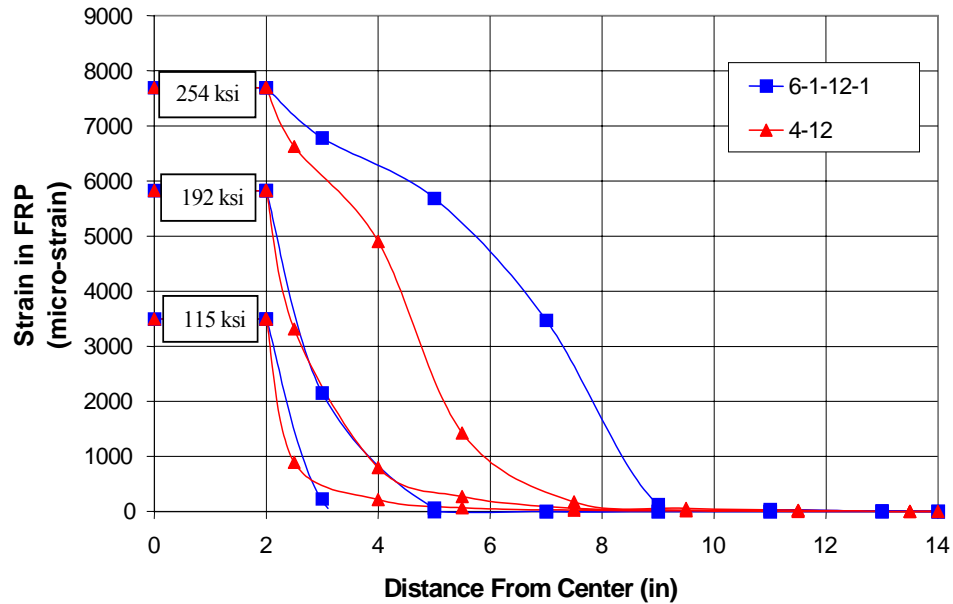
5.4 WIDTH OF SHEET

Two specimens were tested in order to prove that the width of the sheet did not change the bond strength of the CFRP sheet. The expected results of this testing is that the ultimate load would be twice that of Series I, and the strain distribution would stay the same. It was also expected that the failure mode would be the same as Series I. Table 5.5 shows the comparison of the ultimate load for specimens with 2-inch (51-mm) wide and 4-inch (102-mm) wide sheets. The loads are compared for specimens with the same bonded length. The ultimate load for the 2-inch (51-mm) wide sheet is the average of two specimens while the ultimate load for the 4-inch (102-mm) wide sheet is from only one specimen. The last column of the table shows the ratio of the ultimate loads. As expected, the load did approximately double. Figure 5.13 shows the comparison of the strain distribution for specimen 6-1-12-1 and specimen 4-12. These two specimens are identical except 4-12 has a 4-inch (102-mm) wide sheet and 6-1-12-1 had a 2-inch (51-mm) wide sheet. The tensile stress is used to label the curves. It can be seen that the first two curves are identical. The last curve is slightly different, but only because specimen 6-1-12-1 has peeled more than specimen 4-12. The failure mode of the specimens was identical, and it was concluded that the width of the sheet did not influence the bond strength.

Table 5.5: Comparison of Ultimate Load for Different Width of CFRP Sheet

Bond Length (in)	Ultimate Load (lb.)		Ratio of Ultimate Loads 4-inch : 2-inch
	2-inch Wide Sheet (avg.)	4-inch Wide Sheet	
8	3380	7890	2.33:1
12	3610	7990	2.21:1

Note: 1 lb = 4.45 N 1 in = 25.4 mm



Note: 1 ksi = 6.89 MPa 1 in = 25.4 mm

Figure 5.13: Comparison of Strain Distributions for Different Widths of CFRP

5.5 TRANSVERSE SHEET

Two specimens were tested in order to determine the contribution of adding a transverse CFRP sheet on top of the longitudinal sheet. This was to be a model of the orientation of the fibers used as $0^{\circ}/90^{\circ}$ in shear reinforcement. The construction and description of these specimens was discussed in Section 4.

It was found that the use of the transverse sheet dramatically increased the bond strength of the sheet. Also, the failure mode of these specimens was due to fracture of the CFRP sheet instead of peeling. The influence on the ultimate load seen by the transverse sheet is shown in Table 5.6. The comparison is made between specimens with the same width and bonded length. The only difference is the addition of the transverse

CFRP sheet. The table shows the ultimate load of each specimen and then the ratio of the specimen with the transverse sheet to the specimen without the transverse sheet. It can be seen that the ultimate load increased 49 percent for the 2-inch (51-mm) wide sheet and 33 percent for the 4-inch (102-mm) wide sheet. Figure 5.14 shows the comparison of the strain distributions for specimens with 2-inch (51-mm) wide sheets with one specimen having the transverse sheet. It can be seen that the existence of the transverse sheet prevented the peeling failure from occurring. At a load of 3000 lb (13.3 kN), specimen 6-1-8-2 is showing significant peeling while specimen 2-0-90 does not show any peeling. It should also be noted that the transverse sheet tends to increase the effective bonded length. Figure 5.15 shows a similar graph for specimens with a 4-inch (102-mm) wide sheet. The same results as in Figure 5.14 are seen in this graph.

Table 5.6: Influence of Transverse Sheet on Ultimate Load

Width of Sheet (in)	Bonded Length (in)	Ultimate Load (lb.)		Ratio of Ultimate Loads
		No Transverse Sheet	Transverse Sheet	
2	8	3380	5030	1.49 : 1
4		7890	10530	1.33 : 1

Note: 1 lb = 4.45 N 1 in = 25.4 mm

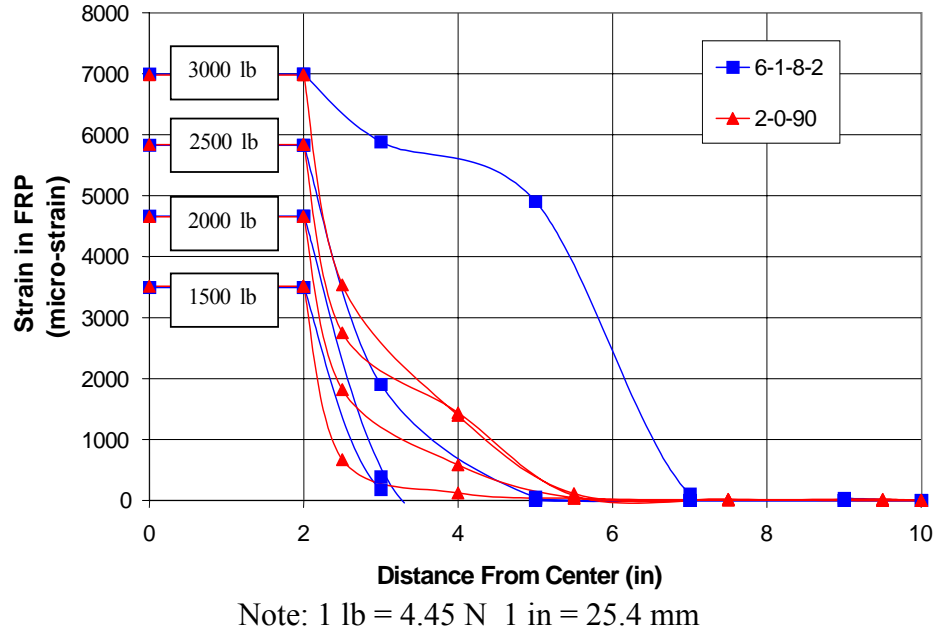


Figure 5.14: Contribution of Transverse Sheet (2-inch (51-mm) Width)

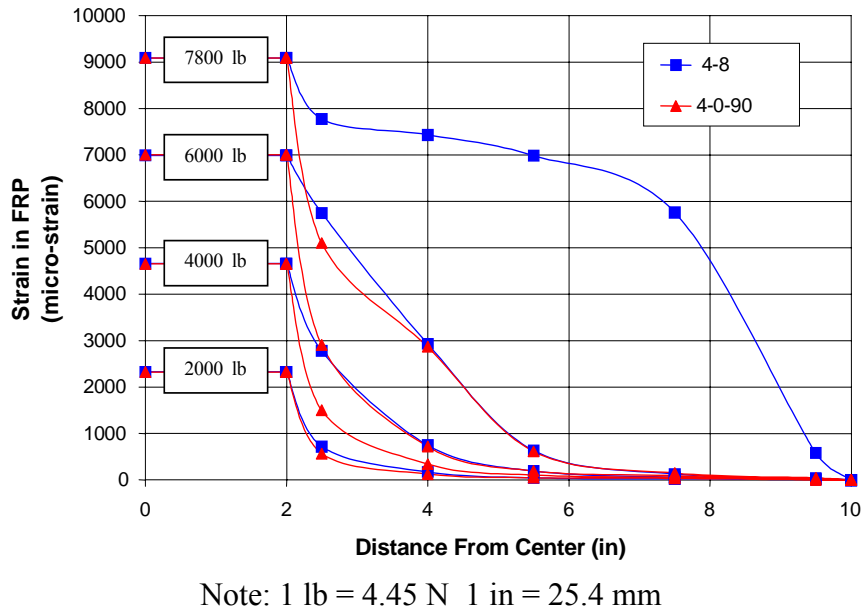


Figure 5.15: Contribution of Transverse Sheet (4-inch (102-mm) Width)

5.6 SURFACE PREPARATION

Table 5.7 shows the difference between specimens with only sandblasted surfaces and a specimen with a surface that was sandblasted and roughened. The procedure for roughening the surface was discussed in Section 3. Figure 5.16 shows the surface of the concrete when sand blasting is used. Figure 5.17 shows the surface as roughened by a hammer and chisel. As the results indicate, the performance of the roughened surface is much better than the sand blasted surface. CFRP rupture was attained with the roughened surface.

Table 5.7: Comparison of Specimens with Different Surface Preparation

Specimen	Surface Preparation	Ultimate Load (lb)	Failure Mode
6-1-12-1	Sandblasted	3830	Peeling
6-1-12-2	Sandblasted	3390	Peeling
6-1-12-S	Roughened	5590	CFRP Rupture

Note: 1 lb = 4.45 kN



Figure 5.16: Sandblasted Surface



Figure 5.17: Roughened Surface

5.7 SUMMARY

In this section, the material that was presented in thus far will be summarized in order to draw overall conclusions.

- The bonded length did not have any effect on the ultimate load of the sheet.
- The concrete strength did not affect the average bond strength because the failure was occurring in the concrete-epoxy interface.
- The number of plies did increase the average bond strength, but the increase from one to two plies did not cause the average bond strength to double. Therefore, it was concluded that the addition of more plies causes the failure to occur at a lower level of normal stress.
- The width of the CFRP sheet was found to have no effect on the average bond strength.
- The addition of a transverse sheet causes the average bond strength to increase considerably by preventing the peeling failure from occurring.

- The roughening of the concrete surface before application of CFRP sheets proved to be the most effective means of improving the average bond strength.
- As the surface becomes rougher, the concrete strength will have an effect on the bond strength because the failure could initiate in the concrete.

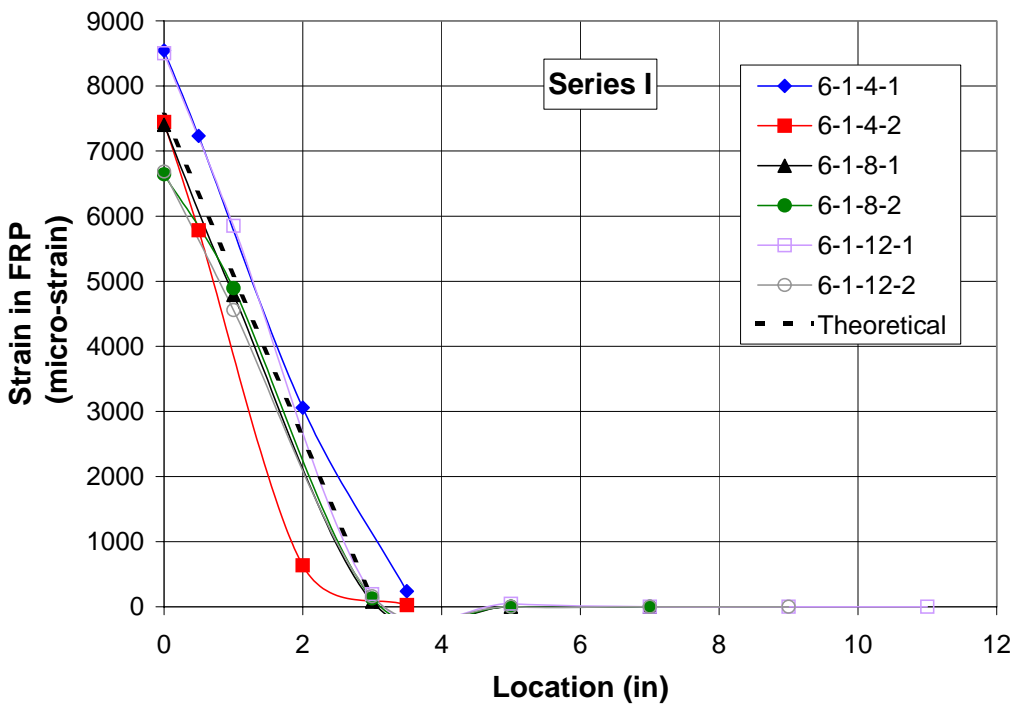
6. MODELING OF RESULTS

In this section, a model to predict the effective bonded length and ultimate load of CFRP sheets based on the results displayed in Section 4 was developed. In order to develop this model, the work by Maeda et al. (1997) was analyzed. Modifications were made to their model and a new model was developed. After the model was developed, a design example was given to demonstrate the use of the equations from the model.

6.1 ANALYTICAL MODEL

The first step in developing the model for the ultimate load of the specimens was to quantify the effective bond length of the sheet. This was accomplished by utilizing the linear shape of the strain distribution at the ultimate stage (see Figure 6.1). Maeda et al. (1997) and Brosens and Van Gemert (1997) also noted the linear shape of the strain distribution. Experimentally, for each specimen a value of the slope ($d\varepsilon/dx$) of the linear portion of the strain location curve was found. The curves used to calculate the slopes are shown in Figure 6.1 and Figure 6.2 for Series I and II respectively. The curves chosen were the strain distributions just before peeling occurred. It should be noted that the value of zero on the x-axis corresponds to the start of the bonded region. The values of $d\varepsilon/dx$ are shown in Table 6.1 for Series I and Table 6.2 for Series II. As can be seen, the value for $d\varepsilon/dx$ is larger for Series I than Series II. Also shown in these two tables is the load that corresponds to the curve from which $d\varepsilon/dx$ was obtained. The strain was then calculated from the load using equation (6-1), and the effective bond length, L_e , was then calculated by equation (6-2). The values for 6-1-4-2 were not used in the calculation for the average, standard deviation, and coefficient of variation for Series I. Likewise, 6-2-4-1 and 6-2-4-2 were not used in the calculations for Series II. The reason for this was

because the value of $d\epsilon/dx$ for these specimens was considerably different as compared to the other specimens of the series. The values of the coefficient of variation based on the remaining specimens show that the results are very consistent. It was found that the effective bond length for Series I and II are very close to the same.



Note: 1 inch = 25.4 mm

Figure 6.1: Curves Used to Calculate $d\epsilon/dx$ for Series I

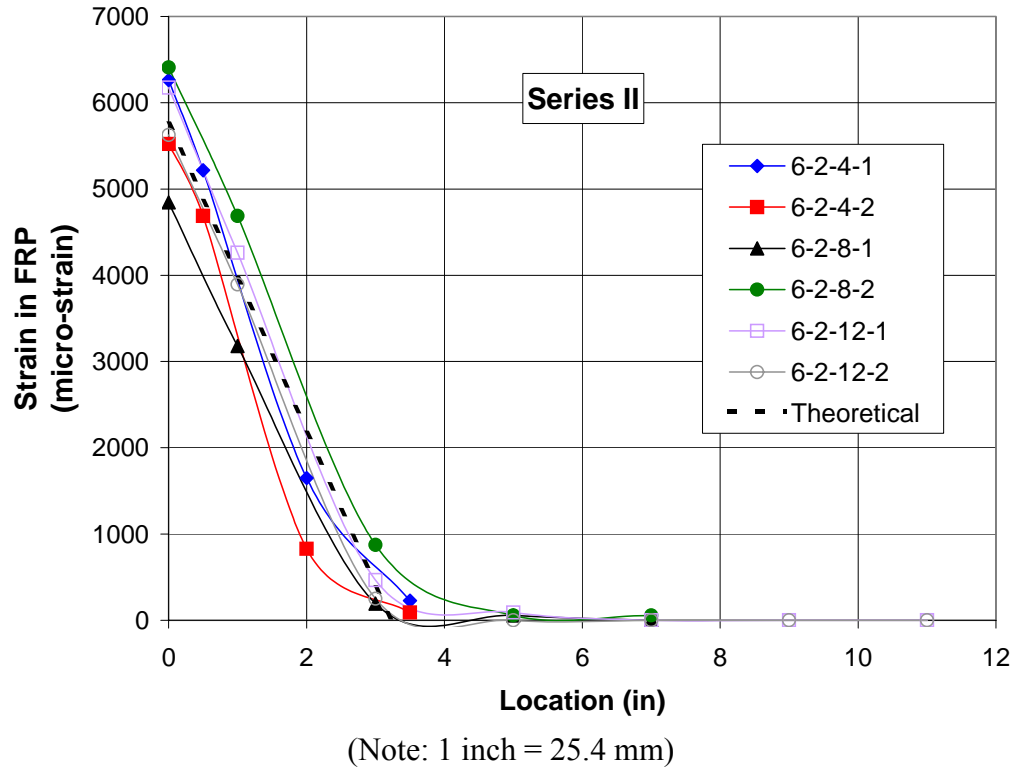


Figure 6.2: Curves Used to Calculate $d\varepsilon/dx$ for Series II

Table 6.1: Values Used to Find L_e (Series I)

Specimen	Load (lb)	$d\varepsilon/dx$ (μ/in)	ε_{max} ($\mu\varepsilon$)	L_e (in)
6-1-4-1	3666	2753	8545	3.10
6-1-4-2	3190	3410	7436	2.18
6-1-8-1	3176	2429	7403	3.05
6-1-8-2	2850	2207	6643	3.01
6-1-12-1	3650	2280	8508	3.06
6-1-12-2	2867	2179	6683	3.07
Average	3242	2470	7557	3.06
Standard Deviation	402	275	936	0.034
Coefficient of Variation	12.4%	11.1%	12.4%	1.1%

Note: 1 lb = 4.45 kN; 1 in = 25.4 mm

Table 6.2: Values Used to Find L_e (Series II)

Specimen	Load (lb)	$d\varepsilon/dx$ (μ/in)	ε_{max} ($\mu\varepsilon$)	L_e (in)
6-2-4-1	5372	2323	6261	2.70
6-2-4-2	4736	2397	5520	2.30
6-2-8-1	4156	1542	4844	3.14
6-2-8-2	5499	1853	6409	3.46
6-2-12-1	5300	1903	6177	3.25
6-2-12-2	4830	1796	5629	3.13
Average	4946	1774	5765	3.25
Standard Deviation	597	160	696	0.15
Coefficient of Variation	12.1%	9.0%	12.1%	4.7%

Note: 1 lb = 4.45 kN; 1 in = 25.4 mm

$$\varepsilon_{max} = \frac{P_{max}}{nt_f w_f E_f} \times 10^6 \quad (6-1)$$

$$L_{e-exp} = \frac{\varepsilon_{max}}{\left(\frac{d\varepsilon}{dx}\right)} \quad (6-2)$$

ε_{max} = Strain corresponding to ultimate load ($\mu\varepsilon$)

P_{max} = Ultimate load (kips or kN)

n = Number of plies

t_f = thickness of CFRP sheet (in or mm)

E_f = Modulus of Elasticity (ksi or GPa)

w_f = width of CFRP sheet (in or mm)

L_{e-exp} = Effective bond length found experimentally (in or mm)

$(d\varepsilon/dx)$ = Slope of the strain distribution curve (μ/in or μ/mm)

The values for L_e shown in Table 6.1 and Table 6.2 were plotted versus the stiffness of the CFRP sheet and can be seen in Figure 6.3. The stiffness is defined as the area multiplied by the tensile modulus of the sheet. However, for FRP sheets a unit width is often considered and the stiffness is considered the thickness multiplied by the tensile modulus. In Figure 6.4, the values reported by Maeda et al. (1997) and their analytical model are shown. The equation for the model is shown in equation (6-3). It can be seen that the results from Maeda et al. (1997) does not agree with the results presented by the current project. The reason for this is that Maeda et al. (1997) considered an average value for $d\varepsilon/dx$ for all stiffnesses. From this they calculated the effective bond length from equation (6-2). These are the values that are plotted in Figure 6.4. The problem with this approach is that since the maximum strain will decrease as the stiffness increases, the effective bond length also decreases. However, the data from this project seems to indicate that $d\varepsilon/dx$ decreases as the stiffness increases. Since the strain decreases also, the effective bond length stays constant. Therefore, it seems to be more appropriate to set the effective bond length to a constant and develop an equation for $d\varepsilon/dx$. Until more testing can be conducted, the conservative value of L_e should be assumed to be 3 in (76 mm). The values of $d\varepsilon/dx$ are plotted in Figure 6.5. A linear approximation is also plotted. Equation (6-4) is the equation for this line.

$$L_{e-M} = \frac{\exp\left[6.134 - 0.58 \ln\left(\frac{nt_f \times E_f}{5.71}\right)\right]}{25.4} \quad (6-3)$$

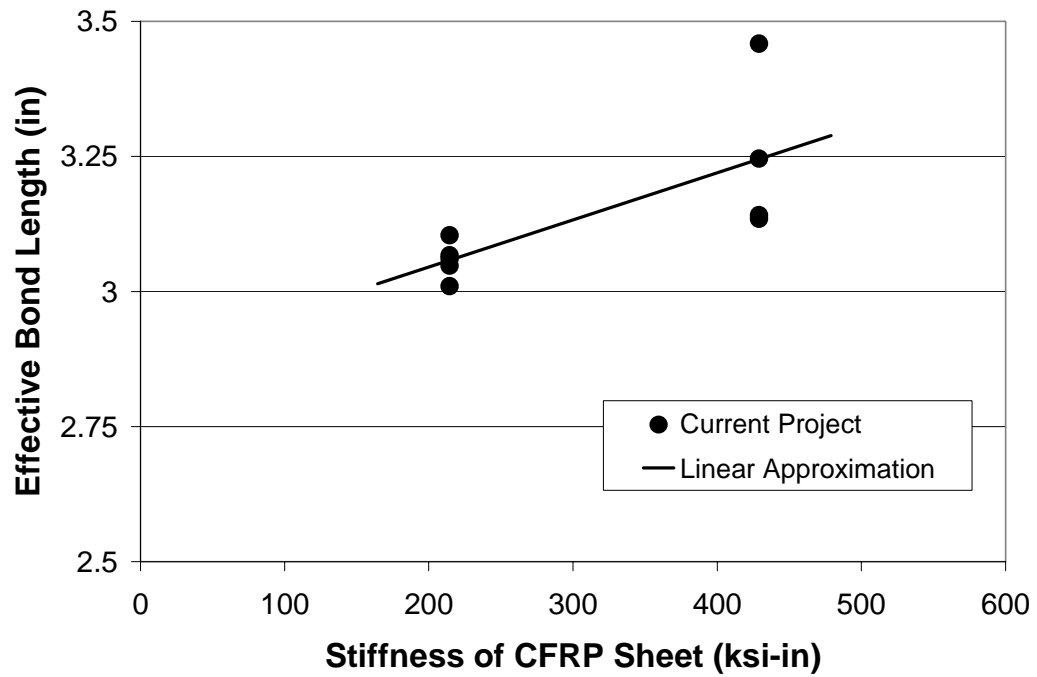
$$L_{e-M} = \exp[6.134 - 0.58 \ln(nt_f E_f)] \quad (6-3M)$$

L_{e-M} = Effective bond length calculated by Maeda et al. (1997) (in or mm)

$$\frac{d\varepsilon}{dx} = -2.915(nt_f E_f) + 3024 \quad (6-4)$$

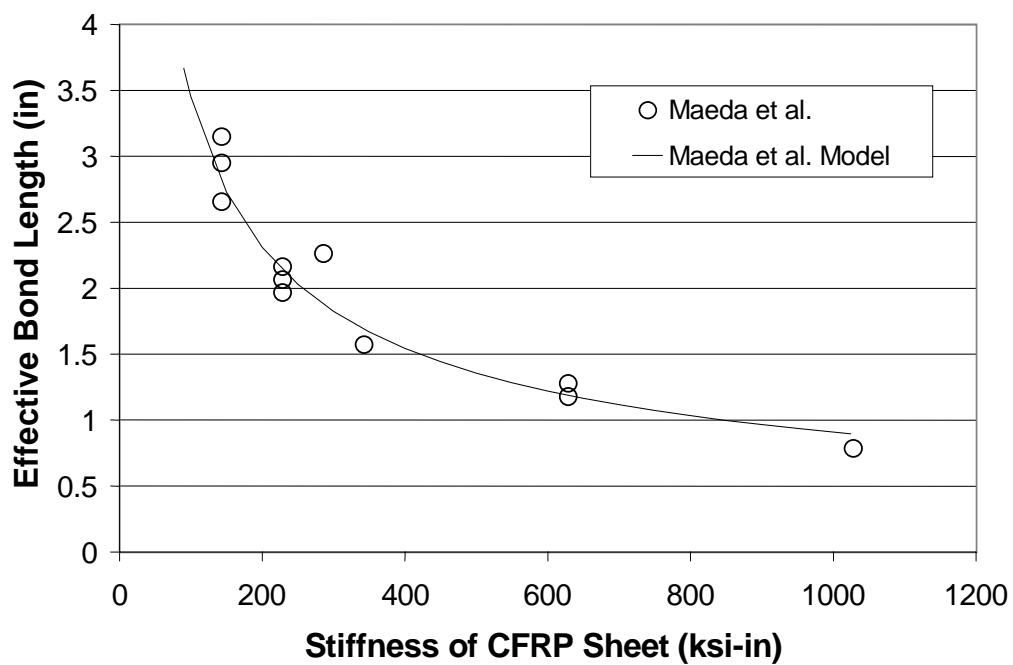
$$\frac{d\varepsilon}{dx} = -0.654(nt_f E_f) + 119.06 \quad (6-4M)$$

Note for equation (6-3) and (6-4), the units for t_f is in. and E_f is ksi. In equation (6-3M) and (6-4M), the units for t_f is mm and E_f is GPa.



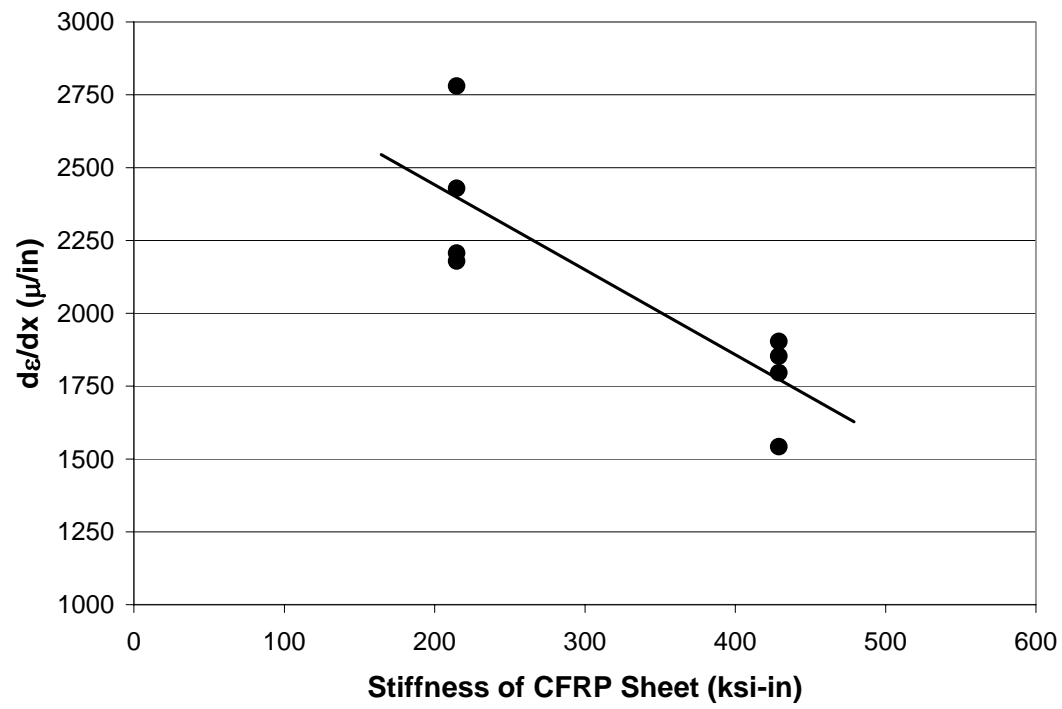
(Note: 1 inch = 25.4 mm; 1ksi-in = 5.71 GPa-mm)

Figure 6.3: Effective Bond Length vs. Stiffness



(Note: 1 inch = 25.4 mm; 1ksi-in = 5.71 GPa-mm)

Figure 6.4: Effective Bond Length vs. Stiffness (Maeda et al.)



(Note: 1 inch = 25.4 mm; 1ksi-in = 5.71 GPa-mm)

Figure 6.5: $d\epsilon/dx$ vs. Stiffness

If the bond stress, τ , is taken as the average bond stress over the effective bonded length, the force P in can be expressed by equation (6-5).

$$P_{\max} = \tau \times L_e \times w_f \quad (6-5)$$

The shear stress, τ , can be found by equilibrium of forces from Figure 6.6. If $P_1 > P_2$, then equation (6-6) can be written.

$$P_1 - P_2 = \tau w_f dx \quad (6-6)$$

The force P can be expressed in terms of strain as in equation (6-7). Equation (6-7) can be substituted into equation (6-6) and noting that E , t , and w are constant gives equation (6-8).

$$P = nt_f w_f \epsilon_f E_f \quad (6-7)$$

$$(\epsilon_1 - \epsilon_2) E_f nt_f w_f = \tau w_f dx \quad (6-8)$$

$(\epsilon_1 - \epsilon_2)$ can be expressed as shown in equation (6-9). Substituting (6-9) into (6-8) and solving for τ gives equation (6-10).

$$(\epsilon_1 - \epsilon_2) = \Delta\epsilon = d\epsilon \quad (6-9)$$

$$\tau = nt_f E_f \left(\frac{d\epsilon}{dx} \right) \times 10^{-6} \quad (6-10)$$

τ = Average bond stress (ksi or GPa)

Substituting equation (6-4) into equation (6-10) gives equation (6-11). Note that for equation (6-11) t_f is in inches and E_f is in ksi, and for (6-11M) t_f is in mm and E_f is in GPa.

$$\tau = [-2.915(nt_f E_f)^2 + 3024(nt_f E_f)] \times 10^{-6} \quad (6-11)$$

$$\tau = [-0.654(nt_f E_f)^2 + 119.06(nt_f E_f)] \times 10^{-6} \quad (6-11M)$$

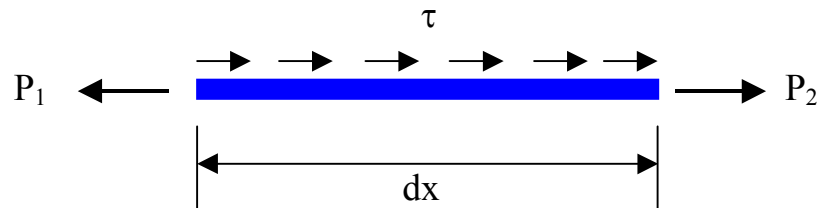


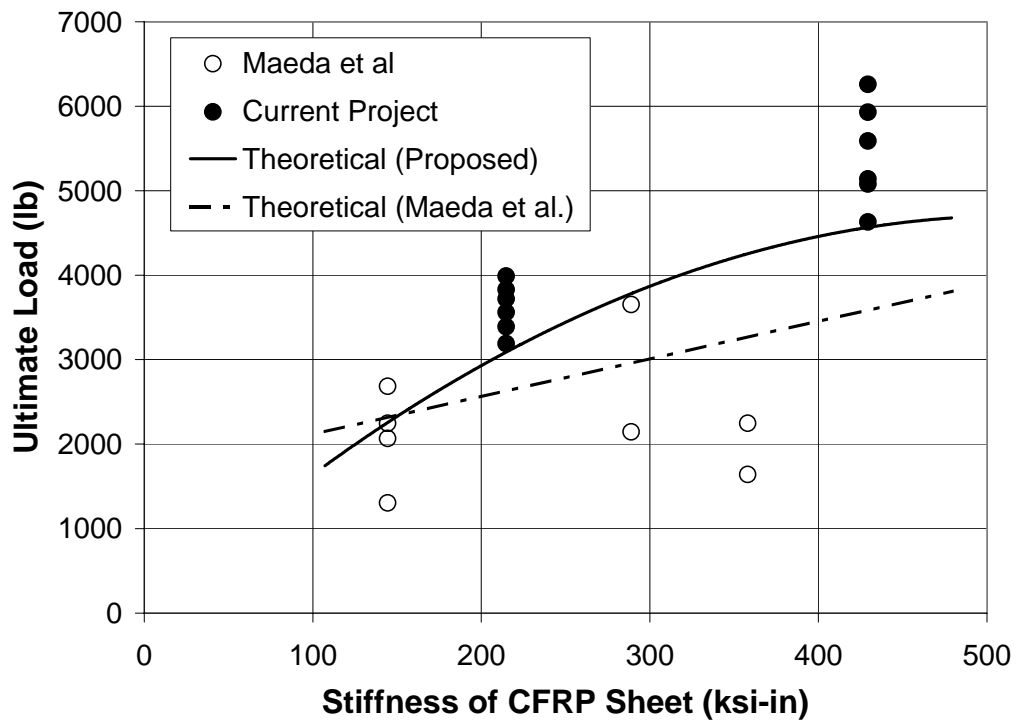
Figure 6.6: Free-Body Diagram of Sheet with Length dx

To summarize the above discussion, the key equations of the model are shown below. Also, since only a limited range of stiffnesses has been tested thus far, limits were placed on the equations. These limits can be removed once more testing has been conducted. Using these equations, the ultimate load was plotted versus the stiffness of the sheet (see Figure 6.7). Also shown on the graph are the experimental values of load versus stiffness. It can be seen that the loads for the current research are higher than the values shown by Maeda et al. (1997). This can be explained by the results of research by Horiguchi and Saeki (1997). They reported that the shear test, which is the test used by Maeda et al. (1997), produces lower ultimate loads than the flexure test.

$$L_e = 3.0 \text{ in} \quad (200 \text{ ksi-in} < n t_f E_f < 450 \text{ ksi-in})$$

$$\tau = [-2.915(n t_f E_f)^2 + 3024(n t_f E_f)] \times 10^{-6} \quad (200 \text{ ksi-in} < n t_f E_f < 450 \text{ ksi-in})$$

$$P_{\max} = \tau \times L_e \times w_f$$



(Note: 1 lb = 4.45 kN; 1ksi-in = 5.71 GPa-mm)

Figure 6.7: Ultimate Load vs. Stiffness of CFRP Sheet

6.2 DESIGN RECOMMENDATIONS

The following section addresses the design considerations that should be made to address the peeling failure. Currently, the ultimate stress of the CFRP sheet for design is based on the ultimate tensile strength of the sheet. There has been no consideration made

for the possibility of premature failure due to peeling. The results of this thesis have shown that if the surface preparation is not sufficient, the failure can occur due to peeling. The problem at present is that there is no means to specify the amount of roughness the concrete surface needs to achieve sufficient bond strength. Therefore, the author recommends that until the effect of surface preparation is better understood, peeling failure should be considered when designing with CFRP sheets.

A design example from the MBrace Design Guidelines (1998) is shown in Appendix C. It can be seen in this design example that no consideration for premature failure due to peeling is made. The design was modified using peeling as the controlling failure at ultimate. The steps in design are the same except the peeling stress must be determined initially and used as the ultimate stress of the CFRP sheet. This value can be calculated using the equations presented in this section.

$$L_e = 3.0 \text{ in}$$

$$\tau = -2.915(nt_f E_f)^2 + 3024(nt_f E_f)$$

$$\tau = -2.915(1 \times 0.0065 \text{ in} \times 33000 \text{ ksi})^2 + 3024(1 \times 0.0065 \text{ in} \times 33000 \text{ ksi}) = 0.5145 \text{ ksi}$$

$$f_{fp} = \frac{\tau L_e}{nt_f}$$

$$f_{fp} = \frac{0.5145 \text{ ksi} \times 3.0 \text{ in}}{1 \times 0.0065 \text{ in}} = \underline{\underline{237 \text{ ksi}}}$$

Some of the key values from the ultimate design method are shown in Table 6.3 for the two cases. It can be seen that the width of the sheet is dramatically increased if peeling failure is considered. Also, the strain in the concrete and steel decreased when peeling was considered. This is because the strain in the FRP is decreased. Table 6.4

shows the key values at service loads. It can be seen that the service loads did not change much when peeling was considered. This is because the stresses are very low at service already, and the change does not affect the stresses dramatically.

Table 6.3: Values for the Ultimate Design

Failure Mode	f_{fu} (ksi)	Width of Sheet (in)	ϵ_{fu}	c (in)	ϵ_c	ϵ_s	ϕM_n (k-ft)
FRP Rupture	550	4	0.017	2.323	0.00251	0.0152	68.4
Peeling	237	9	0.0072	2.830	0.00137	0.00661	67.6

Note: 1 ksi = 6.89 MPa; 1 in = 25.4 mm; 1 kip = 4450 kN; 1 ft = 305 mm

Table 6.4: Values for Service Loads

Failure Mode	k_d (in)	f_s (ksi)	f_c (psi)	f_f (ksi)	$f_{f,all}$ (ksi)
FRP Rupture	5.185	22.41	1106	15.76	112
Peeling	5.244	22.04	981	16.60	48.3

Note: 1 in = 25.4 mm; 1 ksi = 6.89 MPa; 1 psi = 6.89 kPa

7. RECOMMENDATIONS, CONCLUSIONS AND SUMMARY

7.1 RECOMMENDATIONS FOR FUTURE RESEARCH

There are several issues that should be clarified in the area of bond. Since only one type of FRP sheet was used in this research, other types should be investigated. In particular, sheets with different stiffnesses should be tested in order to improve the model that was presented in this thesis. Table 7.1 shows the recommended stiffnesses of sheet that should be tested to gain a better understanding of its effect. It should be noted that the values for thickness and tensile modulus are typical values. The purpose is to test a range of stiffnesses as shown in the last column. Also, a comparison between different fiber types with the same stiffness would be beneficial.

Table 7.1: Recommended Sheet Stiffness to Test

Fiber Type	Thickness (in)	Tensile Modulus (ksi)	Number of Plies	Stiffness (ksi-in)
E-Glass	0.014	10500	1	147
E-Glass	0.014	10500	2	294
Aramid	0.011	17000	1	187
Aramid	0.011	17000	2	374
High Modulus Carbon	0.0065	54000	1	351
High Strength Carbon	0.0065	33000	3	643.5
High Modulus Carbon	0.0065	54000	2	702
High Modulus Carbon	0.0065	54000	3	1053

Note: 1 in =25.4 mm; 1 ksi = 6.89 MPa

The testing of possible anchorage systems is also recommended. The particular anchorage system of interest is described by Khalifa et al. (1999). The system involves cutting a groove into the concrete, applying the sheet to the concrete, and anchoring the sheet in the groove. This can be accomplished either by using a rod and epoxy paste or by using paste alone as seen in Figure 7.1. This anchor can only be applied to the ends to prevent catastrophic failure from occurring. It will not improve the bond strength.

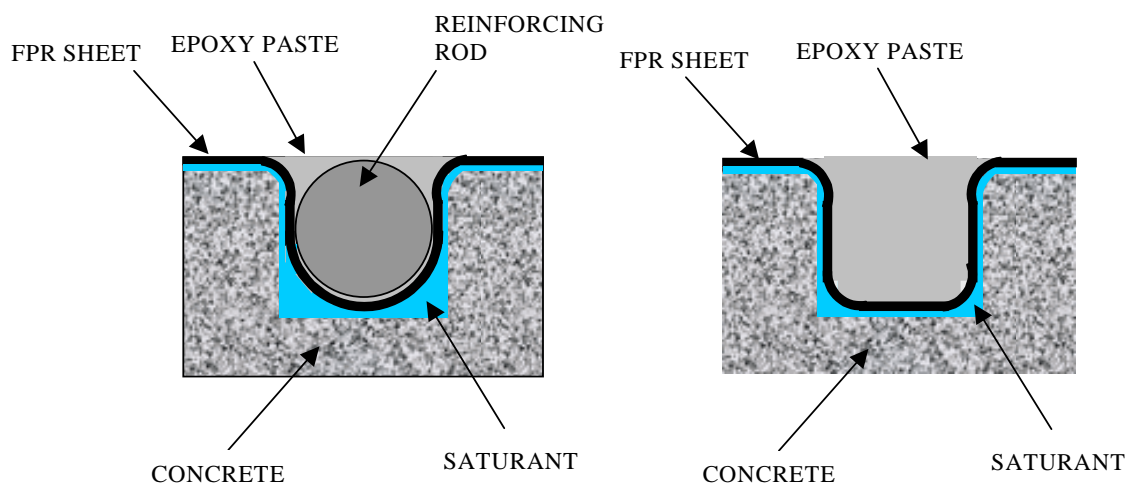


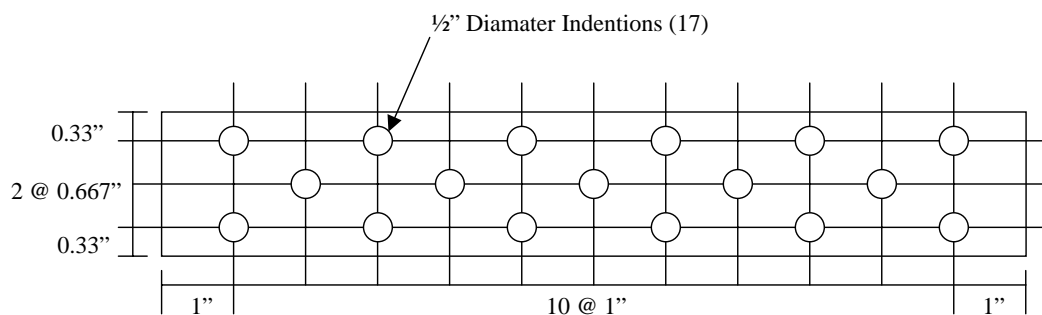
Figure 7.1: Anchor System for FRP Sheets

A test was conducted to determine whether improved surface preparation could cause the FRP to rupture before peeling occurred. A beam in which the surface was roughened as shown in Figure 7.2 was tested. The surface was roughened by making indentions in the concrete with a hammer and chisel in the locations shown in Figure 7.3.

The roughness of the surface is probably excessive, but the purpose of the testing was to see if a difference could be achieved. The test was successful in that CFRP rupture was attained.



Figure 7.2: Surface Before Application



Note: 1 in = 25.4 mm

Figure 7.3: Location of Indentations

From this test, it was concluded that the failure of CFRP sheets bonded to concrete seems to be controlled somewhat by the surface preparation. A study should be conducted to quantify the affect of different degrees of surface preparation. The common means of preparing the surface at present is by sandblasting. If this remains the method of choice, steps should be taken to quantify the amount of sandblasting required to attain sufficient bond strength to cause CFRP rupture. Also, other means of surface preparation should be considered.

7.2 CONCLUSIONS

As stated by several researchers, the use of FRP for reinforcement for concrete structures has emerged as an exciting and promising technology in materials and structural engineering (Nanni, 1995). However, there is still need for research to gain a better understanding of the behavior of the FRP materials.

The focus of this research has been on the bond between CFRP sheets and concrete. One of the main goals of this research was to address how the bonded length, compressive strength of concrete, and number of plies (stiffness) of CFRP affect bond.

The bonded length of the CFRP sheet had no affect on the bond strength of the CFRP sheets. This occurred because of the existence of an effective bond length. The effective bond length is less than the bonded length and is constant no matter the bonded length. This caused the failure load to be constant for each of the bonded lengths that were tested. This effective bond length has been reported by other researchers (Maeda et al, 1997; Takahashi et al, 1997; Brosens and Van Gemert, 1997; Bakis et al, 1998).

The concrete strength did not have an affect on the bond strength. The cause of this was that the peeling failure occurred in the concrete-epoxy interface. It seems that

the surface preparation has more of an effect than the actual concrete strength. However, as the surface is improved, the concrete strength should have more of an impact.

The number of plies (stiffness) of CFRP sheet was found to have an influence on the bond between CFRP and concrete. Based on the stiffness, a model was developed by modifying the model proposed by Maeda et al. (1997). The model predicts the load (or stress) at which the CFRP sheet will experience peeling failure. A design example was given to show how to use the model to design for peeling failure.

Other testing was also performed to see if the width of the sheet had an effect on the bond. It was found that the width does not affect the bond. Also tested was the influence that $0^\circ/90^\circ$ orientation of fibers has on the bond. It was found that this greatly increased the bond strength, and the failure mode was by fiber rupture instead of peeling.

7.3 SUMMARY

The research conducted in this investigation should be viewed as the foundation for future research on bond between CFRP sheets and concrete. The factors affecting the bond were addressed through an experimental investigation, and the results were analyzed and discussed. Based on the experimental results, a method for determining the stress at which peeling occurs was presented. Also, future work was suggested in order to build on the findings in this research.

APPENDIX A.

STRAIN vs. LOCATION DIAGRAMS

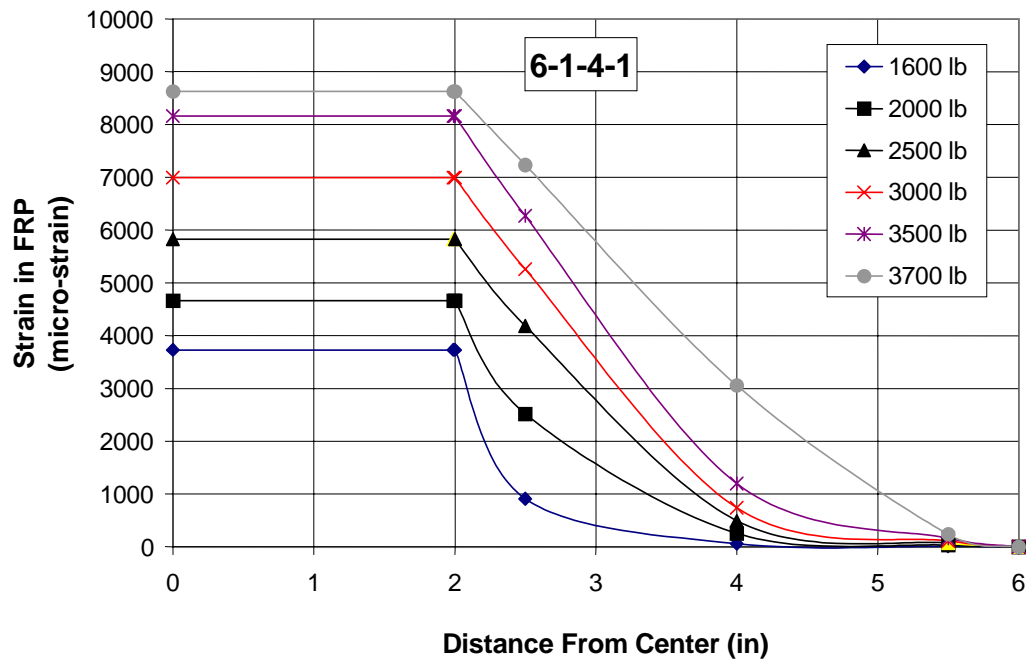


Figure A1: Strain-Location Diagram for 6-1-4-1

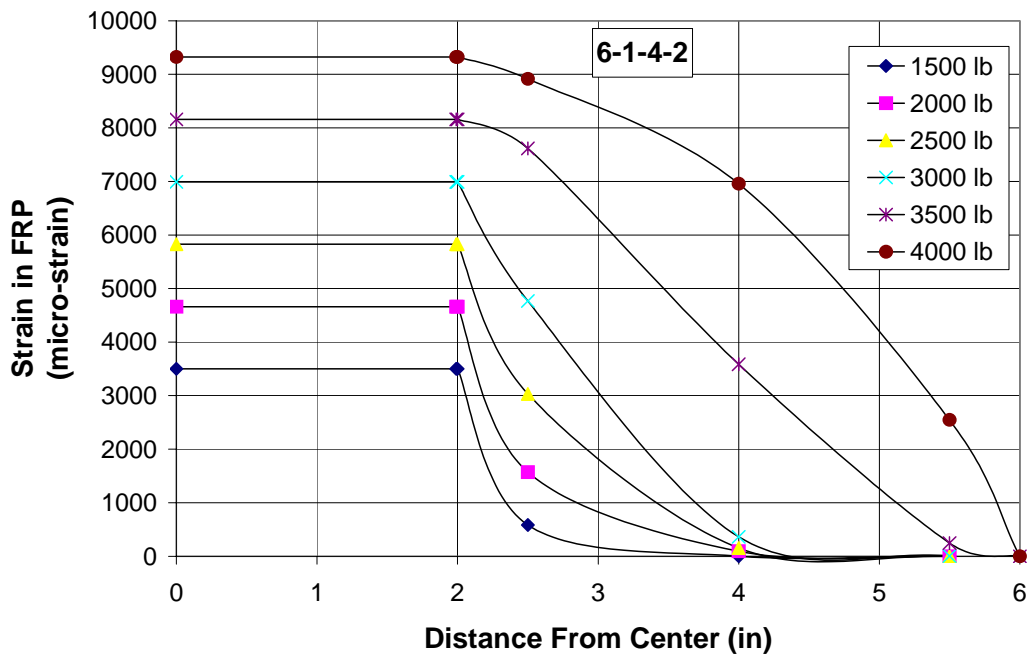


Figure A2: Strain-Location Diagram for 6-1-4-2

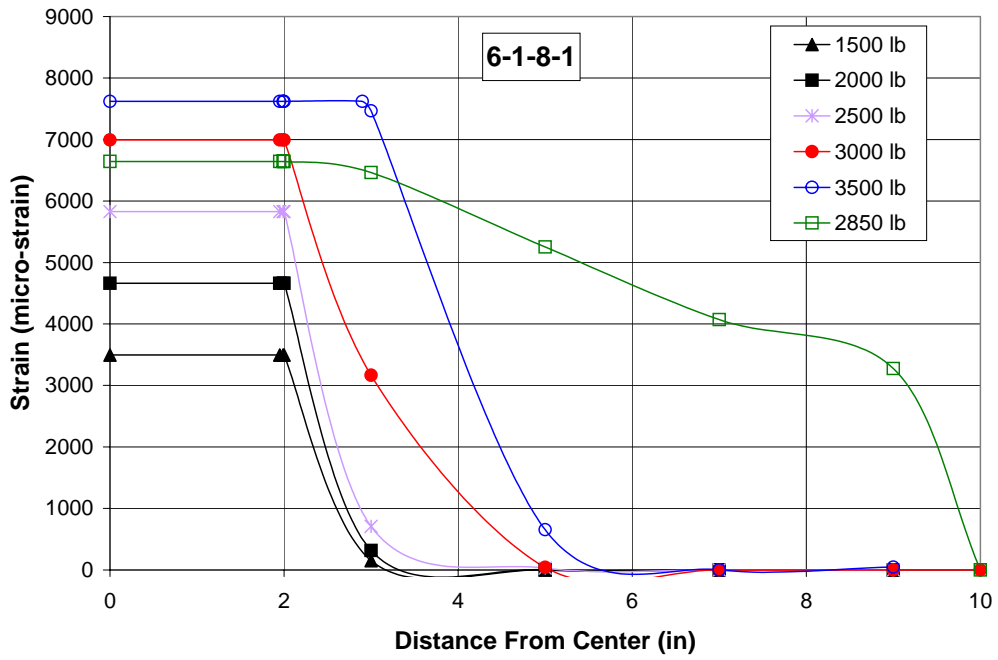


Figure A3: Strain-Location Diagram for 6-1-8-1

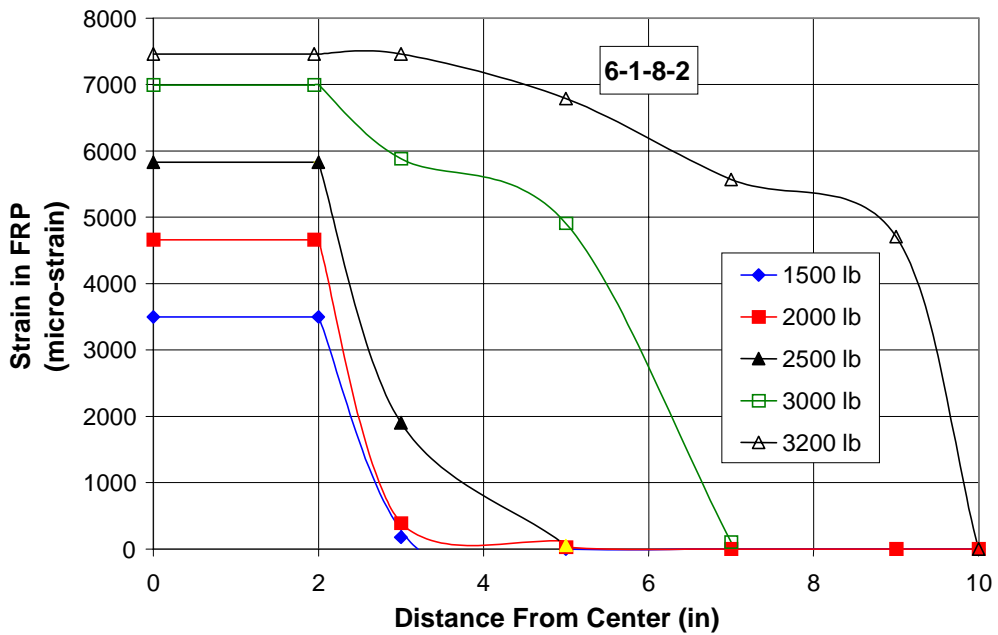


Figure A4: Strain-Location Diagram for 6-1-8-2

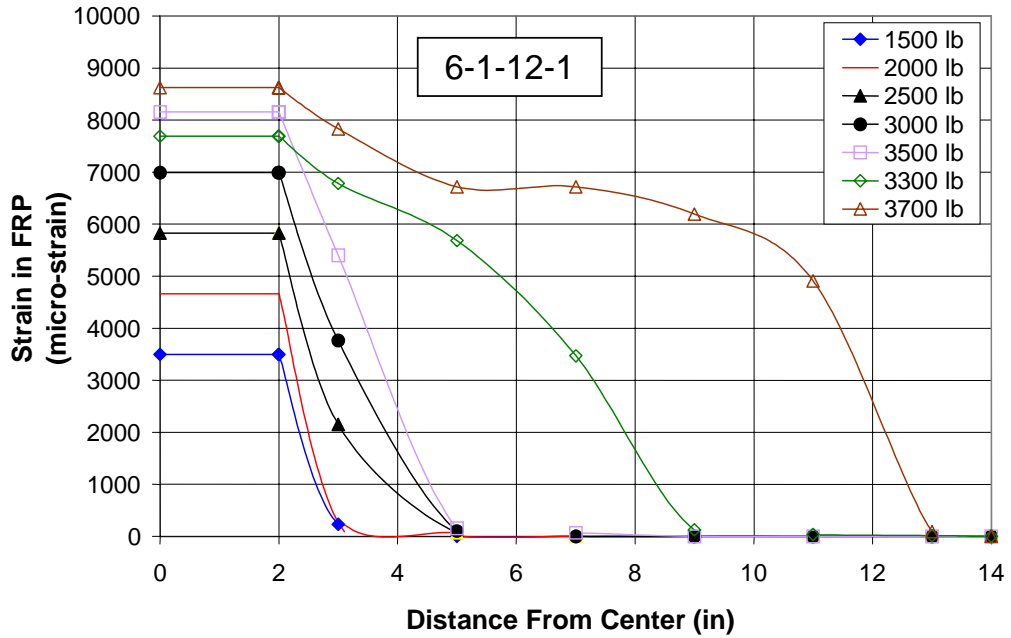


Figure A5: Strain-Location Diagram for 6-1-12-1

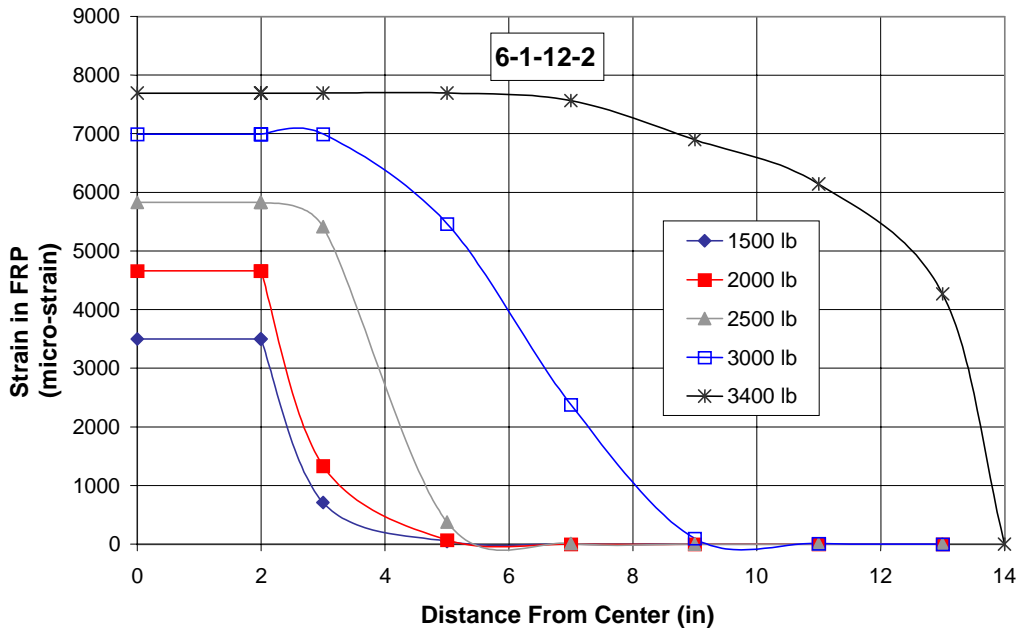


Figure A6: Strain-Location Diagram for 6-1-12-2

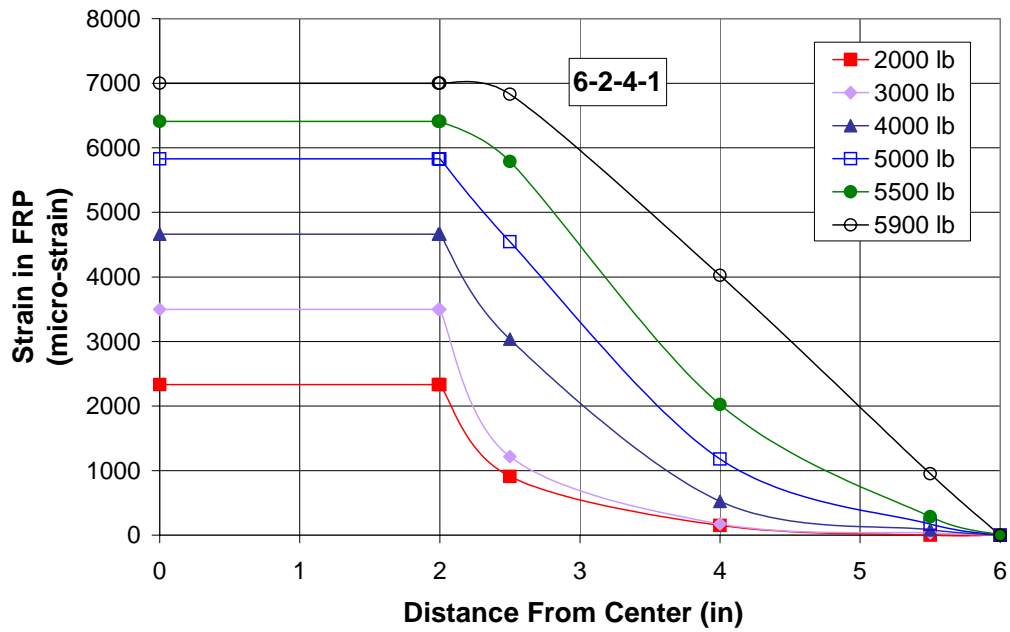


Figure A7: Strain-Location Diagram for 6-2-4-1

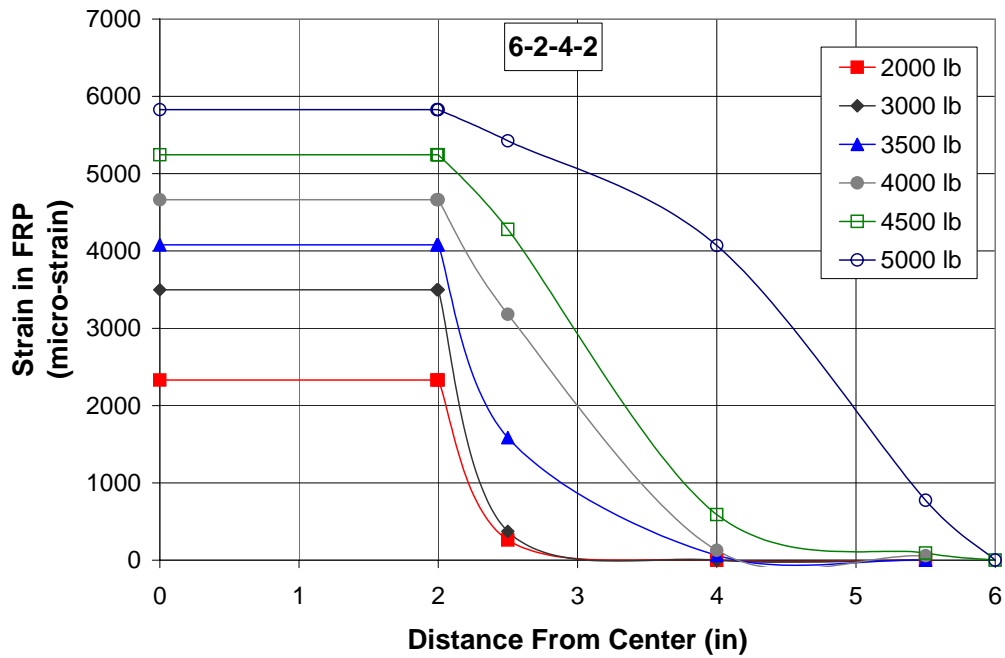


Figure A8: Strain-Location Diagram for 6-2-4-2

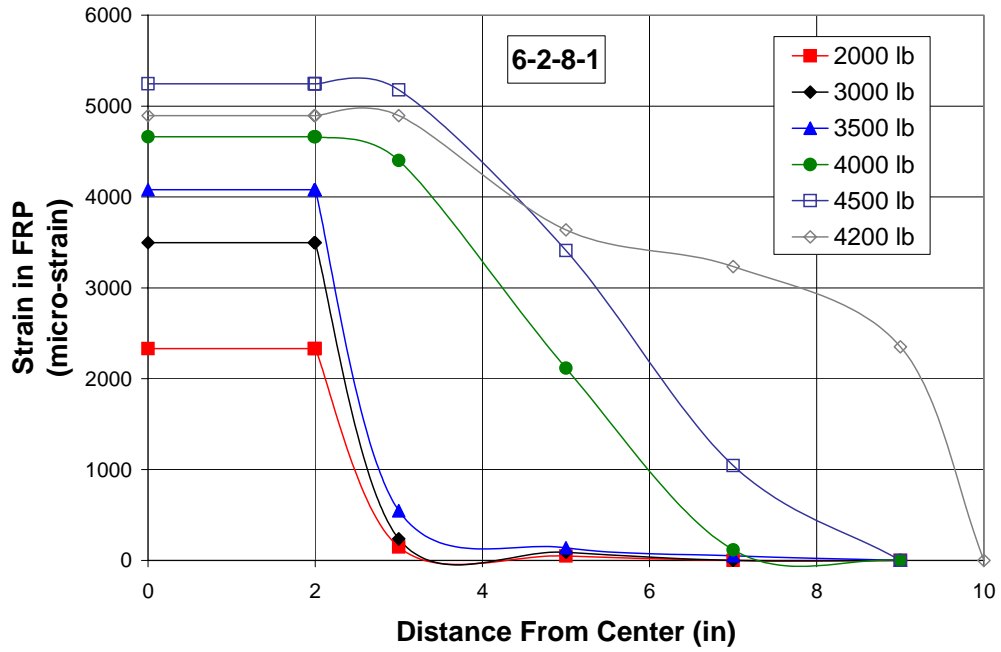


Figure A9: Strain-Location Diagram for 6-2-8-1

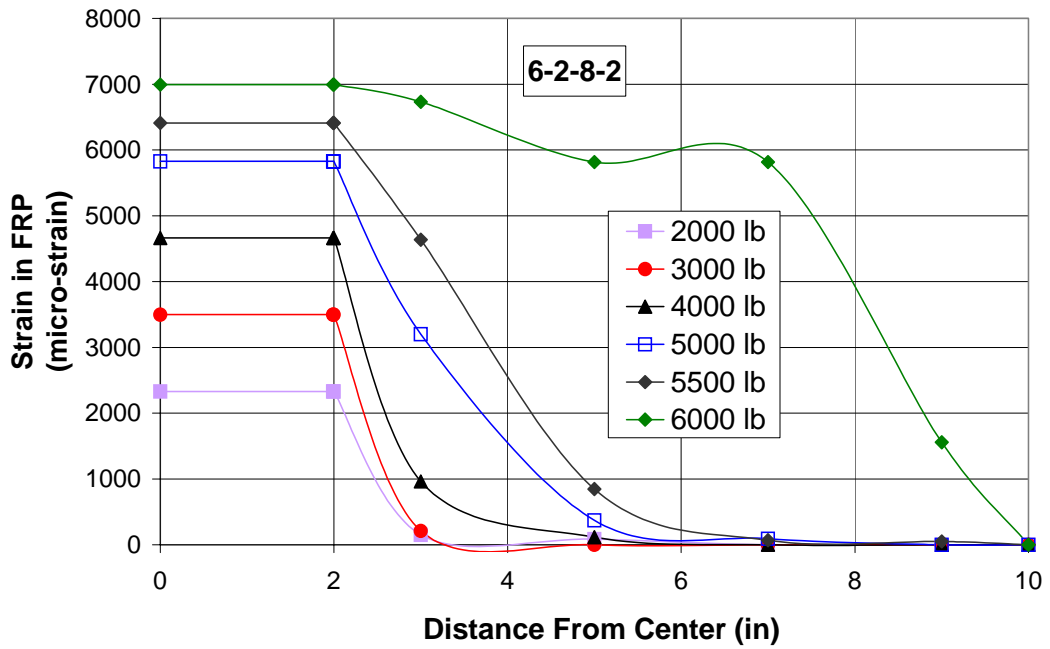


Figure A10: Strain-Location Diagram for 6-2-8-2

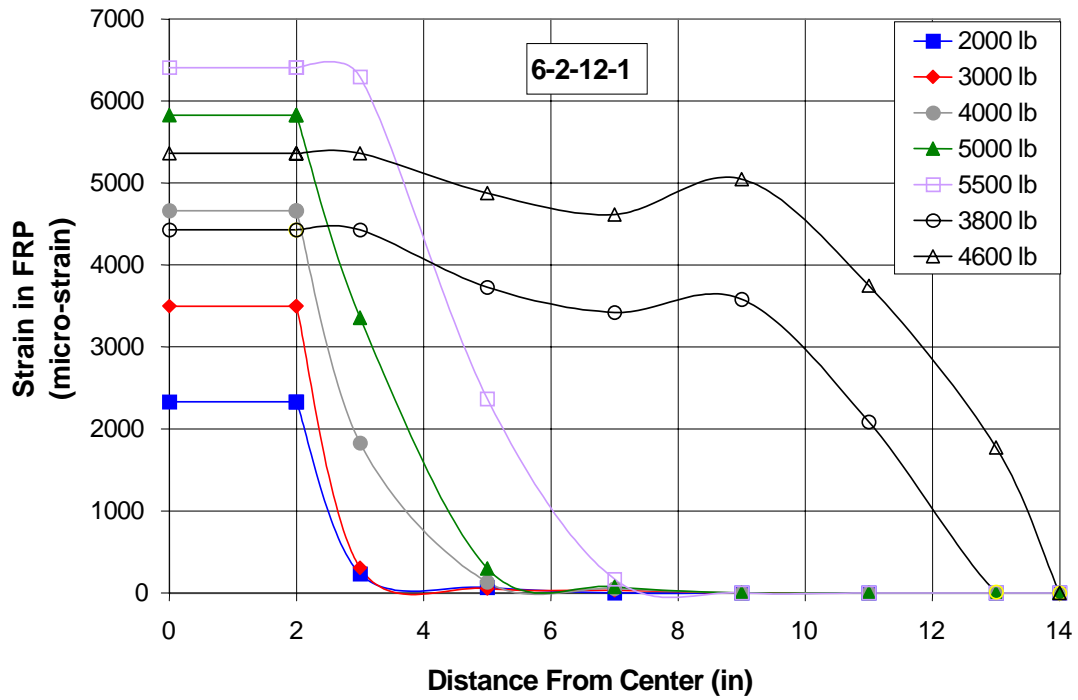


Figure A11: Strain-Location Diagram for 6-2-12-1

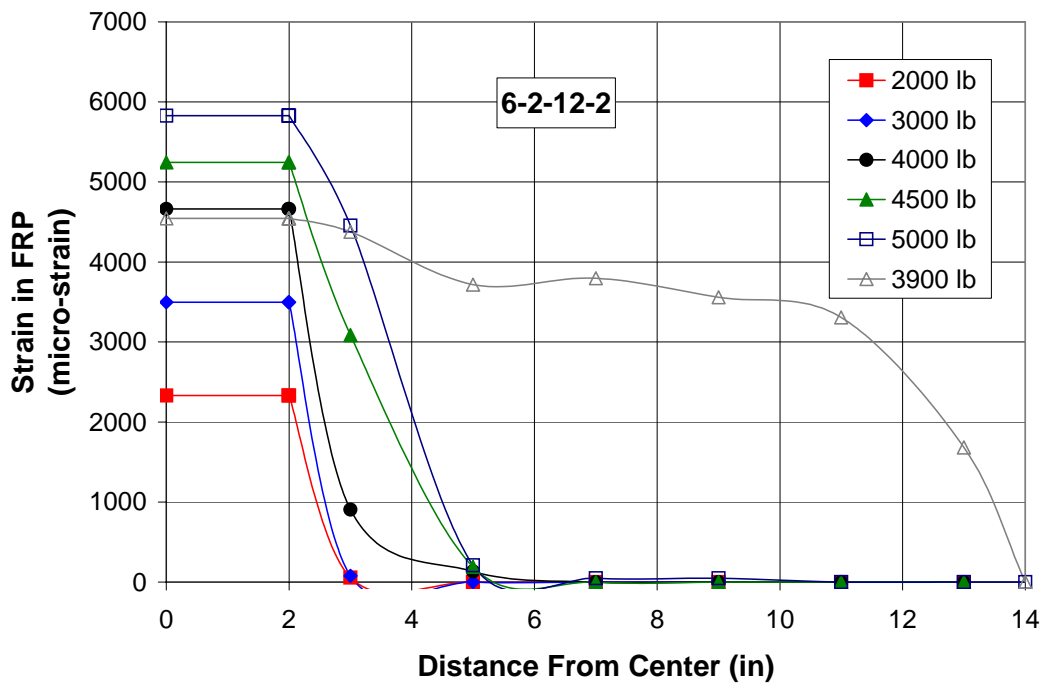


Figure A12: Strain-Location Diagram for 6-2-12-2

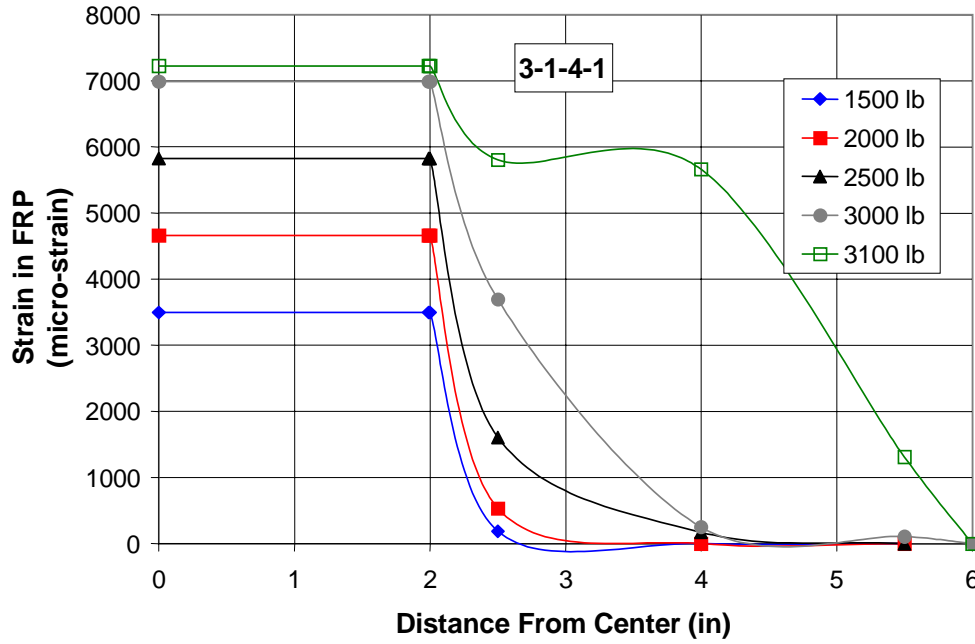


Figure A13: Strain-Location Diagrams for 3-1-4-1

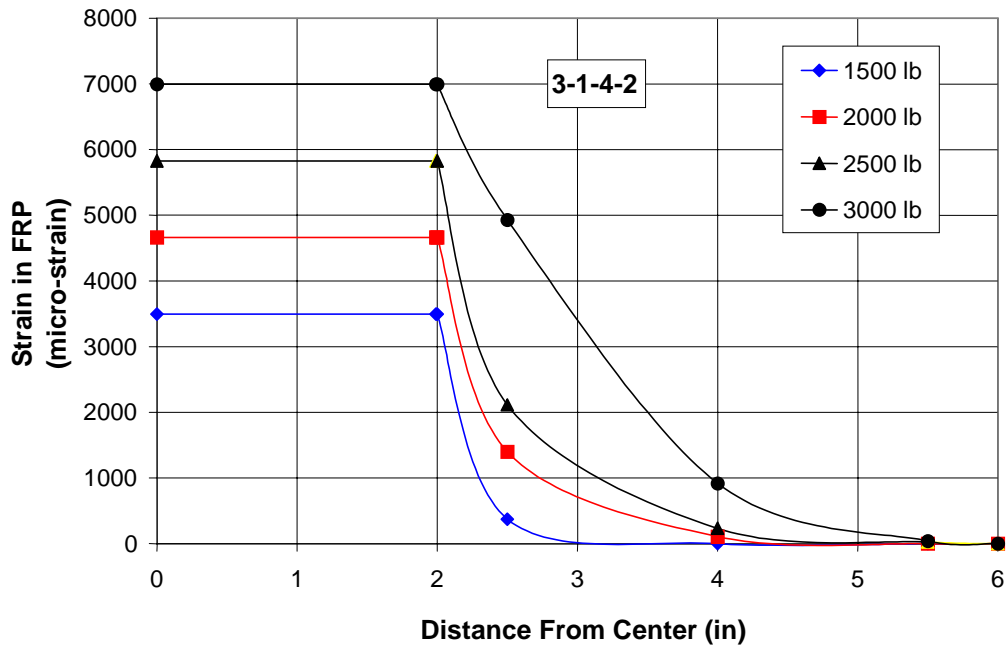


Figure A14: Strain-Location Diagrams for 3-1-4-2

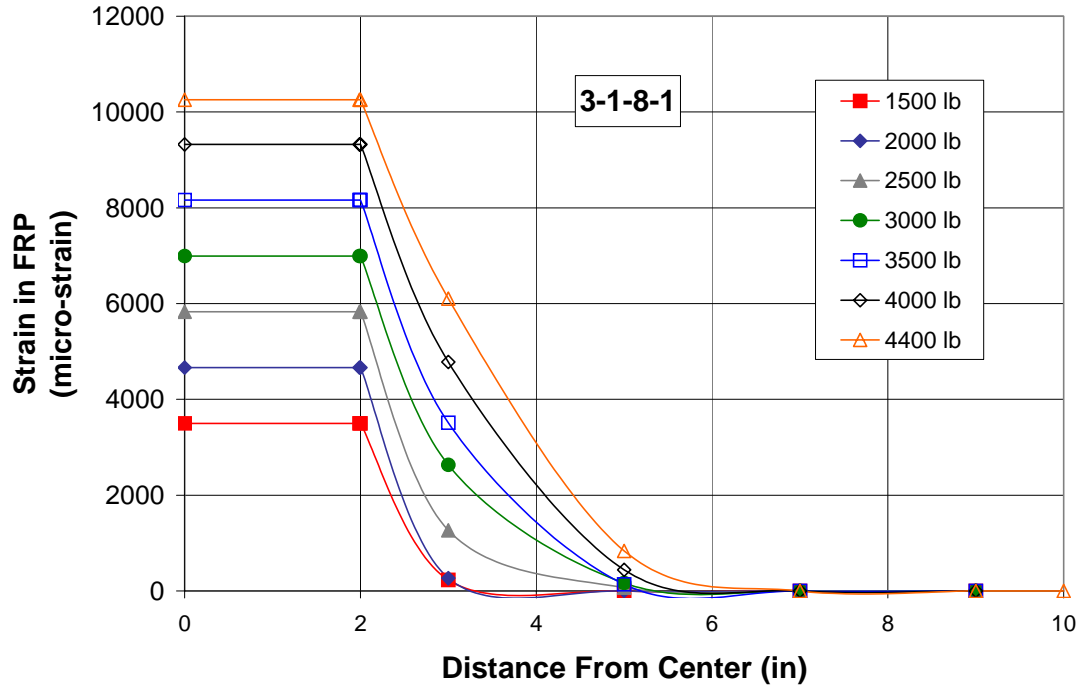


Figure A15: Strain-Location Diagram for 3-1-8-1

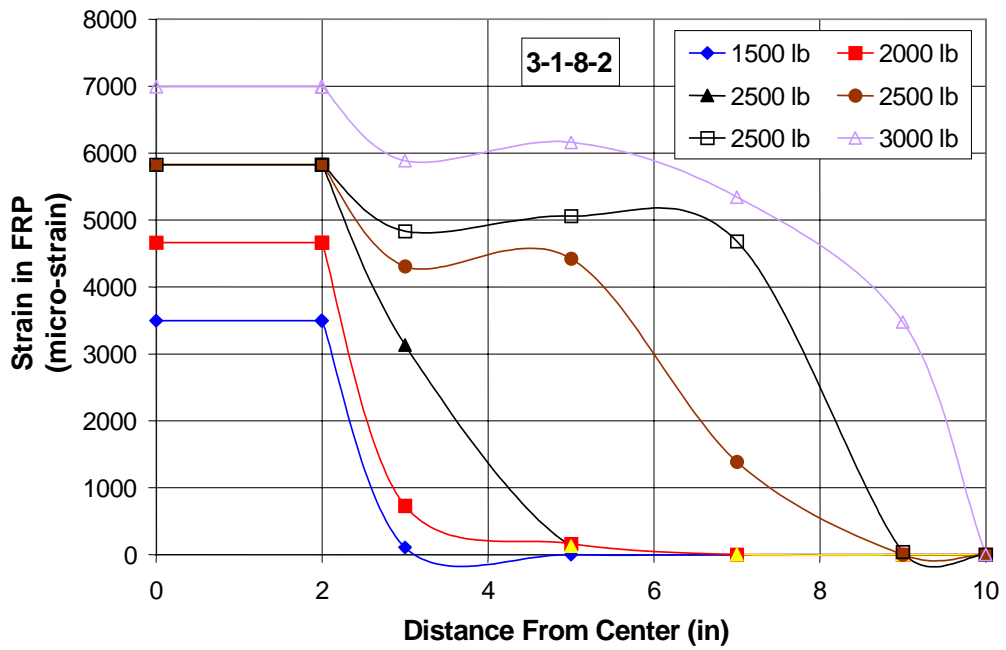


Figure A16: Strain-Location Diagram for 3-1-8-2

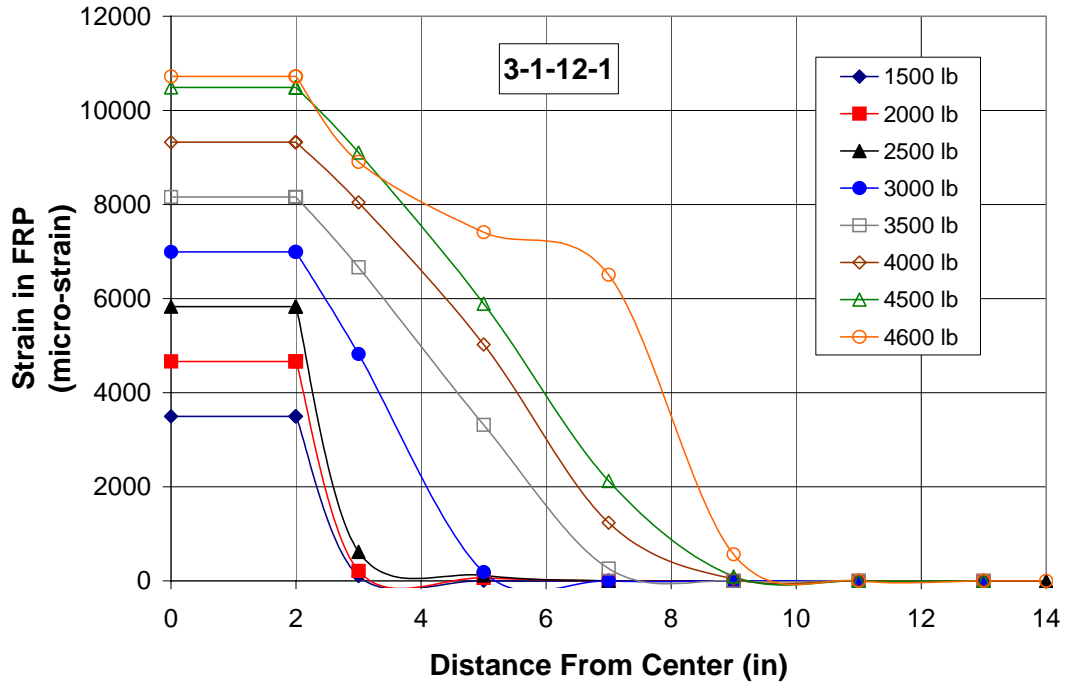


Figure A17: Strain-Location Diagram for 3-1-12-1

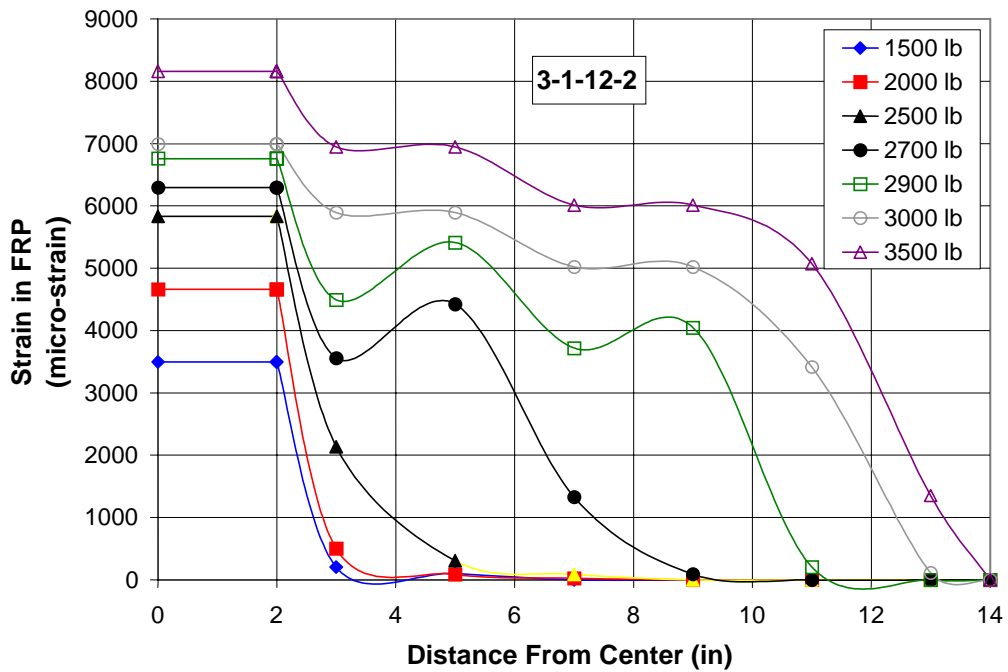


Figure A18: Strain-Location Diagram for 3-1-12-2

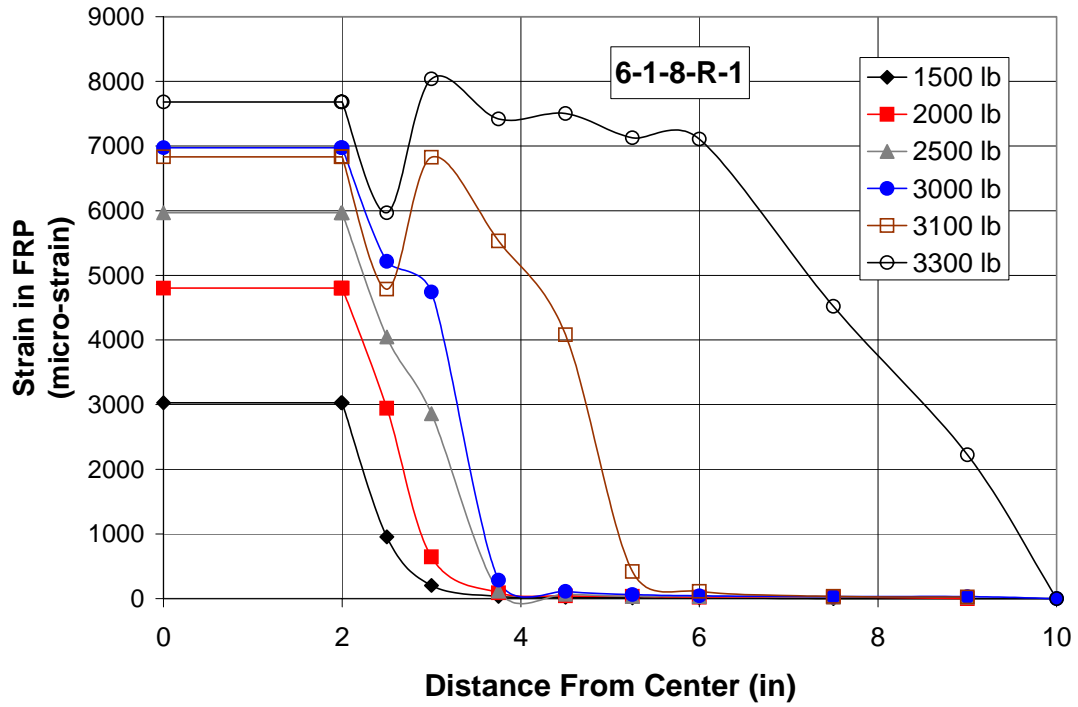


Figure A19: Strain-Location Diagram for 6-1-8-R-1

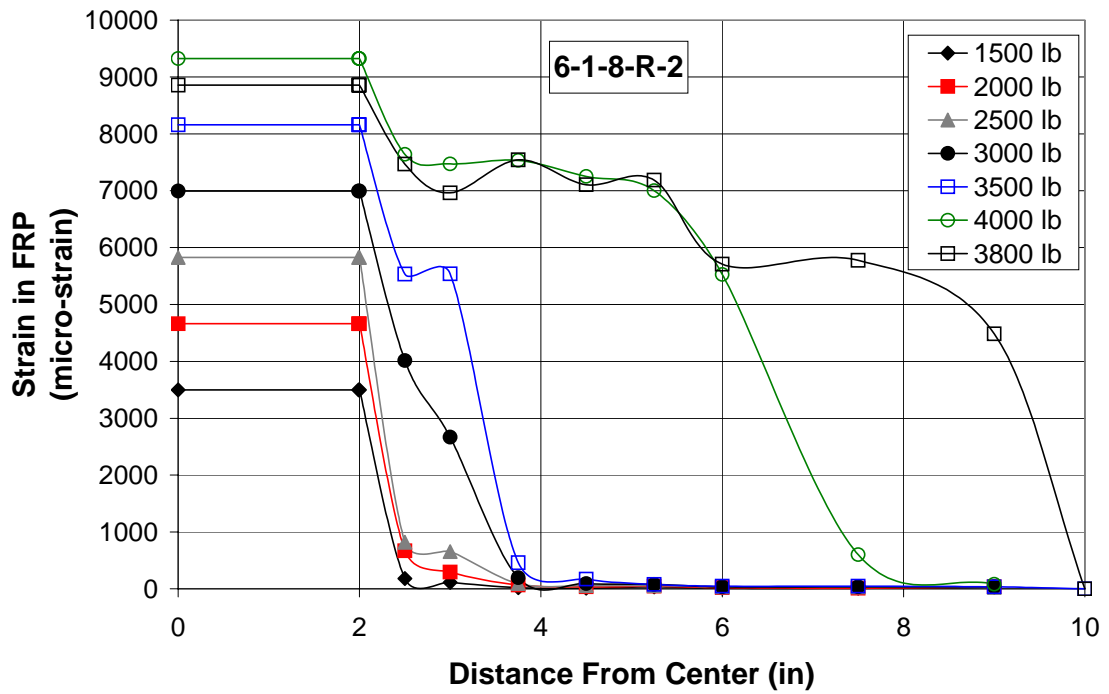


Figure A20: Strain-Location Diagram for 6-1-8-R-2

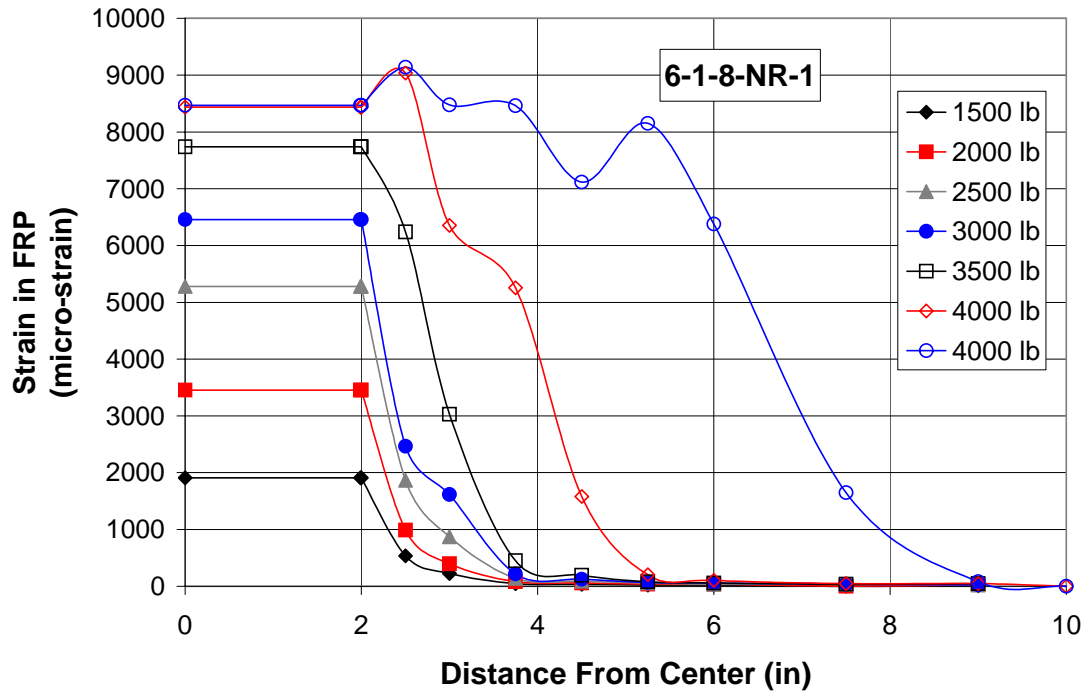


Figure A21: Strain-Location Diagram for 6-1-8-NR-1

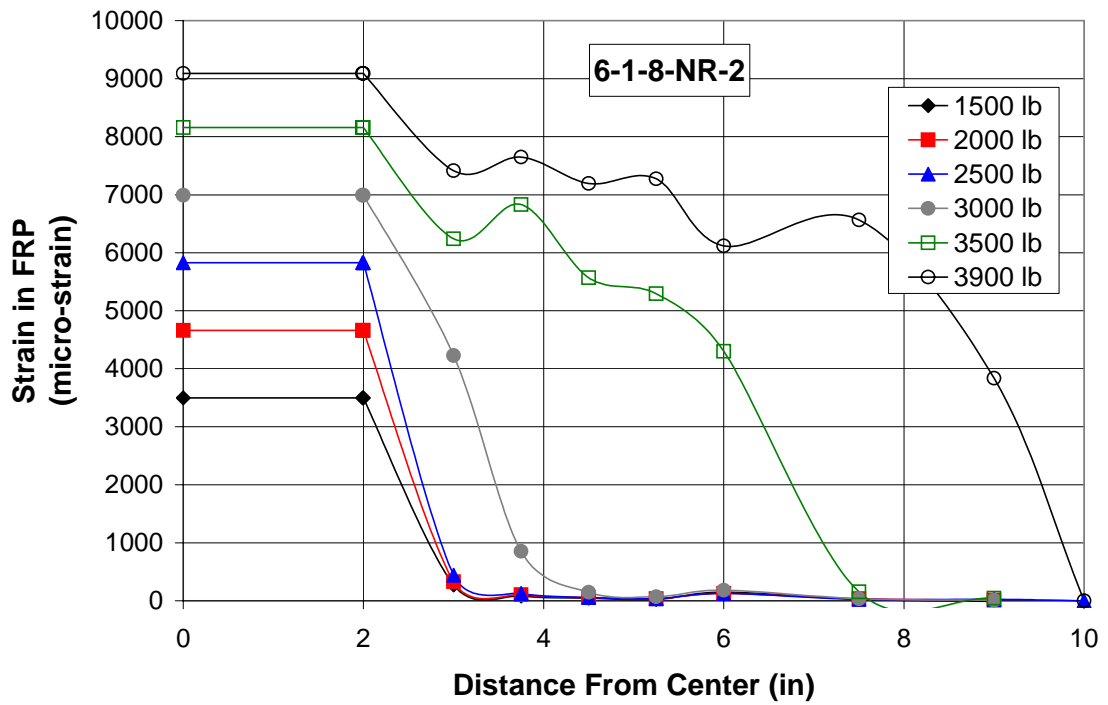


Figure A22: Strain-Location Diagram for 6-1-8-NR-2

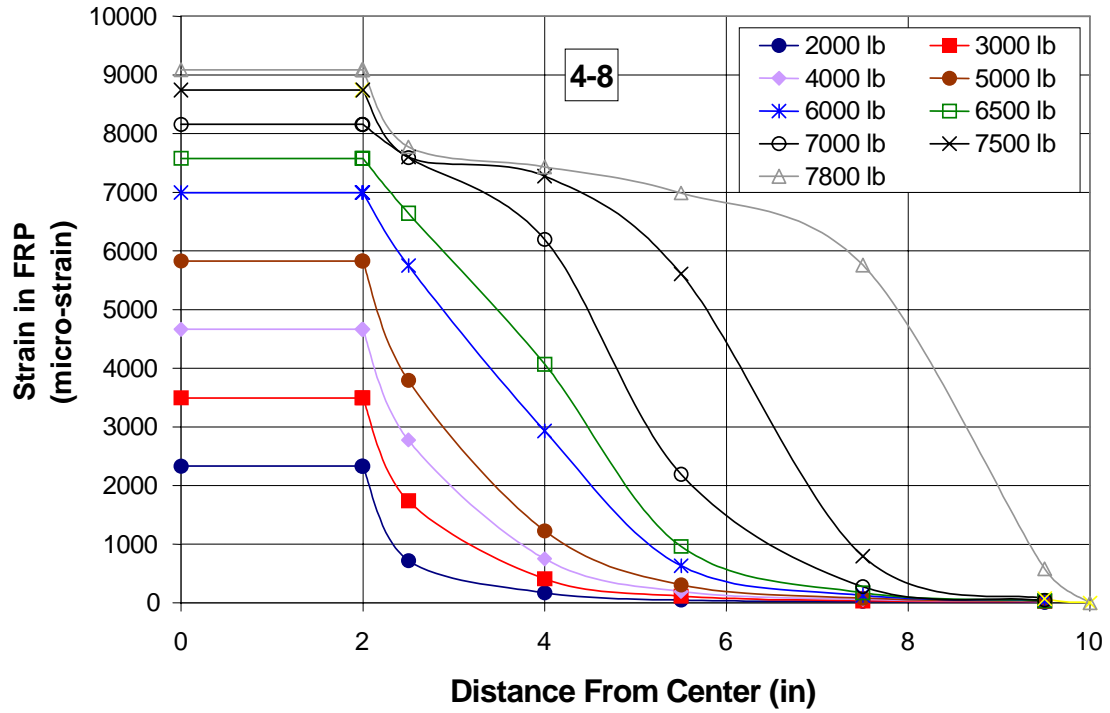


Figure A23: Strain-Location Diagram for 4-8

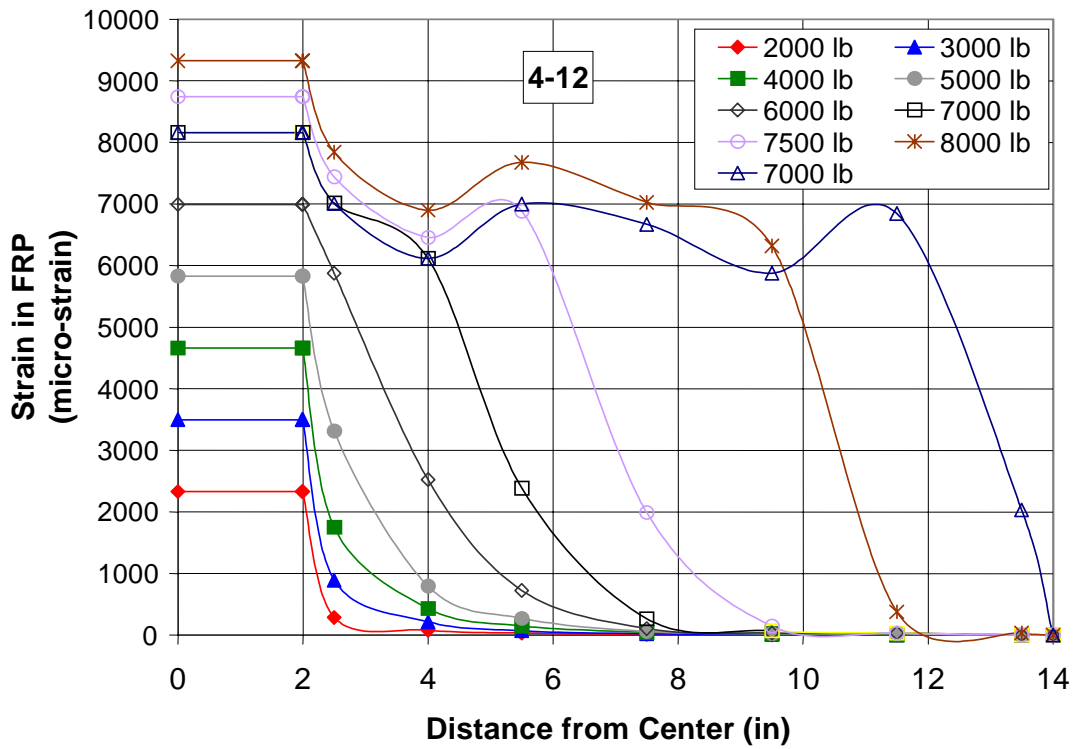


Figure A24: Strain-Location Diagram for 4-12

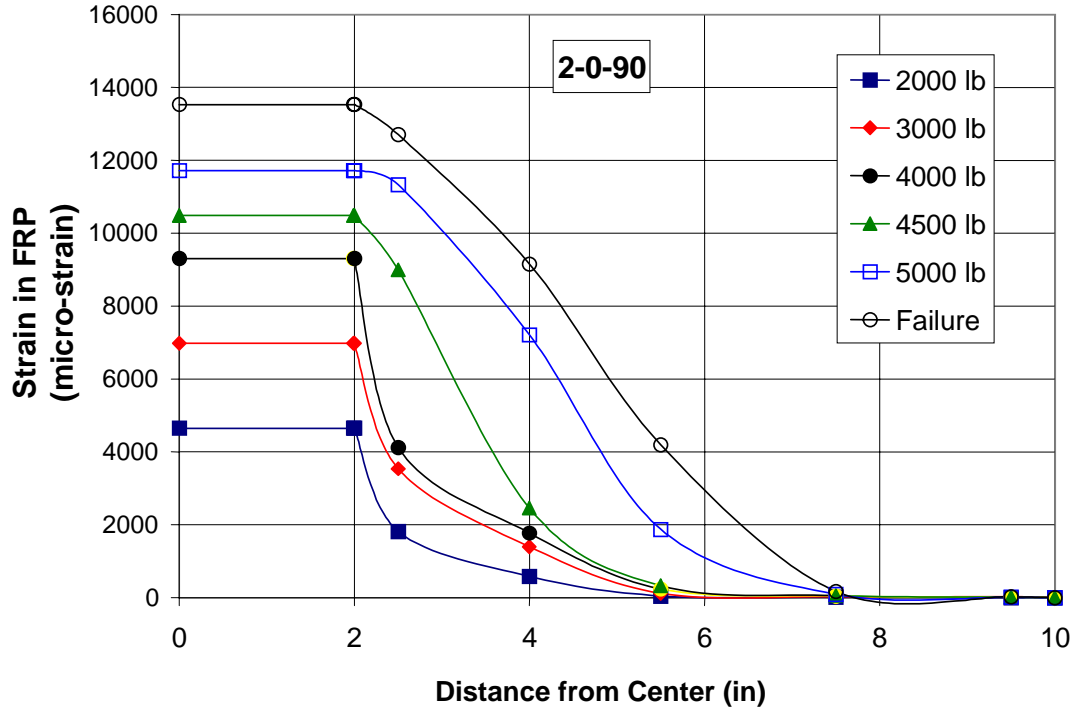


Figure A25: Strain-Location Diagram for 2-0-90

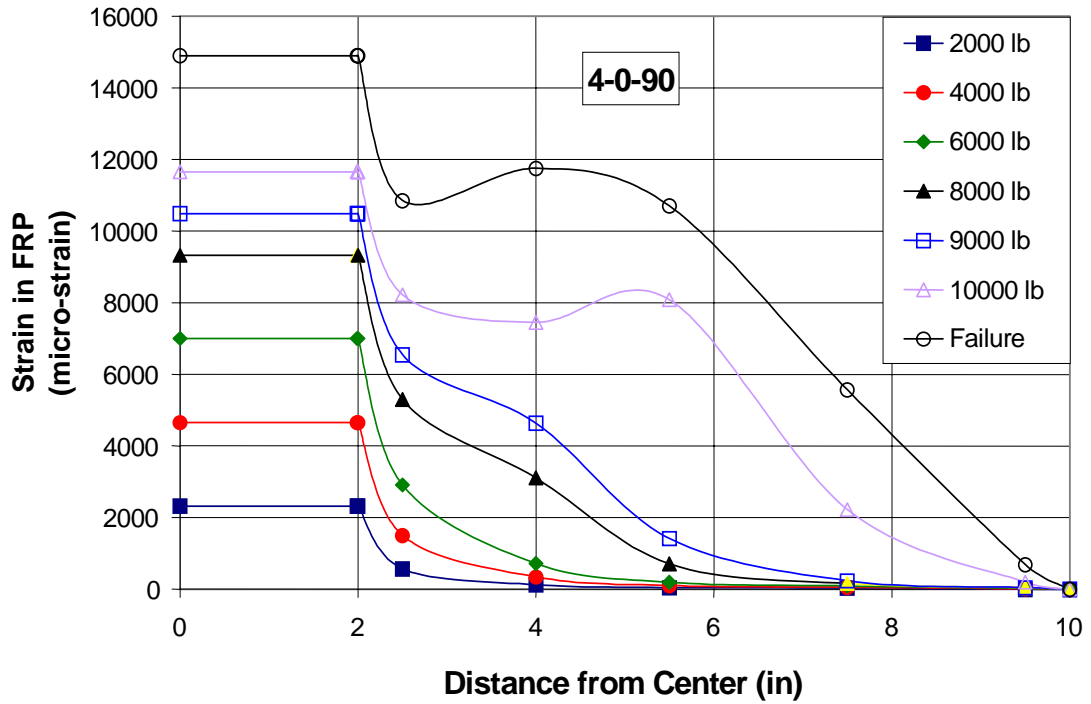


Figure A26: Strain-Location Diagram for 4-0-90

APPENDIX B.

LOAD vs. DEFLECTION DIAGRAMS

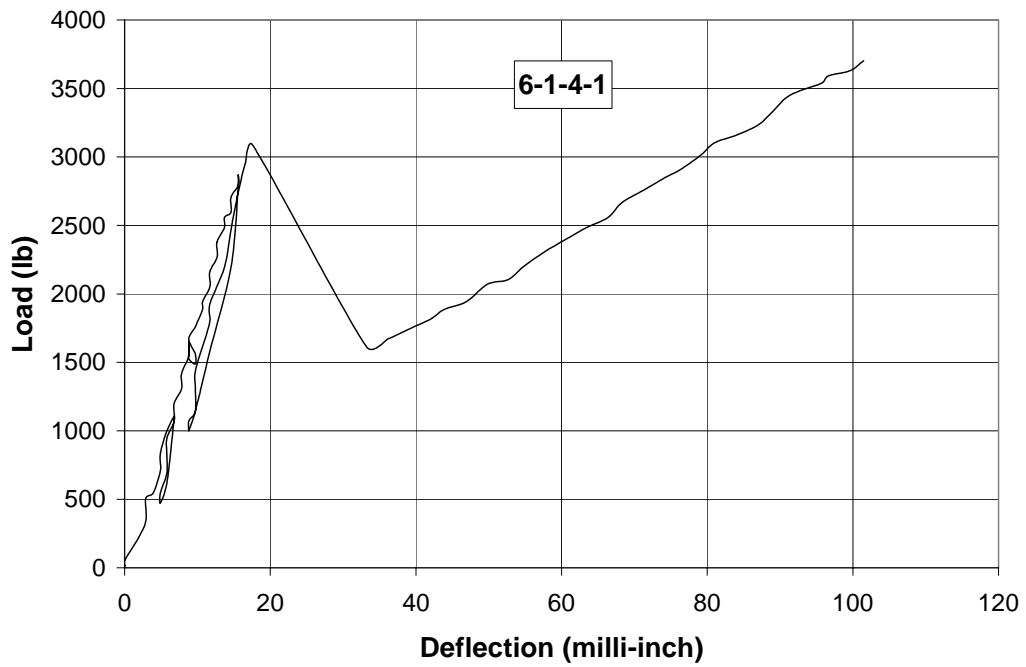


Figure B1: Load-Deflection Diagram for 6-1-4-1

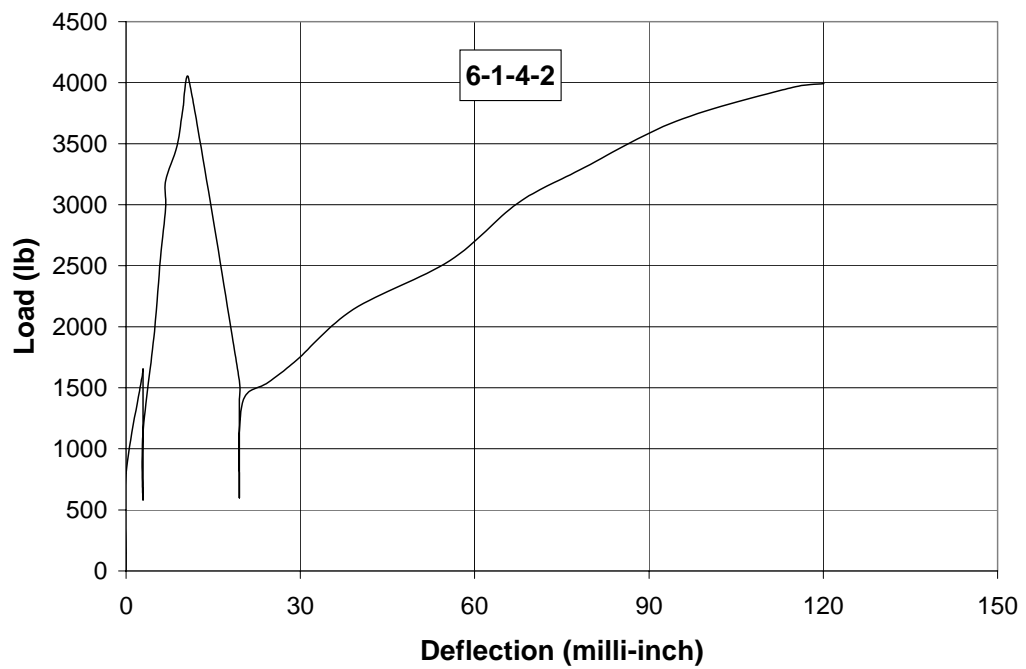


Figure B2: Load-Deflection Diagram for 6-1-4-2

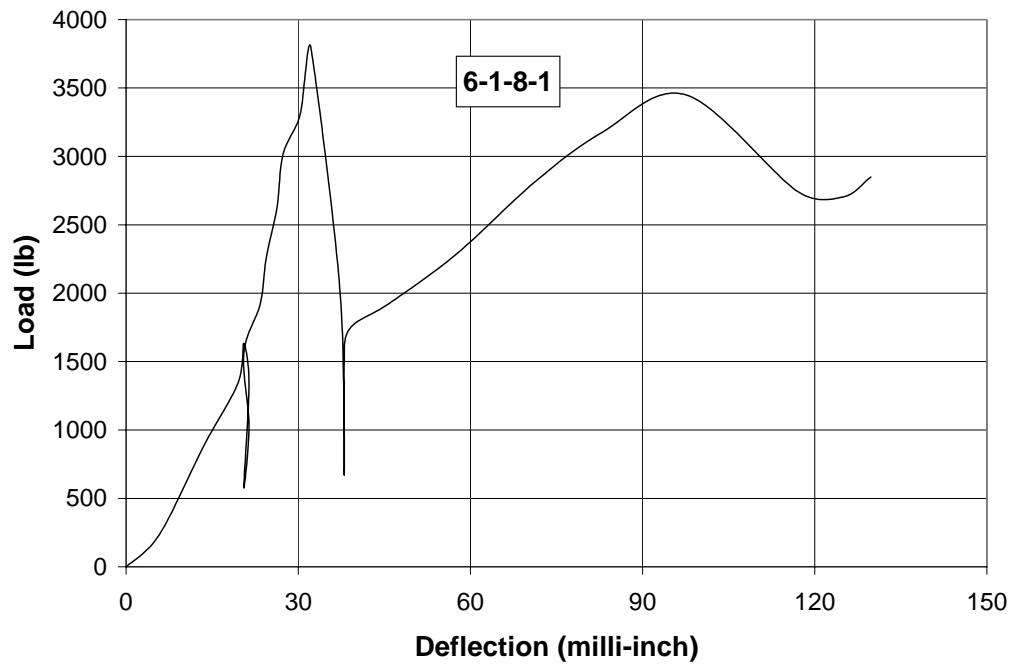


Figure B3: Load-Deflection Diagram for 6-1-8-1

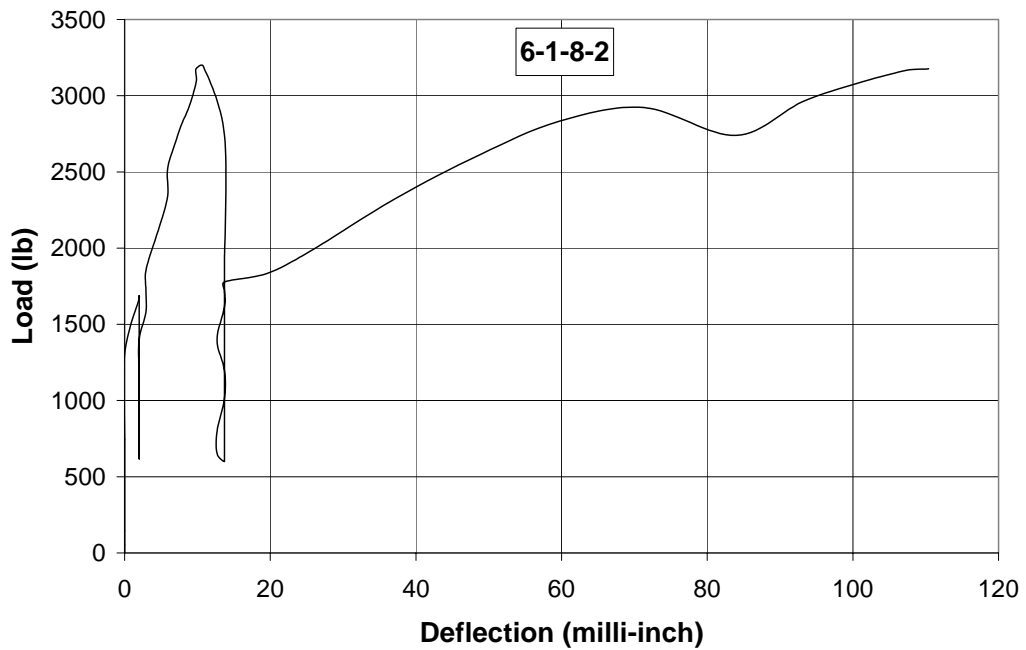


Figure B4: Load-Deflection Diagram for 6-1-8-2

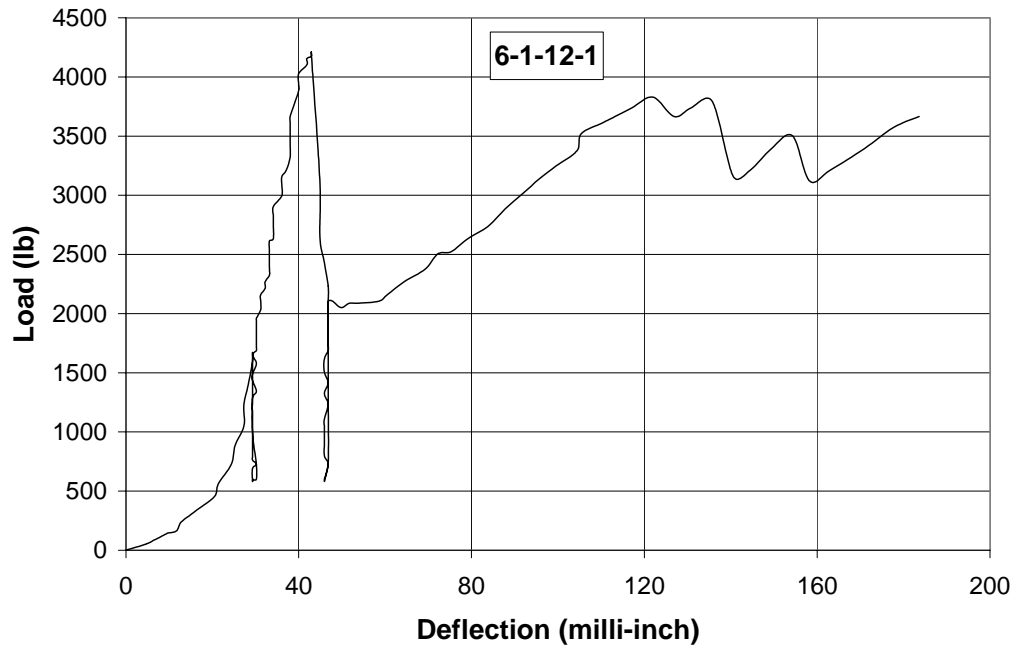


Figure B5: Load-Deflection Diagram for 6-1-12-1

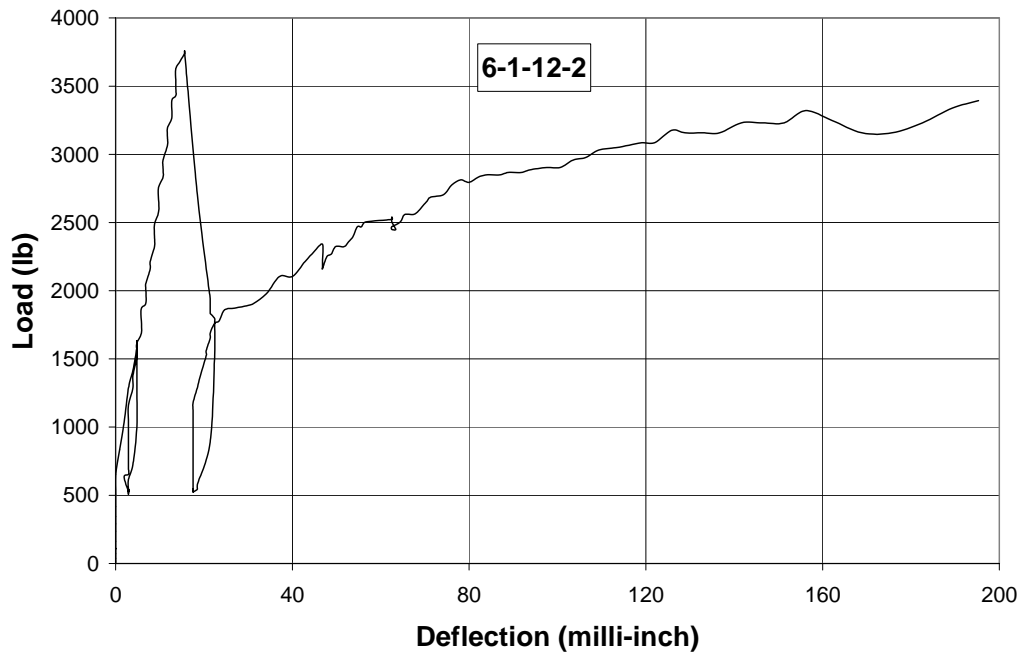


Figure B6: Load-Deflection Diagram for 6-1-12-2

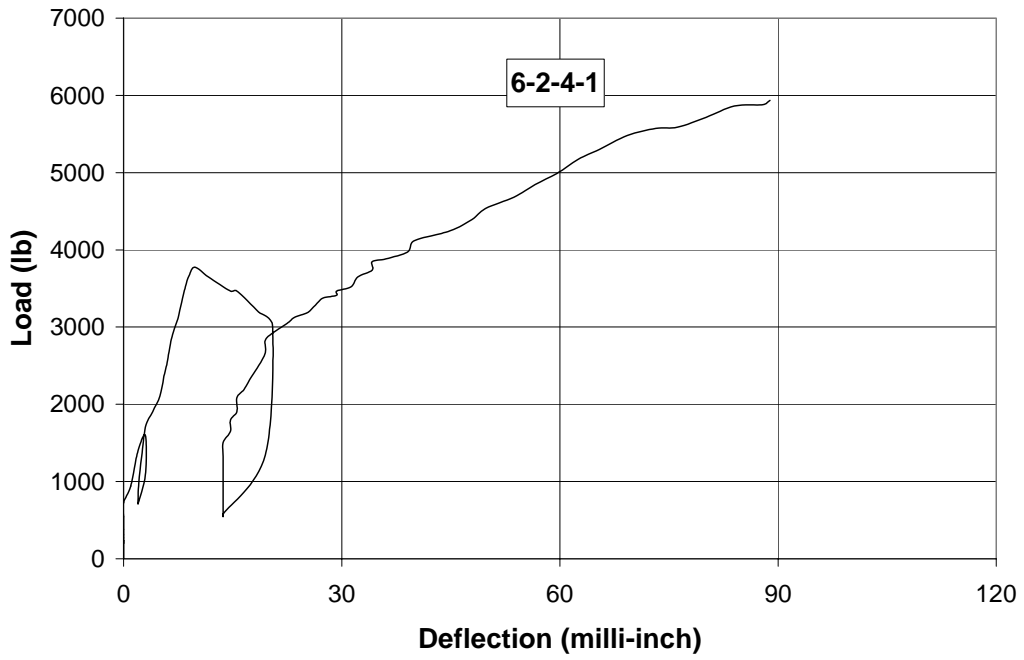


Figure B7: Load-Deflection Diagram for 6-2-4-1

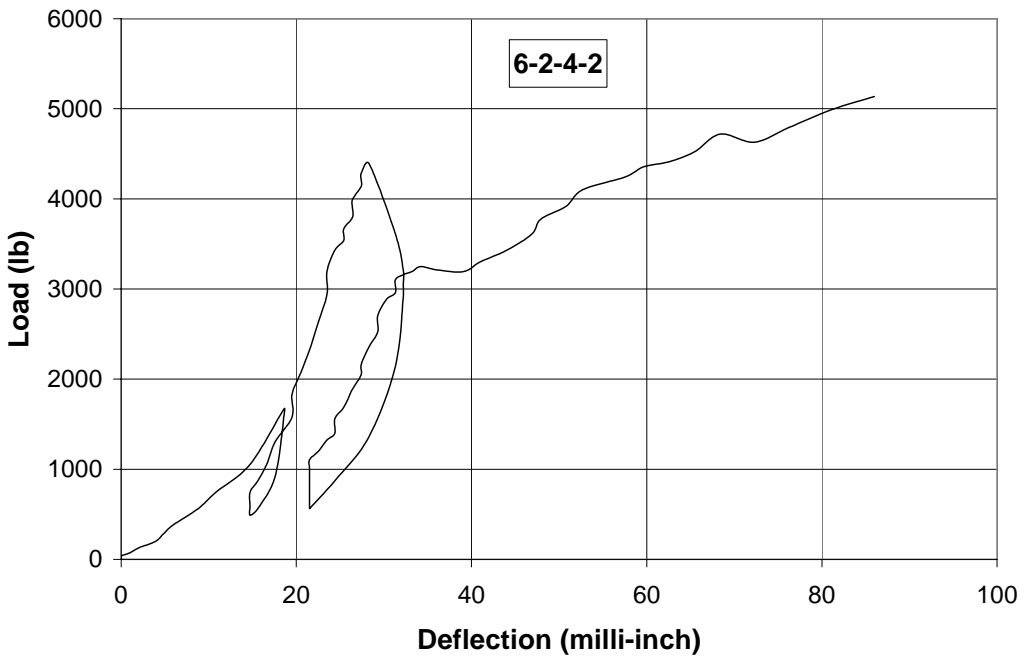


Figure B8: Load-Deflection for 6-2-4-2

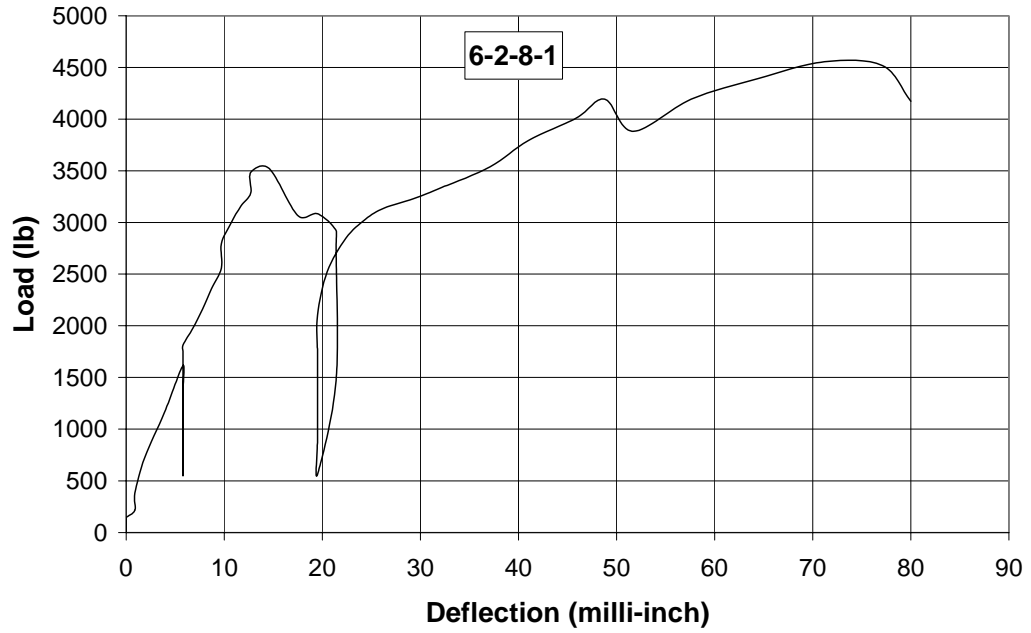


Figure B9: Load-Deflection for 6-2-8-1

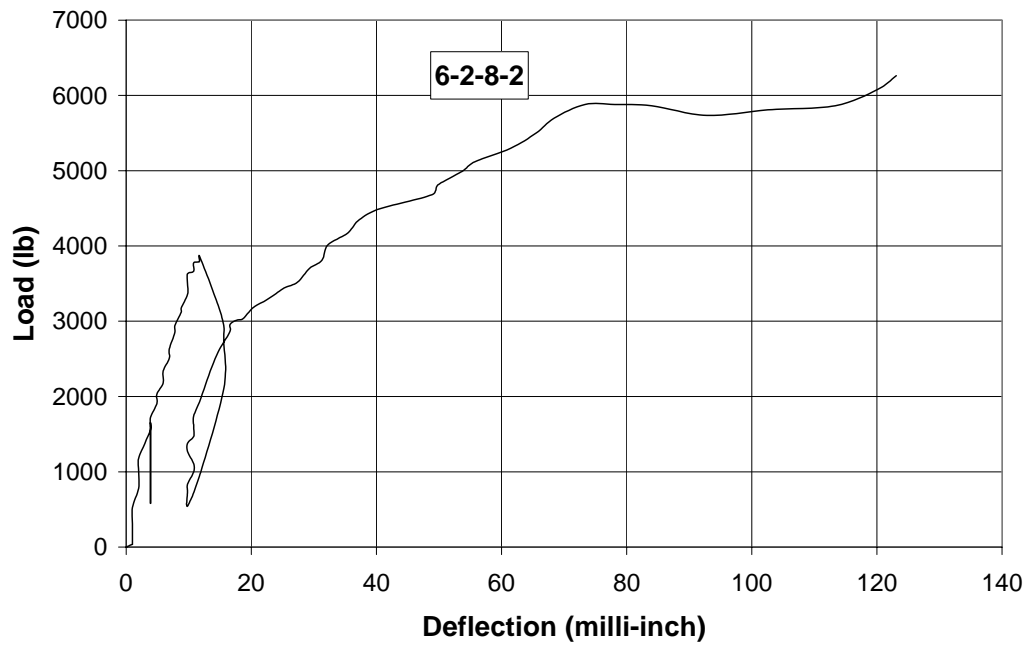


Figure B10: Load-Deflection for 6-2-8-2

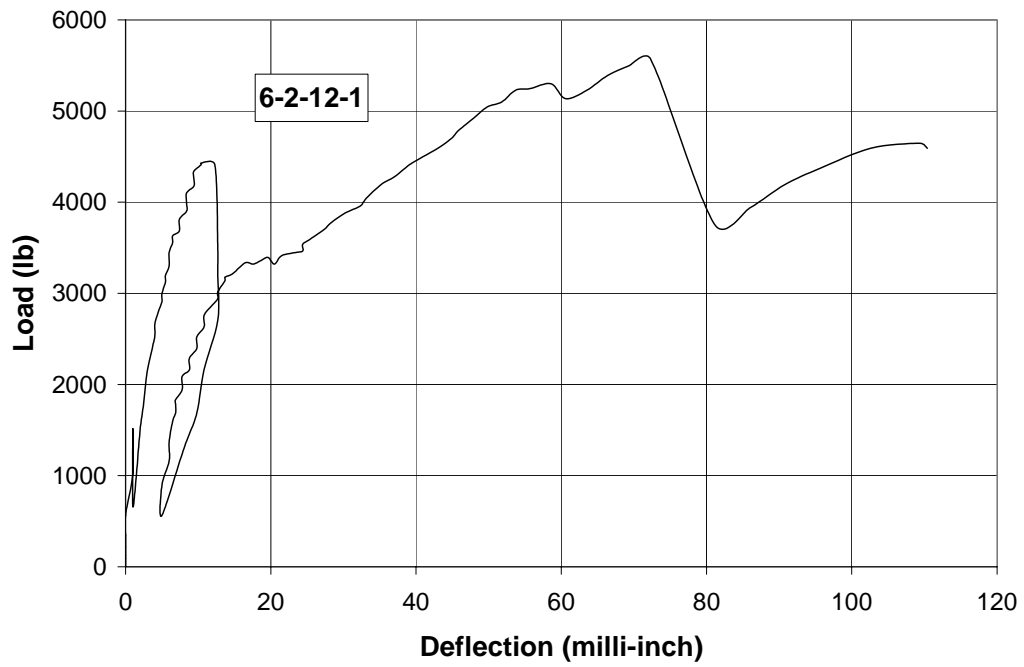


Figure B11: Load-Deflection for 6-2-12-1

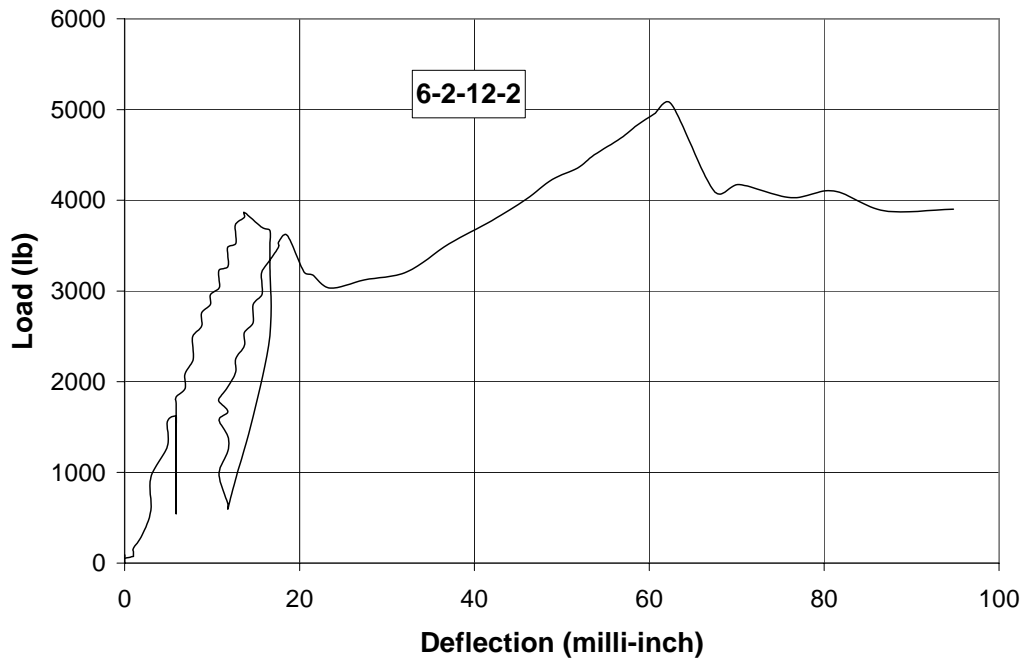


Figure B12: Load-Deflection for 6-2-12-2

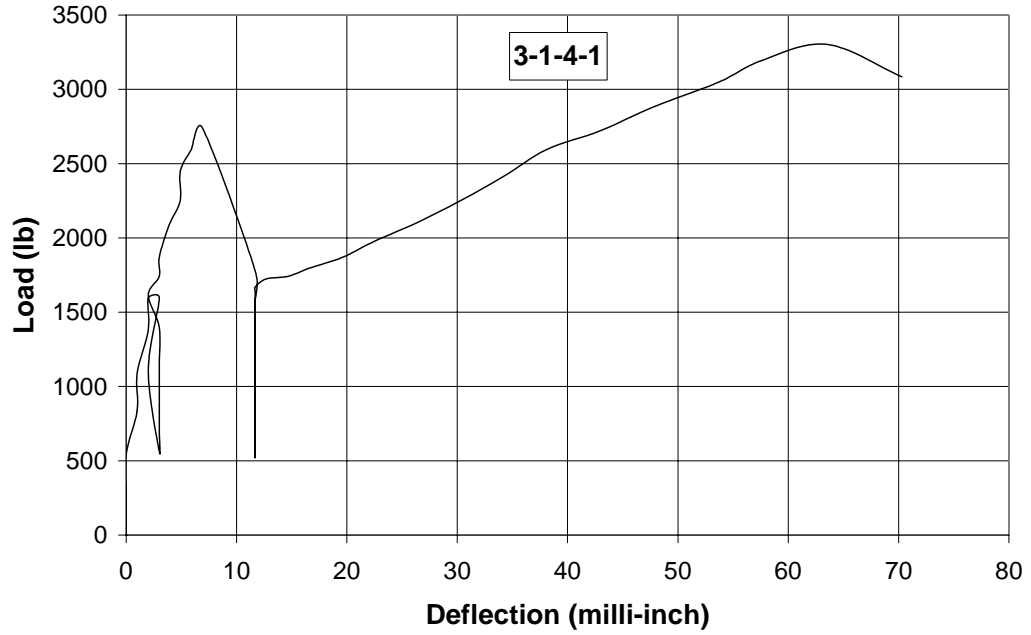


Figure B13: Load-Deflection Diagram for 3-1-4-1

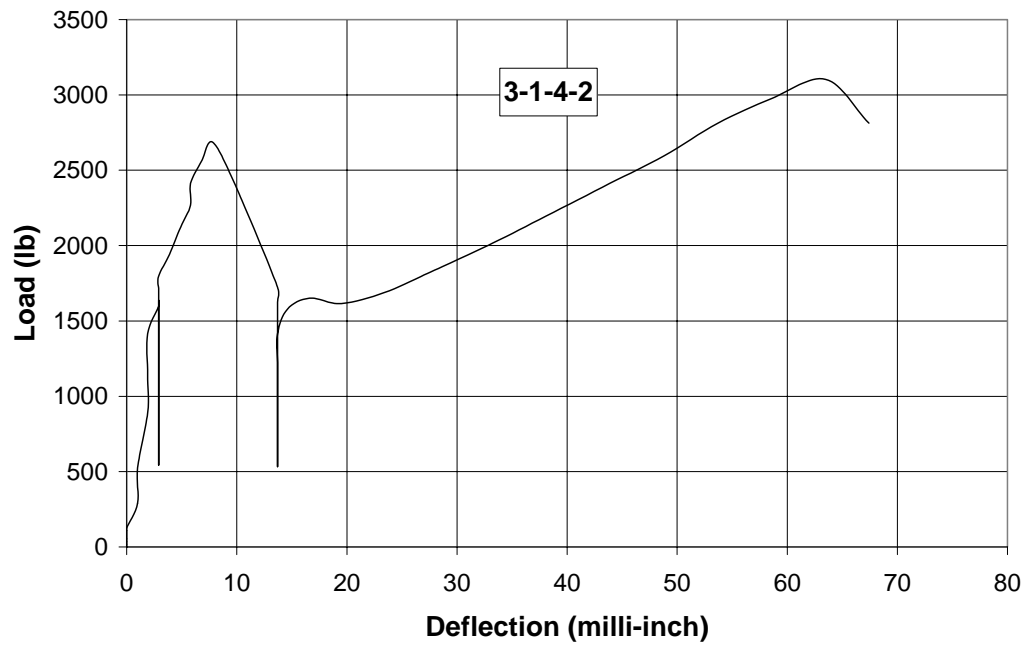


Figure B14: Load-Deflection Diagram for 3-1-4-2

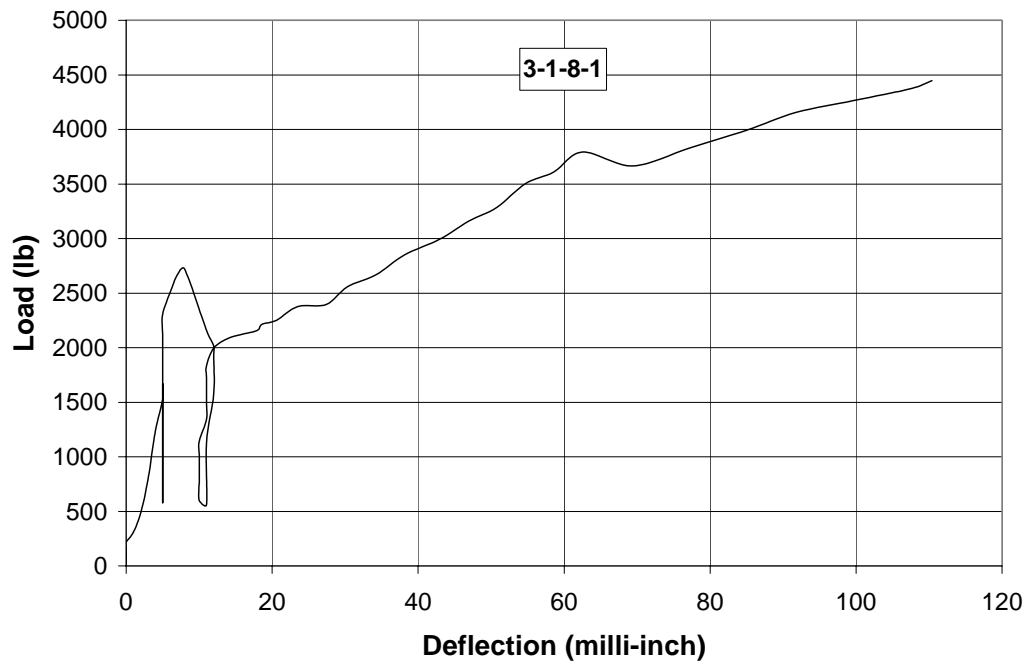


Figure B15: Load-Deflection Diagram for 3-1-8-1

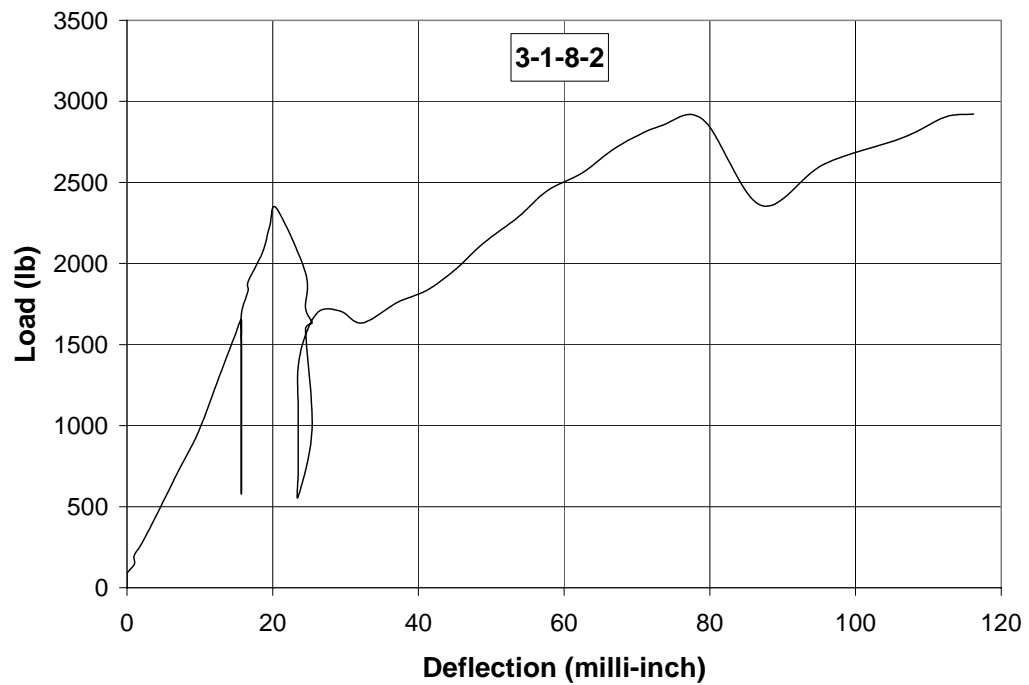


Figure B16: Load-Deflection Diagram for 3-1-8-2

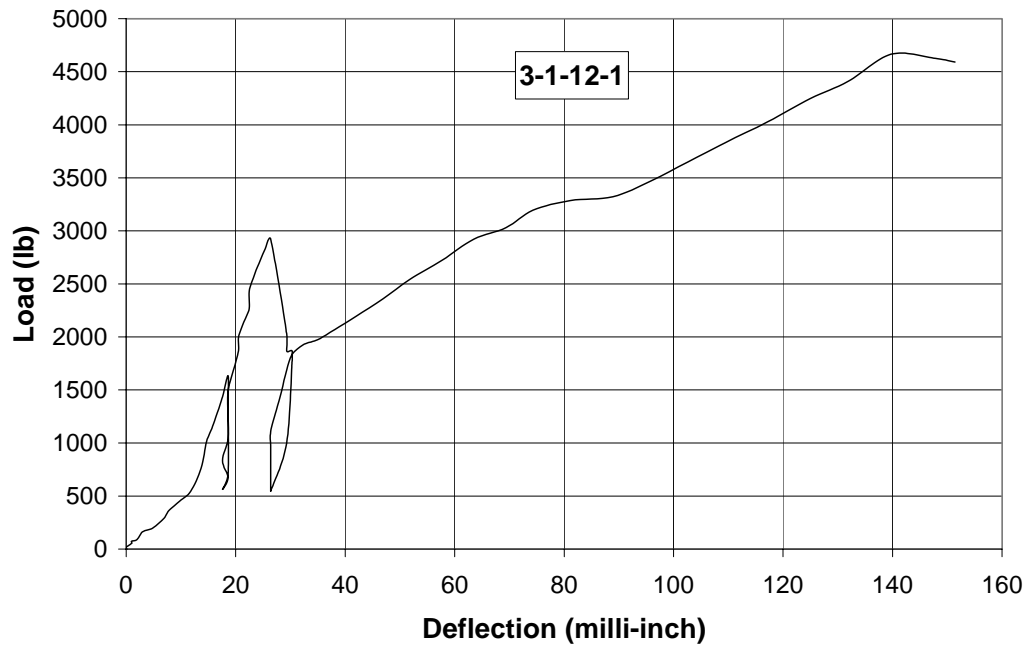


Figure B17: Load-Deflection Diagram for 3-1-12-1

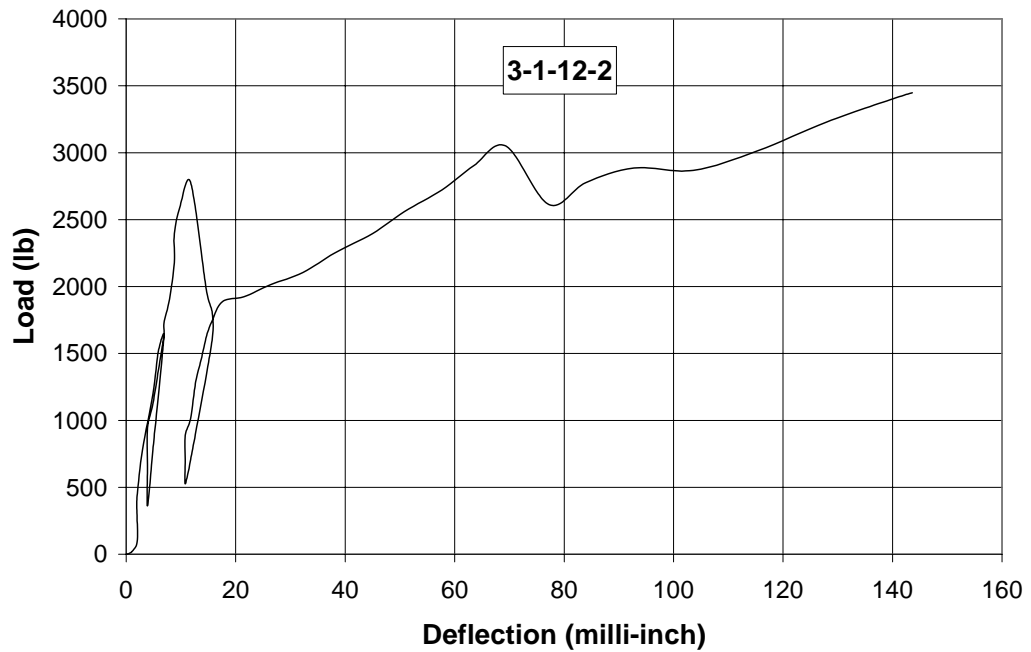


Figure B18: Load-Deflection Diagram for 3-1-12-2

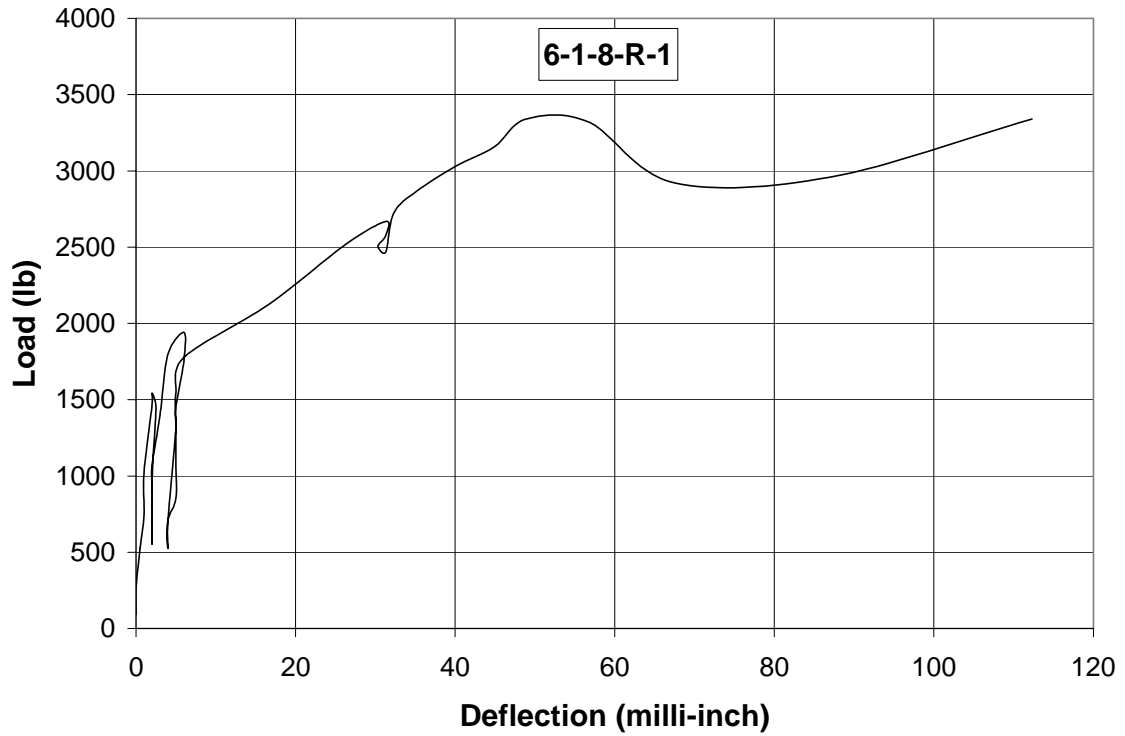


Figure B19: Load-Deflection Diagram for 6-1-8-R-1

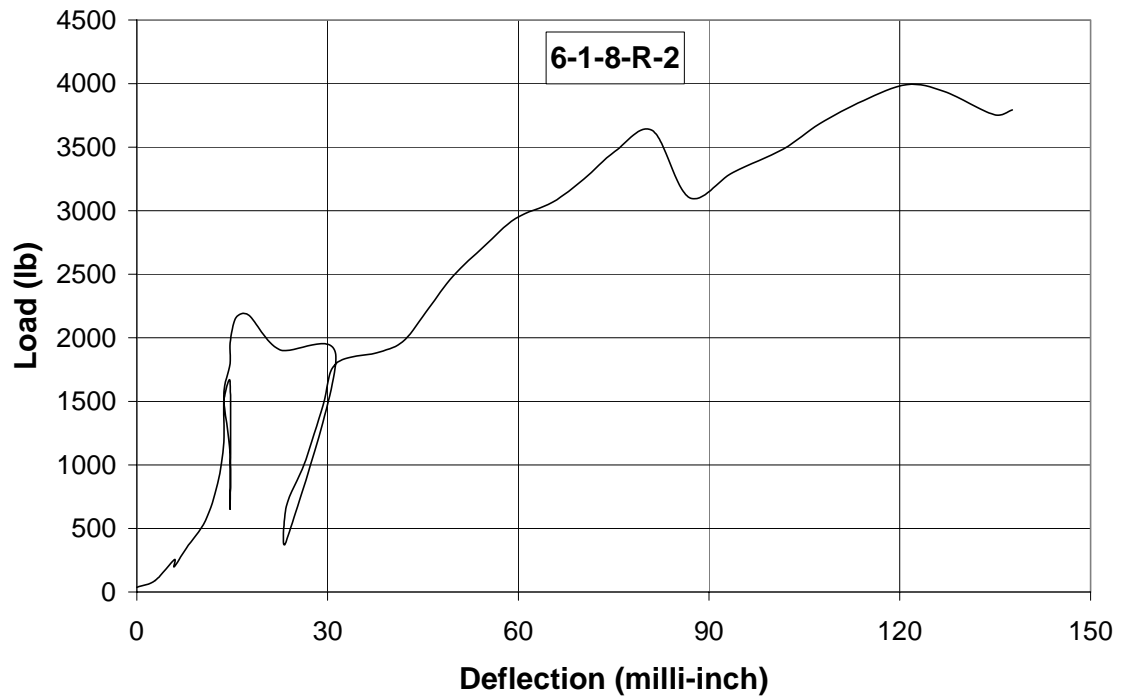


Figure B20: Load-Deflection Diagram for 6-1-8-R-2

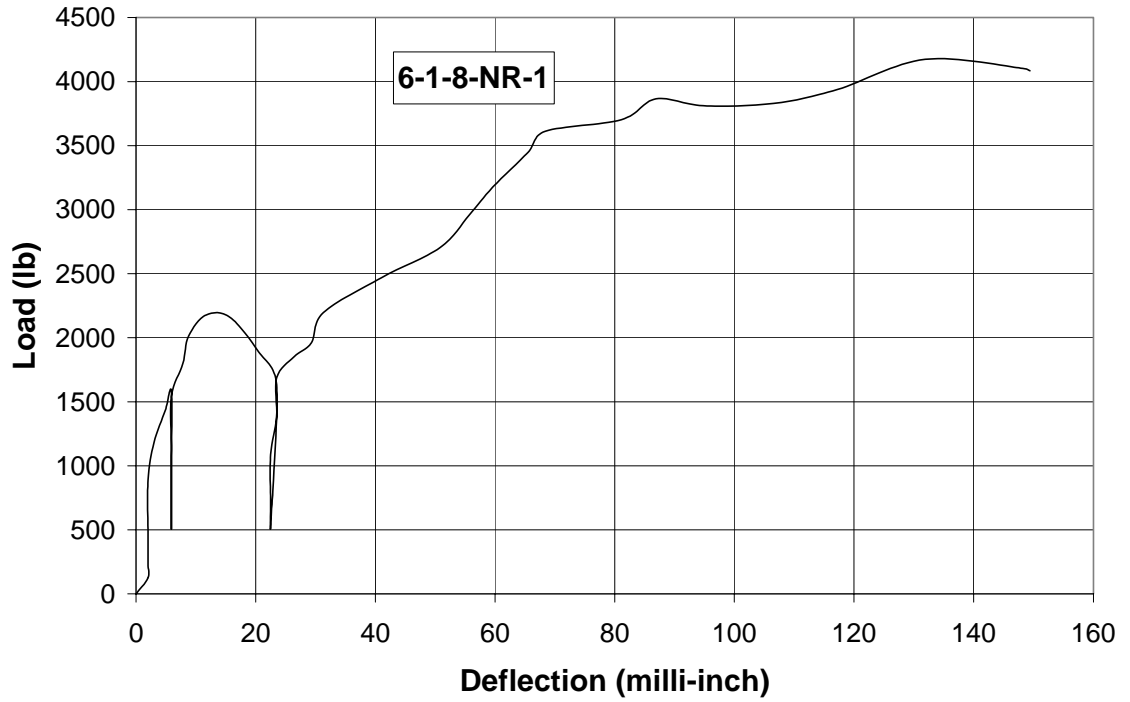


Figure B21: Load-Deflection Diagram for 6-1-8-NR-1

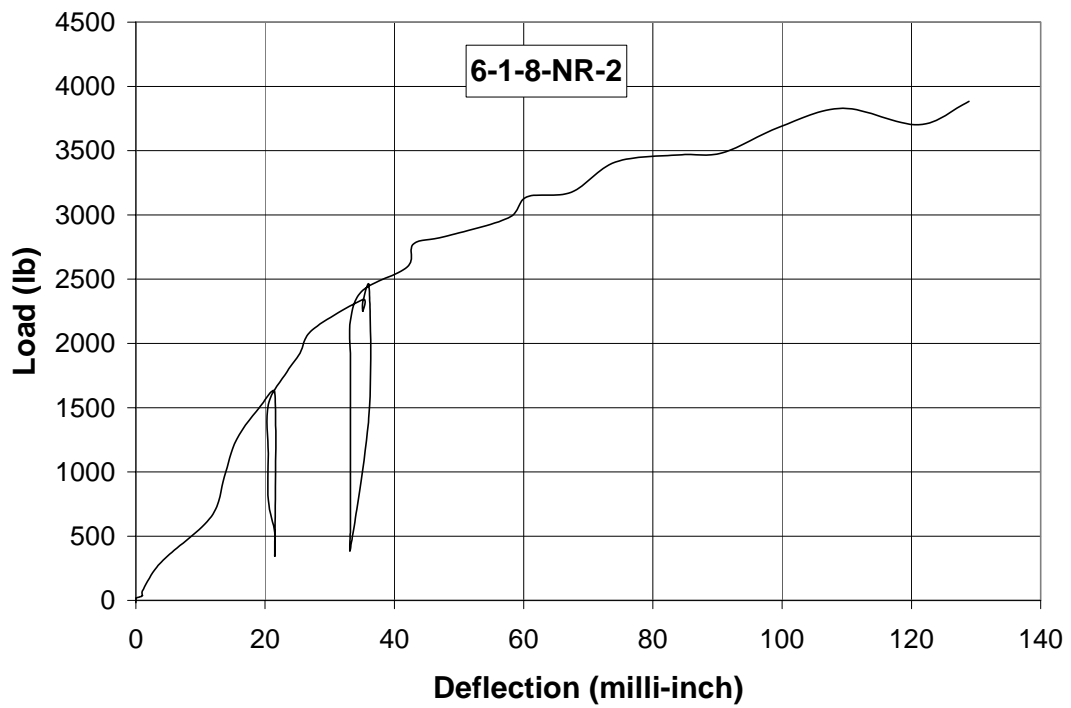


Figure B22: Load-Deflection Diagram for 6-1-8-NR-2

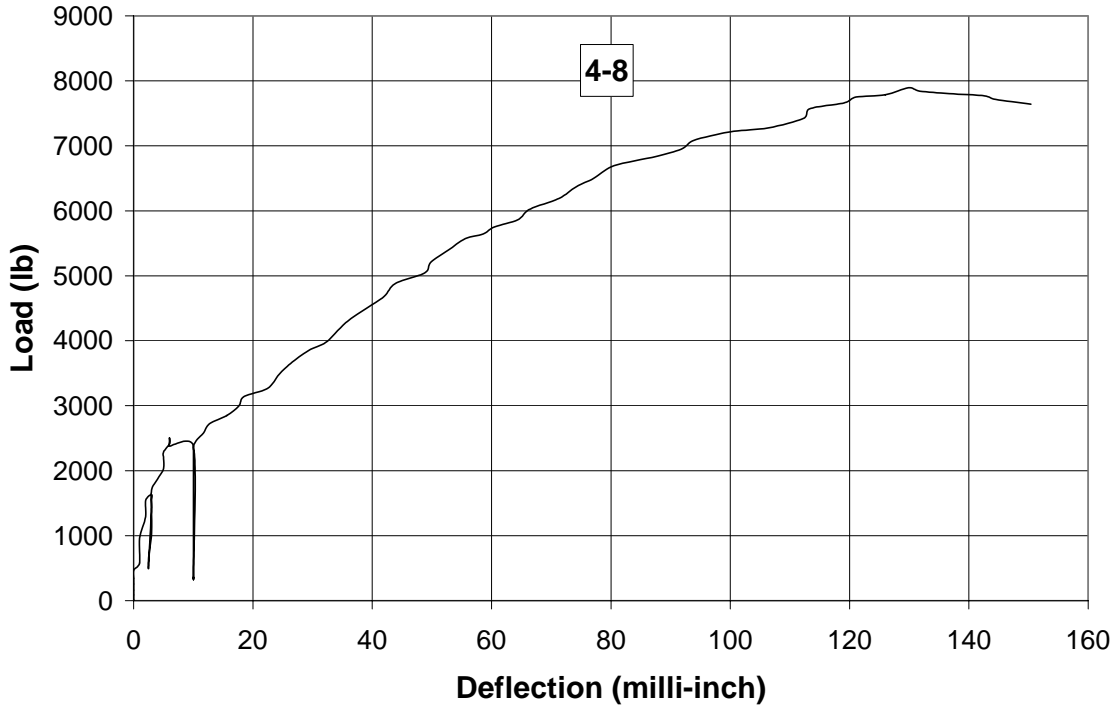


Figure B23: Load-Deflection Diagram for 4-8

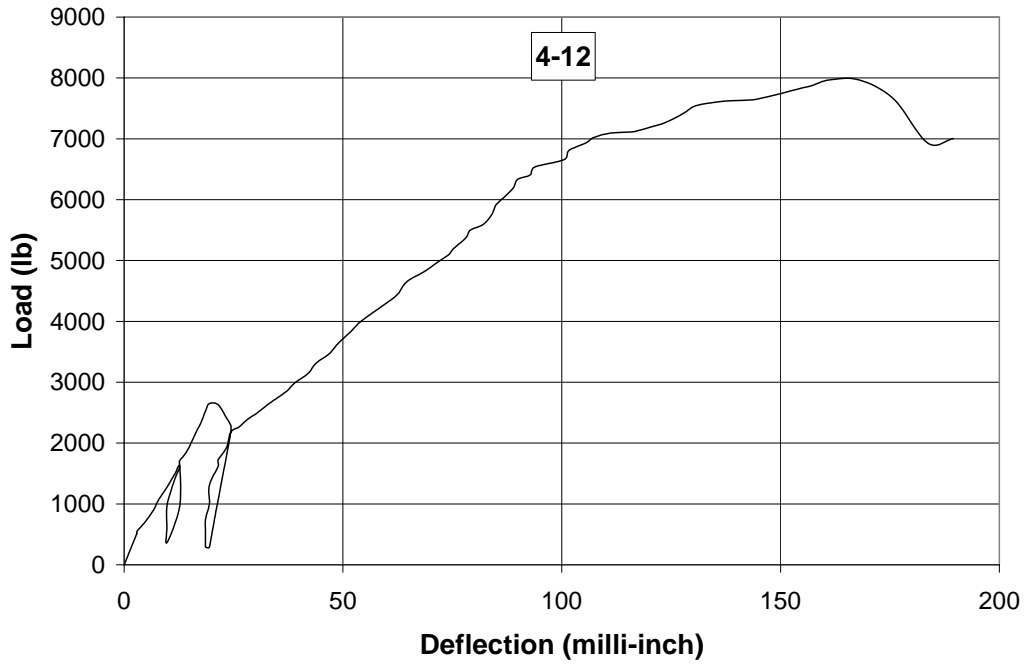


Figure B24: Load-Deflection Diagram for 4-12

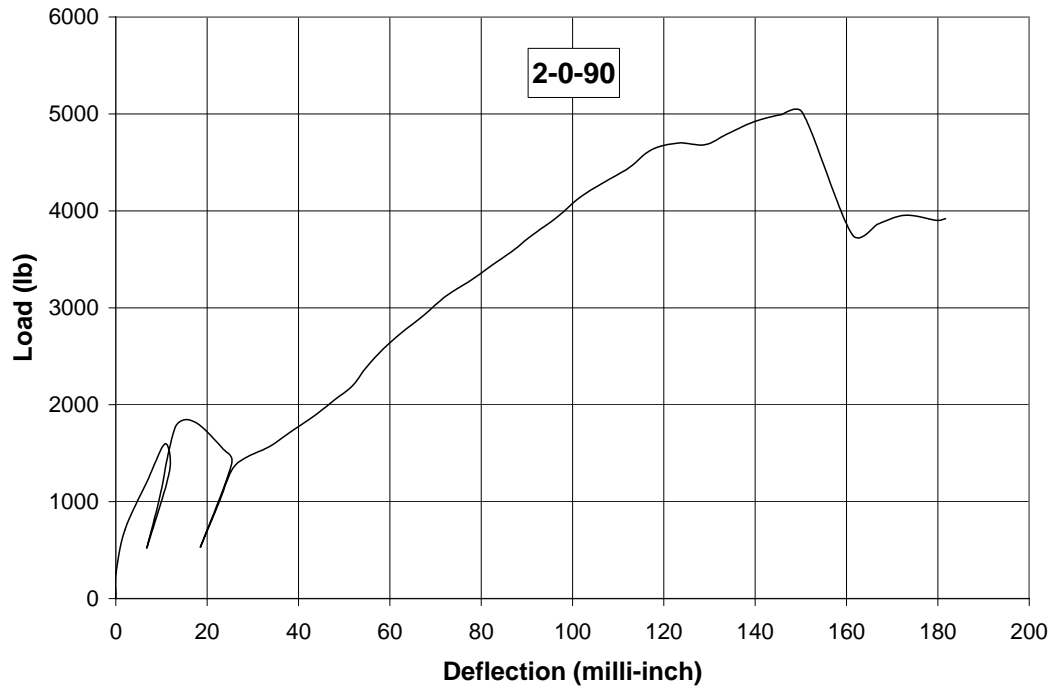


Figure B25: Load-Deflection Diagram for 2-0-90

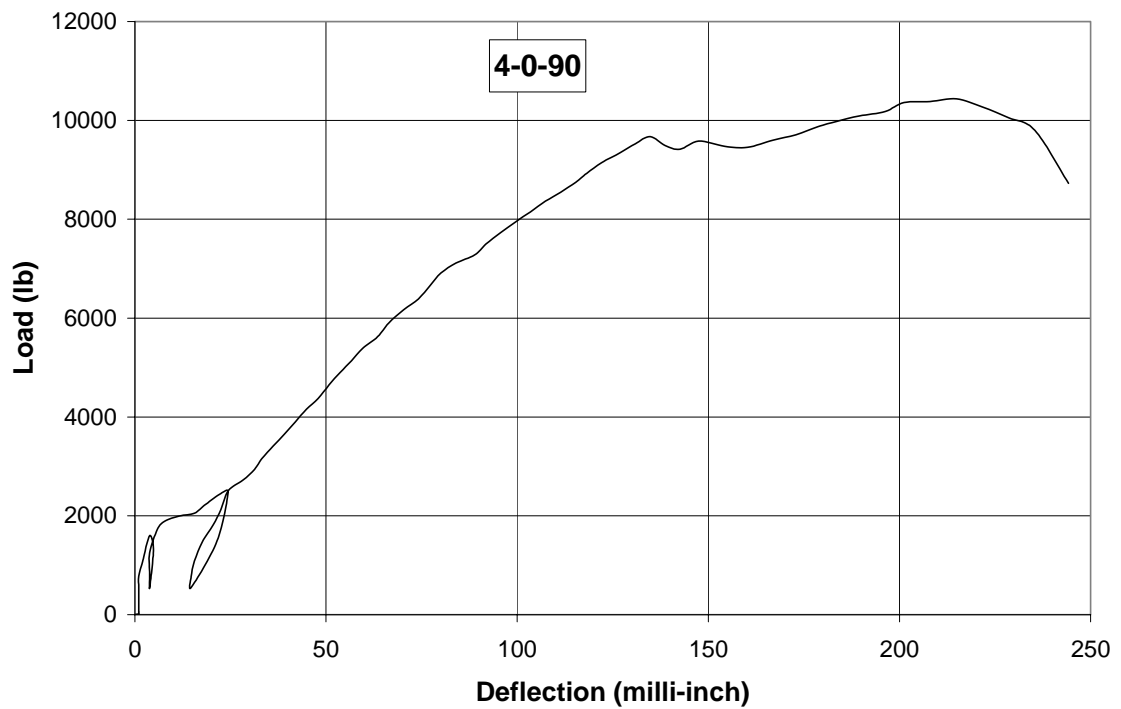


Figure B26: Load-Deflection Diagram for 4-0-90

APPENDIX C.

DESIGN EXAMPLE

The following design example was taken from the MBrace Design Guide (1998). It is the retrofit of an existing bridge slab.

A 70-year-old, solid-slab, concrete bridge requires strengthening in order to accommodate current traffic loads. Based on analysis, the new service loads will produce a maximum positive bending moment of $M_s = 42 \text{ kip}\cdot\text{ft}/\text{ft}$, and the total factored loads result in a design moment of $M_u = 66 \text{ ki}\cdot\text{ft}/\text{ft}$. An assessment of the existing bridge condition yields the section information given in Figure C1. Testing and research into the material properties result in a nominal concrete strength $f'_c = 3000 \text{ psi}$ and a yield strength for the mild steel of $f_y = 30,000 \text{ psi}$. Upon inspection, the concrete is in good condition and no signs of active corrosion are present.

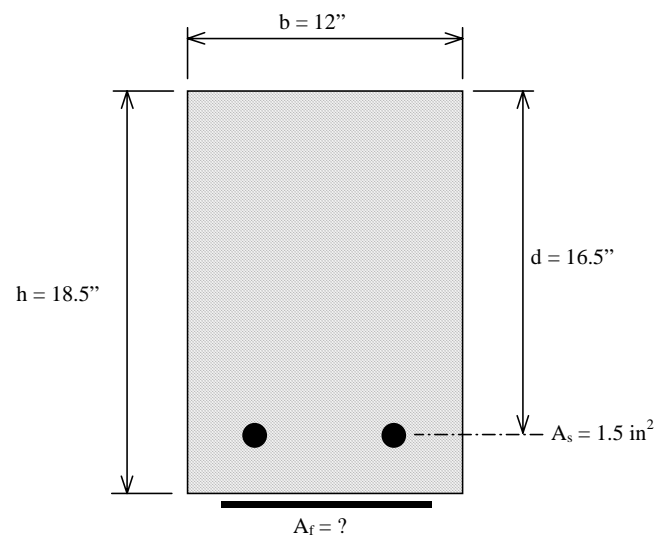


Figure C1: Geometry of unit strip for Design Example

The following illustrates the procedure for designing an MBrace retrofit for this structure.

- **Determine the existing flexural capacity and whether strengthening is required**

$$a = \frac{A_s f_y}{0.85 \cdot f_c' b} = \frac{(1.5 \text{ in}^2)(30,000 \text{ psi})}{0.85(3000 \text{ psi})(12 \text{ in})} = 1.47 \text{ in}$$

$$\phi M_n = \phi A_s f_y \left(d - \frac{a}{2} \right) = 0.90(1.5 \text{ in}^2)(30,000 \text{ psi}) \left(16.5 \text{ in} - \frac{1.47 \text{ in}}{2} \right) = 638,500 \text{ in} \cdot \text{lbs}$$

$$\phi M_n = 638,500 \text{ in} \cdot \text{lbs} = 53.2 \text{ kip} \cdot \text{ft} < M_u = 66 \text{ kip} \cdot \text{ft} \quad \therefore \text{Strengthening req'd}$$

The existing capacity is 25% below the design moment capacity. It is reasonable that the MBrace Composite Strengthening System will be capable of correcting this deficiency. MBrace CF-130 is selected for its high strength and excellent performance under sustained and cyclic loading.

- **Estimate the amount of CF-130 required.**

It is recommended to design the area of FRP by making a rough estimate of the required area based on the additional tensile force, T, required to equilibrate the moment deficiency. Do note, however, that this is a rough estimate and should be modified based on a full analysis.

$$T = \frac{M_u - \phi M_n}{0.90 \cdot d} = \frac{(66 \text{ kip} \cdot \text{ft} - 53.2 \text{ kip} \cdot \text{ft}) \times 12 \text{ in/ft}}{0.90(16.5 \text{ in})} = 10.34 \text{ kips}$$

$$A_{f,est} = \frac{T}{\phi \cdot 0.85 \cdot f_{fu}} = \frac{10.34 \text{ kips}}{0.90 \cdot 0.85 \cdot 550 \text{ ksi}} = 0.0246 \text{ in}^2$$

Based on this area, the width of FRP may be computed. For a slab, a series of evenly spaced FRP strips is typically used. Thus, the estimated width becomes:

$$w_f = \frac{A_f}{n \cdot t_f} = \frac{0.0246 \text{ in}^2}{1(0.0065 \text{ in})} = 3.8 \text{ in} \quad \therefore \text{Try 1 ply, 4 in. wide} \quad A_f = 0.026 \text{ in}^2$$

The actual flexural capacity must now be computed.

- **Find the existing state of strain on the soffit**

Based on an existing condition assessment, the total moment in place at the time that the FRP will be installed is $M_{ip} = 20 \text{ kip}\cdot\text{ft}$. The existing state of strain may be computed for this moment assuming that the section is cracked.

$$\varepsilon_{bi} = \frac{M_{ip}(h - kd)}{I_{cr}E_c}$$

The multiplier on the beam depth, d , to find the cracked neutral axis position is $k = 0.326$. Further, the cracked moment of inertia is $I_{cr} = 2570 \text{ in}^4$. The strain level on the soffit at the time of FRP installation, thus becomes:

$$\varepsilon_{bi} = \frac{(20 \text{ kip}\cdot\text{ft} \times 12 \text{ in} / \text{ft})(18.5 \text{ in} - 0.326 \cdot 16.5 \text{ in})}{(2570 \text{ in}^4)(2850 \text{ ksi})} = 430 \mu\varepsilon$$

- **Estimate c , and adjust by trial and error**

A first estimate of $c = 0.15d$ is used. Thus, $c = 0.15(16.5 \text{ in}) = 2.475 \text{ in}$ is the first estimate.

- **Find the mode of failure for the estimated c**

$$\varepsilon_{fu} + \varepsilon_{bi} \quad ? \quad \varepsilon_{cu} \left(\frac{h - c}{c} \right)$$

$$0.017 + 0.000430 \quad ? \quad 0.003 \left(\frac{18.5 - 2.475}{2.475} \right)$$

$$0.01743 < 0.01942 \therefore \text{FRP Rupture}$$

- Find the strain level in each of the materials

$$\varepsilon_f = \varepsilon_{fu} = 0.017$$

$$\varepsilon_c = (\varepsilon_{fu} + \varepsilon_{bi}) \left(\frac{c}{h-c} \right) = (0.01743) \left(\frac{2.475}{18.5 - 2.475} \right) = 0.00263$$

$$\varepsilon_s = (\varepsilon_{fu} + \varepsilon_{bi}) \left(\frac{d-c}{h-c} \right) = (0.01743) \left(\frac{16.5 - 2.475}{18.5 - 2.475} \right) = 0.0149$$

- Find the stress level in the FRP and steel

$$f_f = f_{fu} = 550 \text{ ksi}$$

$$f_s = f_{sy} = 30 \text{ ksi since } \varepsilon_s \gg \varepsilon_{sy}$$

- Find the parameters to define an equivalent concrete stress block

$$\varepsilon'_c = \frac{1.71 \cdot f'_c}{E_c} = \frac{1.71(2500 \text{ psi})}{2,850,000 \text{ psi}} = 0.0015$$

$$\frac{\varepsilon_c}{\varepsilon'_c} = \frac{0.00263}{0.0015} = 1.635$$

$$\beta_1 = 2 - \frac{4[(\varepsilon_c/\varepsilon'_c) - a \tan(\varepsilon_c/\varepsilon'_c)]}{(\varepsilon_c/\varepsilon'_c) \ln(1 + \varepsilon_c^2/\varepsilon'^2)} = 2 - \frac{4[(1.635) - a \tan(1.635)]}{(1.635) \ln(1 + (1.635)^2)} = 0.847$$

$$\gamma = \frac{0.90 \ln(1 + \varepsilon_c^2/\varepsilon'^2)}{\beta_1 \varepsilon_c/\varepsilon'_c} = \frac{0.90 \ln(1 + (1.635)^2)}{0.847(1.635)} = 0.845$$

- Check the estimate on c

$$c = \frac{A_s f_s - A'_s f'_s + A_f f_f}{f'_c \beta_1 b} = \frac{1.5 \text{ in}^2 (30,000 \text{ psi}) - 0 + (0.026 \text{ in}^2)(550,000 \text{ psi})}{0.845(2500 \text{ psi})0.847(12 \text{ in})} = 2.300 \text{ in}$$

2.300 in \neq 2.475 in \therefore A revision is required by iterating values of c.

- A summary of the trial and error procedure is given in Table C1.

Table C1: Summary of trial and error calculations to obtain c

c_{est} (in)	Failure Mode	ε_f	f_f (ksi)	ε_s	f_s (ksi)	ε_c	β_1	γ	c_{calc} (in)
2.475	FRP	0.017	550	0.0152	30	0.00269	0.847	0.845	2.300
2.400	FRP	0.017	550	0.0152	30	0.00259	0.840	0.849	2.311
2.330	FRP	0.017	550	0.0152	30	0.00251	0.833	0.851	2.323

Thus, the value of c is taken as 2.33 in.

- **Compute the nominal moment capacity**

$$M_n = A_s f_s \left(d - \frac{\beta_1 c}{2} \right) + A'_s f'_s \left(\frac{\beta_1 c}{2} - d' \right) + 0.85 A_f f_f \left(h - \frac{\beta_1 c}{2} \right)$$

$$= 1.5(30) \left(16.5 - \frac{0.833(2.33)}{2} \right) + 0 + 0.85(0.026)(550) \left(18.5 - \frac{0.833(2.33)}{2} \right)$$

$$M_n = 912 \text{ kip} \cdot \text{in} = 76 \text{ kip} \cdot \text{ft}$$

- **Compute the design moment capacity**

Because the strain in the steel at ultimate is much greater than twice its yield strain, the section retains sufficient ductility. The ϕ factor is therefore taken as 0.90.

$$\phi M_n = 0.90(76 \text{ kip} \cdot \text{ft}) = 68.4 \text{ kip} \cdot \text{ft} > M_u = 66 \text{ kip} \cdot \text{ft} \quad \checkmark \text{O.K.}$$

Check serviceability by checking working stresses

- **Compute the elastic depth to the cracked neutral axis, kd.**

By taking the first moments of the areas of concrete, steel (transformed to concrete), and FRP (transformed to concrete), the following expression is obtained:

$$\frac{(kd)^2 b}{2} - n_s A_s (d - kd) - n_f A_f (h - kd) = 0$$

$$\frac{(kd)^2 12 \text{ in}}{2} - \left(\frac{29000 \text{ ksi}}{2771 \text{ ksi}} \right) (1.5 \text{ in}^2) (16.5 \text{ in} - kd) - \left(\frac{33000 \text{ ksi}}{2771 \text{ ksi}} \right) (0.026 \text{ in}^2) (18.5 \text{ in} - kd) = 0$$

Solving this quadratic, the depth to the neutral axis is $kd = 5.185$ inches ($k = 0.314$).

Compute the stress in the steel at a service moment of $M_s = 42 \text{ kip-ft} = 504 \text{ kip-in}$.

$$f_s = \frac{\left[M_s + \varepsilon_{bi} A_f E_f \left(h - \frac{kd}{3} \right) \right] (d - kd) E_s}{A_s E_s \left(d - \frac{kd}{3} \right) (d - kd) + A'_s E_s \left(\frac{kd}{3} - d' \right) (kd - d') + A_f E_f \left(h - \frac{kd}{3} \right) (h - kd)}$$

$$= \frac{\left[504 + 0.00039(0.026)(33000) \left(18.5 - \frac{5.185}{3} \right) \right] (16.5 - 5.185)(29000)}{1.5(29000) \left(16.5 - \frac{5.185}{3} \right) (16.5 - 5.185) + 0 + (0.026)(33000) \left(18.5 - \frac{5.185}{3} \right) (18.5 - 5.185)}$$

$$f_s = 22.41 \text{ ksi} < 0.80 f_y = 24 \text{ ksi} \quad \checkmark \text{O.K.}$$

- **Compute the maximum compressive stress in the concrete at service**

$$f_c = f_s \left(\frac{E_c}{E_s} \right) \frac{kd}{d - kd} = 22.57 \text{ ksi} \left(\frac{2771}{29000} \right) \frac{5.185}{16.5 - 5.185} = 1.106 \text{ ksi}$$

$$f_c = 1106 \text{ psi} > 0.45 f'_c = 1350 \text{ psi} \quad \checkmark \text{O.K.}$$

- **Compute the stress in the FRP at service**

$$f_f = f_s \left(\frac{E_f}{E_s} \right) \frac{h - kd}{d - kd} - \varepsilon_{bi} E_f = 22.53 \text{ ksi} \left(\frac{33}{29} \right) \frac{18.5 - 5.45}{16.5 - 5.45} - 0.00044(33000 \text{ ksi}) = 15.76 \text{ ksi}$$

$$f_f = 16.9 \text{ ksi} < 0.33 C_D C_E f_{fu} = 0.33(0.95)(0.65)550 \text{ ksi} = 112 \text{ ksi} \quad \checkmark \text{O.K.}$$

- **Conclusions**

Based on the analysis, one ply of FRP with a width of 4" per 12" width of beam will be sufficient to strengthen the bridge. The final design could call for a 10" wide one-ply strip spaced at 30" on center for constructability and material economy. Because the MBrace CF-130 sheets come in 20" wide rolls, these strips are easily field cut.

LIST OF REFERENCES

- ACI-318-95, (1995). "Building Code Requirements for Reinforced Concrete and Commentary," American Concrete Institute, Detroit, Michigan.
- Bizindavyi, L and Neale KW (1999). "Transfer Lengths and Bond Strengths for Composite Laminates Bonded to Concrete," *Journal of Composites for Construction*, ASCE.
- Brosens, Kris and Van Gemert, Dionys, (1997). "Anchoring Stresses between Concrete and Carbon Fibre Reinforced Laminates," *Non-Metallic (FRP) Reinforcement of Concrete Structures*, Vol 1, Japan Concrete Institute, Japan, 271-278.
- Dolan, BE; Hamilton III, HR; and Dolan, CW (1998). "Strengthening with Bonded FRP Laminate," *Concrete International*, ACI, 51-55.
- Frigo, Elizabeth Mary, (1996). "The Mechanics of Externally Bonded FRP for the Repair of Reinforced Concrete." MSc Thesis Department of Architectural Engineering, The Pennsylvania State University.
- Green, MF; Bisby, L.A.; Beaudoin, Y; and Labossiere, P (1998). "Effects of Freeze-Thaw Action on the Bond of FRP Sheets to Concrete," *Durability of Fiber Reinforced Polymer (FRP) Composites for Construction*, First International Conference CDCC '98. Benmokrane, Brahim and Rahman, Habib Eds., Sherbrooke, Canada, 179-190.
- Horiguchi, Takashi and Saeki, Noboru, (1997). "Effect of Test Methods and Quality of Concrete on Bond Strength of CFRP Sheet," *Non-Metallic (FRP) Reinforcement of Concrete Structures*, Vol 1, Japan Concrete Institute, Japan, pp. 265-270.
- Khalifa, A.; Alkhradaji, T.; Nanni, A.; and Lansburg, S. (1999). "Anchorage of Surface Mounted FRP Reinforcement," *Concrete International*, ACI, submitted.
- Lee, Y-J; Tripi, JM; Boothby, TE; Bakis, CE; and Nanni, A (1998). "Tension Stiffening Model for FRP Sheets Bonded to Concrete," *Second International Conference on Composites in Infrastructure*, ICCI '98. Saadatmanesh H and Ehsani MR, Eds., Tucson Arizona.
- Maeda, Toshiya; Asano, Yasuyuki; Sato, Yasuhiko; Ueda, Tamon; and Kakuta, Yoshio, (1997). "A Study on Bond Mechanism of Carbon Fiber Sheet," *Non-Metallic (FRP) Reinforcement of Concrete Structures*, Vol 1, Japan Concrete Institute, Japan, pp. 279-286.
- Malek, AM; Saadatmanesh, H; and Ehsani, MR (1998). "Prediction of Failure Load of R/C Beams Strengthened with FRP plate due to stress concentration at the Plate End," *ACI Structural Journal*, 142-152.

MBrace Composite Strengthening System Engineering Design Guidelines Second Edition, (1998). Master Builders, Inc. and Structural Preservation Systems.

Nanni, A; Bakis, CE; Boothby, TE; Lee, YJ; and Frigo, E L (1997). "Tensile Reinforcement by FRP Sheets Applied to RC," ICE '97 International Composites Exposition, Nashville, TN, January 26-30.

Takahashi, Y.; Sato, Y.; Ueda, T.; Maeda, T.; and Kobayashi, A. (1997). "Flexural Behavior of RC Beams with Externally Bonded Carbon Fiber Sheet." Non-Metallic (FRP) Reinforcement for Concrete Structures, Proceedings of the Third International Symposium, Vol. 1, Japan Concrete Institute, Tokyo, 327-334.

Taljsten, B, (1997). "Strengthening of beams by Plate Bonding," Journal of Materials in Civil Engineering, ASCE, 206-212.

Tripi, JM; Bakis, CE; Boothby, TE; and Nanni, A (1999). "Global and Local Deformations in Concrete with External CFRP Sheet Reinforcement," Journal of Composites for Construction, ASCE (submitted for publication).

Tumialan, J. G., (1998). "Concrete Cover Delamination in Reinforced Concrete Beams Strengthened with CFRP Sheets," MSc Thesis Department of Civil Engineering, The University of Missouri, Rolla, MO.

Van Gemert, D., (1996). "Special Design Aspects of Adhesive Bonding Plates," Repair and Strengthening of Concrete Members with Adhesive Bonded Plates, SP-165, N. R. Swami, pp. 25-51.

Yoshizawa, Hiroyuki; Myojo, Toru; Okoshi, Masayoshi; Mizukoshi, Mutuki; and Kliger, Howard S. (1996). "Effect of Sheet Bonding Condition on Concrete Members Having Externally Bonded Carbon Fiber Sheet," Fourth Materials Engineering Conference, ASCE Annual Convention, Washington D.C.

VITA

Brian Daniel Miller was born in Searcy, Arkansas on November 18, 1974. Brian received his primary and secondary education in the Bald Knob public school system in Bald Knob, Arkansas. He then attended Arkansas State University in Jonesboro, Arkansas. In the December of 1997, Brian received his Bachelor of Science in Engineering, graduating Cum Laude.

Following his graduation, Brian enrolled at the University of Missouri – Rolla (UMR) in January of 1998 in pursuit of a graduate degree. Brian conducted his study in the Center for Infrastructure Engineering Studies. Brian also held the Chancellor's Fellowship for the duration of his graduate work.

While studying at UMR, he won a research competition sponsored by the Missouri Chapter of ACI. The competition was for graduate students studying in the area of concrete.